INFORMATION TO USERS

The negative microfilm of this dissertation was prepared and inspected by the school granting the degree. We are using this film without further inspection or change. If there are any questions about the content, please write directly to the school. The quality of this reproduction is heavily dependent upon the quality of the original material.

The following explanation of techniques is provided to help clarify notations which may appear on this reproduction.

1. Manuscripts may not always be complete. When it is not possible to obtain missing pages, a note appears to indicate this.

2. When copyrighted materials are removed from the manuscript, a note appears to indicate this.

3. Oversize materials (maps, drawings and charts are photographed by sectioning the original, beginning at the upper left hand corner and continuing from left to right in equal sections with small overlaps.

UMI®

UMI Number: 3227178

UMI®

COSMIC STRINGS IN THE BRANE WORLD

A Dissertation

Presented to the Faculty of the Graduate School

of Cornell University

in Partial Fulfillment of the Requirements for the Degree of

Doctor of Philosophy

by

Benjamin Simon Percival Shlaer

August 2006

This document is in the public domain.

BIOGRAPHICAL SKETCH

Benjamin Simon Percival Shlaer was born in Albuquerque, NM on May 3rd, 1977. His education began at the Rio Grande Elementary School in Santa Fe, which was extremely rewarding due to both the self-paced learning and school-wide community fostered by the teachers and administrators. Growing up in New Mexico evoked a strong love of the outdoors, especially through backpacking in the Sangre de Cristo mountains. After continuing through the public schools of Santa Fe, Ben attended The Colorado College where he studied physics, and to a lesser extent German. While completing his Bachelors degree, he spent a year abroad at the University of Freiburg. Ben enrolled at Cornell University in the Fall of 2001, where he completed his Masters in the Spring of 2005. While in Ithaca, Ben spent a large part of his free time sailing and windsurfing on Cayuga Lake, inner tubing down Fall Creek, flying model airplanes, and playing ultimate.

To my loving parents
Robert, Susan, Lidian, and Danny.

iv

ACKNOWLEDGEMENTS

Foremost I would like to thank Henry Tye, my advisor. Henry has provided me with tremendous guidance and always surprised me with his remarkable insight into what direction next deserves pursuit to further elevate the state of the art of string cosmology. Our group travels, meetings, and outings have been both enjoyable and invigorating.

My studies at Cornell have also been greatly enriched through discussions and interactions with my other committee members, Ira Wasserman and Seámus Davis. Their perspectives as scientists has been extremely enlightening. I am greatly indebted to my collaborators, Sarah Shandera, Horace Stoica, Mark Wyman, and of course Henry Tye, all of whom have contributed significantly to the work contained in this dissertation. I have also enjoyed my many discussions and interactions with David Chernoff, Hassan Firouzjahi, Girma Hailu, Nick Jones, Sash Sarangi, Jaijun Xu, and especially Louis Leblond, whose heated discussions have left me understanding a great deal more about string theory than could have been possible without him. I have also greatly enjoyed the many conversations I've had with Ferdinand Kümmeth, who along with Louis Leblond, Sarah Shandera, and Marie Göritz have made my time in Ithaca truly wonderful.

TABLE OF CONTENTS

LIST OF TABLES

LIST OF FIGURES

CHAPTER 1

INTRODUCTION

1.1 Motivation

As physicists and non-physicists alike, we are intrigued by the most fundamental questions about The Universe, namely: 'What is space, what is time, and what is matter?' In the form of General Relativity and Quantum Field Theory, fundamental physics has made tremendous progress in addressing these questions, and as scientific theories they have proven very robust in their ability to describe physical reality. Both of these theories have made highly non-trivial predictions which have been empirically verified with tremendous confidence; Cosmology, armed with the tools of general relativity and statistical mechanics, has predicted and verified the expansion of the universe, gravitational radiation, the cosmic microwave background radiation (CMB), and has singled out the theory of cosmological inflation as the paradigm in which we should investigate the earliest moments in our universe's history. Quantum field theory (in the form of the standard model) has predicted and found new particles, and made empirical predictions verifiable to seven decimal places, the most accurate of any scientific theory.

By any previous standard, GR and the SM are fundamental theories. But it can be shown that the predictions of these theories must become inaccurate in certain (not yet possible) experiments. Firstly, GR is not a quantum theory. This means it is a theory of waves, and not of quantized waves (which we call particles in QFT). In the year 1900, it was shown by Max Planck that by postulating electromagnetic waves to be quantized waves (photons), one could exactly account for the observed radiation of hot objects. A similar experiment cannot be performed directly for

1

gravity. Efforts to quantize gravity in the same spirit as the other fields in the SM have been unsuccessful. Classically speaking, gravity is surprisingly similar to the other forces we have identified in our universe; all are geometric. Gravitational forces can be attributed to curvature of spacetime, while the Strong, Weak, and Electromagnetic forces can be attributed to curvature in a richer spacetime called a fiber bundle. Quantum mechanically, these four forces are naturally described in terms of particle exchanges, the photon for electromagnetism, and the graviton for gravity. Because gravity is so weak, no experiment in the foreseeable future can provide direct evidence for the existence of gravitons.

Lacking a quantum gravity, problems arise within QFT when one tries to incorporate GR. Specifically, it appears that information is lost when the particles in our universe interact with black holes. While this is not in violation with any experiment, it is at odds with the predictive nature we assume quantum theories to have.

The word we use to describe attempts to reconcile two separate theories is 'unification.' The only theory which has done this for gravity and quantum field theory is string theory. The largest problem facing string theory is due to the tremendous success of GR and the SM: The predictions of string theory are that we live in a universe that contains both gravity and gauge theory, both of which are already known. The point where string theory predicts this to be observably different from GR+QFT is out of reach of all foreseeable experiments. One partial exception to this is supersymmetry, which is possibly detectable at the LHC. Of course string theory allows for there to be no supersymmetry, too! The versatility of string theory is both frustrating and unexpected. String theory is highly constrained as a theory, meaning it cannot be consistently modified. As an analogy,

string theory would be like a magic square. Change any number and it doesn't work. In this picture, the standard model of particle physics would be more like one's phone number: almost *any* one could work provided it has ten digits, but only one is *the right one.*

Such mathematical stringency led early string theorists to assume they had found the *theory of everything,* and so by improving our computational power we could make arbitrarily many predictions about spacetime and matter. Unfortunately it seems there are quite a few magic squares, although only one of them can describe the universe around us. It is very possible that there is no theory of everything, but if string theory is to be the closest we have, it needs to at least be correct; its rows and columns must model the nature we observe. Of course there is no way to measure each row and column of our universe, but much progress would be made by predicting just one new number in the specific "magic square" representing our string vacuum. There is much confidence among physicists that string theory is correct, partially due to it being the only candidate for unification of all observed forces in nature, but without a falsifiable prediction this confidence is too subjective to be science. If we were a strange species living on a small comet, we might have discovered string theory before we discovered gravity. Then string theory would have the credibility of an empirical science. Alas this is not the case, and so the search continues.

1.2 String Theory

String theory is built on the assumption that fundamental particles are actually one-dimensional objects ('strings') whose individual properties are characterized by which vibrational modes have been excited. By applying quantum mechanics

to these strings, one is automatically forced to accept that these strings propagate in nine spacial dimensions according to the laws of quantum mechanical supersymmetric GR and gauge theory. In addition, the theory contains higher dimensional membranes and a dynamical coupling constant. The theory has several dynamical 'parameters' which smoothly interpolate between *many* different vacuum (lowest energy) configurations, a small fraction of which closely resemble our universe. The many dynamical fields in string theory can be easily expressed in geometric terms, and even the coupling constant can take on the geometric character of a tenth spacial dimension. This is known as M-theory, and is remarkable because strings and membranes can interchange roles as fundamental degrees of freedom. Some predictions that are inescapable in string theory are the existence of extra dimensions, an infinite tower of ever heavier and higher spin particles, and gravity as we know it (GR). Unfortunately, the two not-yet-measured predictions are unlikely to ever be tested by experiment. Still, the remarkable success of string theory are overwhelming. String theory predicts a consistent quantum gravity through the exceedingly delicate cancellation of inconsistent behavior (anomalies and divergences), it predicts supersymmetry (which may soon be discovered at the LHC), and it contains Dirichlet Branes which can generate exponential hierarchies of different forces and drive inflation. All this makes string theory a very promising scientific theory worthy of continued investigation. Calculational difficulty in the strongly coupled regimes of string theory has been partially addressed through profound dualities such as the AdS/CFT correspondence whereby certain supersymmetric gauge theories are equivalent to complimentary regimes of string theory.

1.3 String Cosmology

String theory's most resolute predictions (like the existence of extra dimensions) are most likely out of reach of all future experiments. This is because the energy scales required to probe the expected features are astronomically high. These high energy scales seem irrelevant to physics in the universe today, but we know that the universe was once much hotter than it is now. The farther back we look in the universe's history, the larger the relevant energy scales are, and at some early time, string theory (if correct) must have been the only valid description of it. For this reason, cosmology seems to be the most promising tool for investigating the viability of string theory. This is especially true in light of recent progress in early universe cosmology. The recent data produced by the Wilkenson Microwave Anisotropy Probe (WMAP) team has decisively selected the theory of cosmological inflation as the correct description of how our universe got so uniform and flat, and how the seeds of galaxies were sewn to allow for our very existence. A remarkably intuitive description of this is possible using string theory: the so called Brane World [1, 2]. This picture is the simplest known paradigm useful for describing the four known forces, and how they conspired to produce the universe we observe today. The Brane World/Brane Inflation scenario is composed of a (possibly warped) string compactification containing stacks of D-Branes upon which the standard model lives. Additional brane anti-brane pairs gave rise to inflation, and the subsequent collision heated up the open string degrees of freedom (SM). Using Brane Inflation and the Brane World as a starting point, we can calculate what features a universe must have, and then search for them using technology available today or in the near future. One of the most straightforward predictions [3, 4] to come out of the Brane World is the existence of so-called cosmic

strings. Cosmic strings are one dimensional topological defects, like ultra-fine tornadoes snaking through the cosmos at rapid speeds. Cosmologists first predicted cosmic strings would kick around the smooth matter in the universe, enabling structures like galaxies to form. We now know that inflation must be responsible for this, eliminating the hypothesis of cosmic string sourced density perturbations. Their relevance was reborn with the invention of the Brane World. Brane Inflation once again necessitates the existence of cosmic strings, at some level. Much of this work is dedicated to understanding and describing these potential fingerprints left on our universe by string theory.

CHAPTER 2

COSMOLOGY

When we look deep into the universe today, we see our entire past light cone projected onto the two dimensional sky. On the largest scales, the features seen are isotropy, homogeneity, and the Hubble expansion rate (and its time variation). These observations determines the geometric evolution of the universe, and we can write down a metric quite easily which satisfies all three constraints as well as Einstein's equations. The coupled Boltzmann-Einstein equations tell us how matter and geometry interact, giving a rather complete picture of the history of the universe. This works quite well all the way back to the last 55 e-folds of inflation, before which essentially nothing can be measured, in principle. Most physicists believe inflation is the earliest empirically relevant phase of the universe, and it is where string theory probably plays a distinguished role in the form of Brane Inflation. Inflation is an exponential expansion of the universe resulting from potential energy domination of spacetime.

2.1 History of the Universe

An open question in quantum cosmology is how the universe was created. The most intuitive approach is analogous to the quantum mechanical production of electron-positron pairs from "nothing" in an external electric field [5]. The instanton approach to this problem seems to allow one to calculate the probability [6] of tunneling to a given inflationary universe from "nothing." Since this is a tunneling process, it is by definition off shell. This is why one speaks of tunneling from "nothing," meaning no classical space time. The earliest point in this universe is an off shell three-sphere of zero volume, and this phase ends with the emergence of a

7

classical (on shell) de Sitter universe. Any initial structure or geometry is rendered unobservable by inflation, especially eternal inflation. Thus the earliest empirically relevant phase of the universe is that of an inflationary (de Sitter) vacuum. This is characterized by a vacuum dominated by positive potential energy, and it is thus exponentially expanding for a length of time over which linear scales are stretched by a factor of at least e^{60} and possibly much more. Toward the end of inflation, the universe is completely empty, cold, and smooth. If the inflationary potential is flat enough, inflation is eternal, meaning the universe will always be dominated by still inflating volume. The vacuum energy is dynamical in the sense that it is the potential energy of a scalar field, and so quantum mechanical variation results in scalar (density) perturbations to the early universe.

These primordial curvature perturbations are due the quantum mechanical variance of the inflaton field. This variance is imposed on every scale smaller than the horizon, and is frozen in as soon as the scale leaves the horizon. As the expansion of the universe slows, the perturbations re-enter the horizon, and subsequently evolve much like acoustic waves. These perturbations leave a visible signature on the surface of last scattering as they evolve. The primordial density (curvature) perturbations are adiabatic, Gaussian, and nearly scale invariant. Some of these will grow large enough to become non-linear, and they survive to the present day in the form of large scale structure.

Because the end of inflation can be viewed as a second order phase transition, one might expect the formation of topological defects. String theory predicts that co-dimension two defects (cosmic strings) will be copiously produced, while other defect production is suppressed [3, 4, 7]. Thus a network of cosmic strings will appear immediately after inflation, formed much in the same way as vortices in

superconductors. Causality forbids the strings to be correlated at lengths greater than the Hubble length, although it is not inconceivable that tachyon perturbations will be correlated with the Gaussian inflaton perturbations. In any case, the non-linear evolution of cosmic strings will result in perturbations that are completely uncorrelated with the adiabatic perturbations.

The universe will have acquired particles (possibly for the first time) through "reheating" when the vacuum potential energy is converted to kinetic energy which excites the fields of all interacting particles (including dark matter) in a highly non-adiabatic process.

Cosmic strings leave wakes of over-density behind them because of their deficit angle geometry. These wakes, as well as finite string loops are additional sources of density perturbations that can seed structure formation. Although a pure tension cosmic string exerts no gravitational force on matter (or other strings), small scale wiggles including cusps and kinks endow the string with an effective matter density, which contributes to formation of density perturbations [8]. Perturbations can be classified by how their spacial components transform. Density perturbations are scalar perturbations because they perturb the local 3-D curvature scalar, or what turns out to be equivalent, the scalar Newtonian potential. The other perturbations are thus vector (sourced by defects like cosmic strings) and (symmetric traceless) tensor, which are gravity waves. Non-adiabatic perturbations are called isocurvature perturbations. Isocurvature perturbations correspond to local perturbations to the equation of state (but not density). Sub-horizon isocurvature modes subsequently evolve to produce density perturbations, since matter is pushed around. Tensor perturbations are primordially generated by the quantum mechanical variation of the graviton field. They are suppressed relative to scalar

perturbations by the slow-roll parameter $\epsilon \lesssim 1/60$. Because tensor perturbations are not coupled to density perturbations (or vector perturbations, for that matter) they are proportional only to the Hubble rate during inflation. $P_{+,\times}(k) = \frac{8\pi G H^2}{k^3}$

The homogeneity and isotropy of the universe is preserved on large scales, and so we may calculate the evolution of the now hot radiation dominated universe with the Friedmann-Robertson-Walker metric, whose only degree of freedom is the scale factor $a(t)$. The Hubble rate is defined as $H = \frac{\dot{a}}{a}$. Thermal equilibrium is maintained for all particles whose interaction rate is greater than the expansion rate.

The Boltzmann-Einstein equations predict not only how the size of the universe will evolve, but how the matter in the universe will evolve, specifically: The energy density of radiation will scale like $1/a^4$, of matter like $1/a^3$, and of non-interacting cosmic strings like $1/a^2$. A remaining vacuum energy density does not scale with expansion. This correctly predicts that matter will begin to dominate the universe as the radiation is scaled away. We observe that cosmic strings do not dominate, as their $1/a^2$ scaling would naively imply. But cosmic string scaling is naturally modified by inter-commutation, which leads to kink and loop formation. Loops decay to gravitational radiation, which scales like $1/a^4$. Simulations suggest a scaling solution whereby the number of long strings per Hubble volume is constant at about ten. String theory could modify this due to lower inter-commutation probability and network formation [9-12]. Today, as scaling would predict, the universe is vacuum energy dominated. The matter content of the universe determines both the evolution of the scale factor and the evolution of perturbations [13]. During the matter era, perturbations can finally grow large and become non-linear. This is because diffusion is mainly due to radiation. Baryonic

matter cannot grow perturbations, because it remains coupled to the photon fluid until well after matter-radiation equality, and even for a while after recombination, due to the large number of photons present.

When the primordial density perturbations re-enter the horizon, evolution occurs whereby over-dense regions begin gravitational collapse and heat up until the radiation pressure of the baryon-photon fluid builds enough to stop and reverse this infall. These are appropriately called acoustic oscillations, and the oscillation frequency depends on the sound speed of the baryon-photon fluid. Each perturbation's amplitude is related to the baryon density present. This is because more baryons mean the initial pressure is farther from the equilibrium pressure. Similarly, more matter causes the return bounce (underdensity) to be less impressive, since the overdensity gravitationally prevents photons from leaving the potential well. Isocurvature perturbations first need to create overdensities before they can collapse. Isocurvature perturbations are 90 degrees out of phase with adiabatic perturbations of the same frequency [14]. Like all sound waves, diffusion is important for wavelengths shorter than the mean free path of the fluid. This will damp the perturbations, and so one expects smaller scale perturbations to die out before last scattering. Because diffusion prevents the growth of perturbations, the matter dominated era marks the time when perturbations can grow and become non-linear. Inflation predicts density perturbations that are six times larger than the observed temperature perturbations. Photon perturbations are not fast growing, unlike matter perturbations, and hence photon perturbations remain linear even up to the present time. [13] Perturbations at t_{eq} of order 10^{-5} are exactly what is needed to produce non-linear structure in the range of 1 Mpc to 10 Mpc [15]

Last Scattering is the relatively short epoch around $z = z_* = 1100$ when elec-

trons and protons combined, making the universe transparent. Before this time, the universe consisted of a baryon-photon fluid and cold dark matter. We know that large modes re-entered the horizon at later times, and so one would expect those that entered after last scattering would not have undergone acoustic oscillations. More specifically, one would expect that the length of time between horizon entering and last scattering would determine the phase of oscillation at last scattering. The acoustic peaks seen in the microwave anisotropy thus correspond to scales that evolved to maximum (or minimum) density just before last scattering. The density troughs (but Doppler peaks) correspond to scales that were transitioning between maximum and minimum density when the photons decoupled. Because the sound speed is lowered when more matter is present, the oscillations take longer, and the acoustic peaks are shifted to higher k. Additionally, the slower fluid speeds caused by more matter will cause the Doppler effect to be less important. Doppler peaks are 90 degrees out of phase with density peaks since velocity is 90 degrees out of phase with density in a sound wave. Cosmic strings contribute to Doppler peaks because of the velocity fields they induce in passing matter. When diffusion is important, light can travel far enough to exhibit local quadrapole anisotropy. This quadrapole anisotropy is necessary for polarization to occur (via Compton scattering).

The inhomogeneities at last scattering describe the anisotropy we see today. Because the plasma is optically dense for most scales, any co-moving observer at the time of recombination would observe mainly a monopole and, for smaller scales some dipole anisotropy. When diffusion is important, light can travel far enough to even transmit local quadrapole anisotropy. The effective monopole anisotropy at the time of recombination $(\Theta(k, \eta_*)_{l=0} + \Psi(k, \eta_*))$ is converted to the anisotropy

we see today simply by relating linear scales to angular scales at the distance to the surface of last scattering. (The flatness of the universe is measured by this correspondence.) Notice the effective photon anisotropy depends on the sum of the photon and gravitational potential inhomogeneities. This is the Sachs-Wolfe effect. The hotter regions at last scattering correspond to the more dense regions, and so the light we see must have climbed out of the gravitational potential to reach us. This effect is so strong for large scales that the over-dense (and thus hotter) regions appear cold on the sky. For smaller scales, which entered the horizon earlier (radiation dominated era) the radiation pressure acts to cancel the Newtonian potential. Matter-radiation equality occurs not much earlier than recombination, and so after recombination, left over radiation is significant. Unlike in a matter dominated universe, this causes gravitational potentials to vary with time, and so light traveling into and out of a gravitational potential will not emerge at the same frequency. This integrated Sachs-Wolfe effect thus contributes to temperature perturbations on smaller scales. They are of order ten percent. When cosmic strings push matter around after t_{eq}, their potentials distort the adiabatic perturbations through both the Sachs-Wolfe and Doppler effects.

In the tightly coupled limit, the baryon-photon fluid can be described entirely by its monopole (pressure) and dipole (velocity, and hence Doppler) contribution (perfect fluid like). This is because in the tightly coupled regime, the wavelength of any lasting perturbation has $k << 1/\lambda_{mfp}$ and so all directions look very similar [13]. A quadrapole moment is relevant only when diffusion is important. A local quadrapole ($\Theta_2(k, \eta_*)$) anisotropy to temperature perturbations leads to linear polarization via Compton scattering.

Because scalar perturbations are axially symmetric, the polarization associated

with them will be E-mode (gradient) polarization. The quadrapole anisotropy induced by vector and tensor perturbations, however can also contribute to B-mode (curl) polarization. Two important sources of B-mode polarization are those due to vector mode polarization from cosmic strings, and those due to tensor perturbations. E-mode polarization corresponds to a gradient in the polarization strength that is parallel to the direction of polarization. The observables from the CMB include not only temperature correlation (C_l^{TT}) but also E-mode, B-mode, and temperature-E cross correlation. Parity conservation predicts $C_l^{TB} = C_l^{EB} = 0$.

As the CMB free streams from the surface of last scattering to us, it may interact with moving Cosmic Strings. Unlike a static cosmic string, a moving cosmic string can blue-shift passing light. One would see discrete steps in temperature given by [16]

$$\frac{\omega_f}{\omega_i} = 8\pi G\mu \frac{|\mathbf{v} \times \hat{\mathbf{n}}|}{\sqrt{1 - v^2}} \tag{2.1}$$

where $\hat{\mathbf{n}}$ is the outward pointing unit vector. The radiation is blue-shifted behind the cosmic string. This is a non-Gaussian perturbation, although the combined effects of many randomly moving strings makes detection via non-Gaussianity (non-vanishing three-point function) difficult. The Kaiser-Stebbins effect exists only after last scattering, but similar physics before last scattering is the source of Doppler and integrated Sachs-Wolfe effects due to cosmic strings.

At some point the remaining matter in the universe became re-ionized. This must have happened relatively recently ($z = 17 \pm 5$), and it is not observed to be important in the CMB A complete CMB observation allows one to know the polarization and temperature seen in any direction (or equivalently its deviation from the mean) $\frac{\delta T}{T} = \Theta(\theta, \varphi, \eta_0)$. We can expand this information into spherical

harmonics via

$$a_{l,m} = \int \Theta(\theta, \varphi) Y_{l,m}(\theta, \varphi) d\Omega \qquad (2.2)$$

For Gaussian perturbations we would expect

$$< a_{l,m} > \; = \; 0$$

$$< a_{l,m} a_{l',m'} > \; = \; C_l \delta_{m,m'} \delta_{l,l'}$$

$$< a_{l,m} a_{l',m'} a_{l'',m''} > \; = \; 0$$

as is the case with free quantum fields. Because we have only one universe to observe, it is difficult to test these equations completely. But since the number of ms for each value of l is $2l + 1$, and the right hand side of each equation is independent of m, one can measure the RHS of each equation by treating m as the ensemble index. This gives us the empirical value of C_l with statistical error

$$\frac{\Delta C_l}{C_l}\Big|_{cosmicvariance} = \sqrt{\frac{2}{2l + 1}}. \qquad (2.3)$$

2.2 Inflation

Cosmological inflation is profound due to the striking predictions and subsequent verifications the theory has produced. It is also appealing that so many attractive features are contained in such a concise idea. The early motivation for inflation was to solve the apparent contradiction between the copious amounts of topological monopoles predicted by grand unified theories (GUTs) and the observed age of the universe which requires extremely low abundances of such heavy particles. Another seemingly unrelated conceptual problem remedied by inflation is the so called horizon problem. The FRW metric we use to describe our universe predicts that most of our visible universe has only recently come into causal contact. It

seems odd that the universe could be so uniform after emerging from the big bang singularity, since no causal physics could have played a role in this. A third problem that inflation can solve is the flatness problem. The expansion rate of the universe after the big bang must have been fine tuned to extraordinary accuracy with the matter content to allow for a universe which has lived so many times longer than the Planck time [15], and yet has no obvious negative (or positive) spacial curvature. A generic big bang singularity could have produced a universe with any Hubble rate, so why such a large, but not too large of one?

The most stunning success of inflation comes in the form of the large scale structure seen in the universe today. Absent inflation, today's universe would be a highly uniform, low density gas of hydrogen. In order for stars, galaxies, and clusters to form, the matter density of the universe needs to be perturbed, and these perturbations need to grow large enough that gravity can overcompensate the smoothing effect of cosmic expansion. Cosmic strings are also capable of seeding structure formation, but WMAP has conclusively shown that they play at most a secondary role to inflation.

2.2.1 Monopole, Horizon, and Flatness Problems

The solutions to the monopole, horizon and flatness problems are remarkably straightforward in the inflationary paradigm. Since the GUT scale is around 10^{16} GeV, one can conclude that at least one monopole per Hubble volume is produced when the temperature falls below this scale. Inflation dilutes any previous matter density to insignificant amounts, so if the reheating scale is below the GUT scale, no new monopoles are formed.

The horizon problem is solved by the fact that the largest observable scales (for

definiteness, take as a fiducial scale our current Hubble radius) must have been sub-horizon at some point during inflation. If we follow the scale of our current Hubble radius back to the very end of inflation, it is super-horizon (acausal). This is because the Hubble radius at the end of Inflation was very small (rapid expansion), and this overcompensates for the fact that this fiducial scale has been shrunk by the scale factor. But as we go farther back (into the inflationary epoch) the Hubble radius does not grow any further: a de Sitter phase is defined by a time independent Hubble rate. Since the fiducial scale shrinks with the scale factor, eventually the scale becomes sub-horizon (assuming enough e-folds are present, in this case 60), thus allowing for correlations in physical quantities such as energy density. Thus it is entirely expected that the temperature of the universe on opposite sides of us can be correlated up to one part in 10^5. In effect, inflation predicts that our entire visible universe was once extremely small, and thus in causal contact.

The flatness problem is solved since a de Sitter phase exponentially increases the spacial size of the universe without becoming less dense. This expansion will thus dilute the three-dimensional curvature to near zero even if it starts with a rather large value (like ~ 1 in Planck units). This requires at least 60 e-folds, assuming large initial curvature. When the vacuum energy is thermalized into radiation, the energy density will of course be very near the critical value, since the expansion rate is determined by the inflation scale. The inflation scale is essentially the reheating scale, and this fixes the energy density to be extremely close to the critical density.

2.2.2 Density Perturbations

The most empirically significant signature of inflation is the density perturbations revealed through the CMB and large scale structure. The quantum mechanical variance of the inflaton field produces the primordial curvature (density) perturbations. This variance is imposed on any scale k that is sub-horizon ($k > aH$), and its magnitude is determined by the scale of inflation. Any perturbations become non-dynamical as soon as they leave the horizon, and remain so until they re-enter the local horizon some time after inflation ends. Very short scales were thus frozen toward the end of inflation, and became reanimated soon afterward. The largest scales were the first to freeze during inflation, and they don't begin to evolve again until comparatively late. Of course, we cannot observe perturbations on scales larger than our Hubble radius. The evolution takes place governed by the Boltzmann-Einstein equations. The primordial density (curvature) perturbations are adiabatic, Gaussian, and nearly scale invariant. Adiabatic refers to the fact that curvature perturbations yield zero variation in the number density per co-moving volume over all forms of matter [15]. Gaussianity is due to the fact that the inflaton field has very little self-interaction, and thus consists of effectively independent Fourier modes. Each mode obeys the Schrödinger equation of a damped harmonic oscillator. (The damping is due to the expansion rate.) This leads to a vanishing n-point correlation functions for all but the power spectrum ($n = 2$). Non-Gaussianity (if detected) will reveal deviations from the simple slow-roll class of models. The power spectrum $P_\Phi(k)$ is defined by $< \Phi(k)\Phi^*(k') >= (2\pi)^3 P_\Phi(k)\delta^3(k - k')$ and has k-dependence given by $k^3 P_\Phi(k) \propto k^{n-1}$. It is called scale invariant if $n = 1$. Deviations from scale invariance are due to a non-trivial inflaton potential.
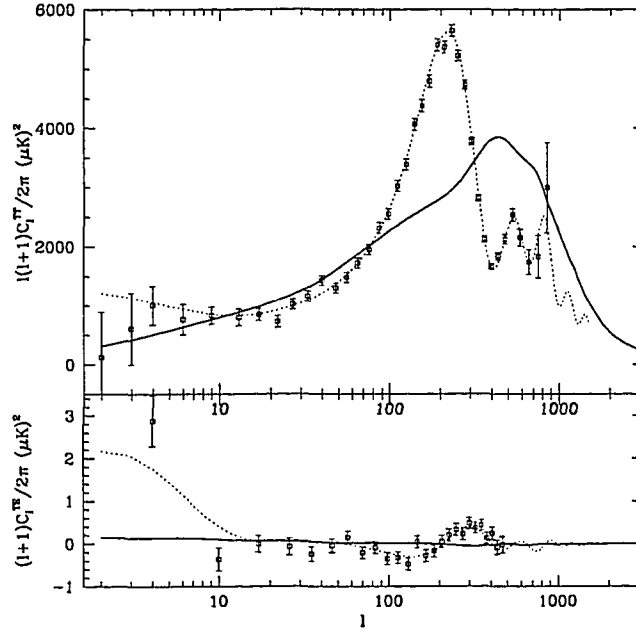
Figure 2.1: WMAP TT (top) and TE (bottom) data superimposed on the seven parameter best fit model (dashed-line) and the contribution coming purely from cosmic strings (solid line). The cosmic string curve is normalized to produce the same TT total power $I = \frac{1}{4\pi}\sum_l l(l+1)C_l^{TT}$(Taken from [8]).

2.3 The CMB: Inflation and Cosmic Strings

Cosmic strings will have contributed to CMB anisotropy both before and after last scattering. The aforementioned Kaiser-Stebbins effect allows one to bound the cosmic string tension by looking for step discontinuities (edges). One may do this statistically by looking at the power spectrum, or individually by looking for visible discontinuities. The power spectrum from this effect is approximately scale invariant, with an amplitude dependent on the energy density in the scaling cosmic string network. Figure 2.1 shows how cosmic strings are ruled out as the primary contribution to CMB power.

On large scales, cosmic strings produce linear density perturbations that can
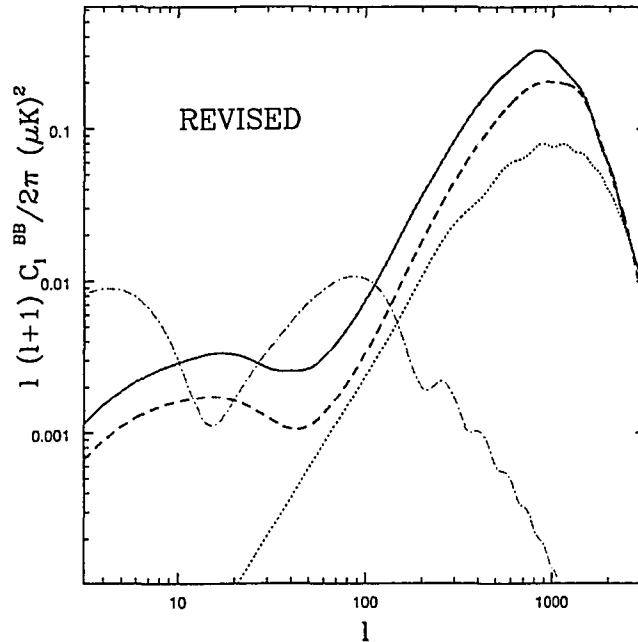
Figure 2.2: Predicted B-mode polarization power spectra for tensor to scalar ratio $r = 0.1$, $\alpha_r = 1.9$ (dashed line) and $\alpha_r = 1$ (solid line) each with total power given by $f = \frac{I^{cs}}{I^{cs} + I^{ad}} = 0.1$. The light dotted line is the B-mode component from gravitational wave converted E-mode, and the light dash-dotted line is the predicted B-mode from tensor mode quadrapole anisotropy(Taken from [18]).

be calculated with the Boltzmann-Einstein equation. The strings will be endowed with a coherence length $\xi(t)$, a tension μ, and a wiggliness parameter α defined by

$$\tilde{\mu} = \alpha\mu \qquad \tilde{T} = \alpha^{-1}\mu \tag{2.4}$$

where $\tilde{\mu}$ is the mass per unit length and $\tilde{T}$ is the effective tension of the wiggly string. The inter-commutation probability may be significantly less than one [12, 17]. This would increase the cosmic string number density.

The B-mode polarization from cosmic strings as well as other sources is summarized in Figure 2.2.

Table 2.1: Best fit results for purely adiabatic perturbations, and adiabatic + cosmic strings. α_r is the wiggliness parameter in the radiation era defined by Eqn.(2.4)

Parameter	$B = 0$	$B > 0$
f	—	$< 0.068\,(68\%)$, $< 0.14\,(95\%)$
B	—	$< 0.029\,(68\%)$, $< 0.062\,(95\%)$
α_r	—	$< 2.3\,(68\%)$, $< 3.6\,(95\%)$
A_s	$0.87^{+0.08}_{-0.16}$	$0.85^{+0.09}_{-0.13}$
n_s	$1.0^{+0.02}_{-0.04}$	1.0 ± 0.026
$\Omega_B h^2$	0.024 ± 0.001	$0.025^{+0.0012}_{-0.0016}$
$\Omega_M h^2$	0.15 ± 0.01	$0.15^{+0.013}_{-0.01}$
h	0.69 ± 0.03	0.71 ± 0.034
τ	0.155 ± 0.057	0.143 ± 0.054
F_b	$1.46^{+0.24}_{-0.22}$	$1.47^{+0.2}_{-0.18}$

2.3.1 Parameters

A best fit to the CMB (as well as SDSS) by varying the usual six cosmological parameters, as well as the galaxy bias factor (F_b) and the cosmic string parameters $(\alpha$ and $\mu)$ was conducted recently by Wyman, Pogosian, and Wasserman [8, 18]. Their results indicate that not more than 7 (14)% of the total power of the CMB anisotropy is permitted at 68(95)% confidence level. The cosmological parameter best fit is summarized in Table 2.1.

CHAPTER 3

BRANE INFLATION

Brane interactions in the brane world have been proposed as the origin of inflation [19-21], an epoch in the early universe that initiated the radiation-dominated big bang. In brane inflation [1] the inflaton is an open string mode, while the brane interaction comes from the exchange of closed string modes. A particularly simple scenario is the Dp-brane-anti-Dp-brane system. To obtain enough inflation in a realistic scenario, all string moduli need to be stabilized. A natural paradigm in which this is successful is flux compactification [22, 23]. An added benefit to such geometries is the natural appearance of warping [24]. Perhaps the most famous scenario is the Klebanov-Strassler (KS) throat [25]. Such throats are expected to be generic features of stable Type IIB compactifications. These smooth, warped, stabilized compactifications allow for a realistic ($\mathcal{N} = 1$) brane world. A stack of N D3 branes is placed at the tip of a cone over $T^{1,1}$ with M D5 branes wrapped over the shrinking two sphere. The resulting warped, deformed conifold can be studied in the context of AdS/CFT, and has led to many interesting inflationary models [26] A distinctly stringy advantage to inflationary models comes in the form of the DBI action, which describes the dynamics of D-branes. Due to the nonlinear kinetic term of the open string degrees of freedom which arise from the geometric nature of extra dimensions, a natural speed limit [27-30] is imposed on the inflaton which is absent in four dimensional models with standard kinetic terms. This results in striking empirical predictions such as non-gaussianity in the

23

CMB.

3.1 Compactification Effects

Although the naive potential between them seems too steep, it was proposed [31,32] that certain compactification effects in the special case of a hyper-cubic torus will flatten the inflaton potential enough for 60 e-folds of inflation. Let us call this the $D\bar{D}$ scenario.

The Poisson equation for the inflaton potential Φ in a compactified manifold possesses a background term [23], the so-called "jellium" term known from solid state physics. As a result, the slow-roll parameter η in the $D\bar{D}$ inflationary scenario (in the simplified version where the stabilization of compactification moduli is independent of the inflaton) becomes

$$\eta \simeq -2/d_\perp \qquad (3.1)$$

where $d_\perp$ is the number of dimensions perpendicular to the branes, $d_\perp = 9 - p \leq 6$. Since we need at least $N_e = 50$ e-folds of inflation, and $|\eta| < 1/N_e$, the $D\bar{D}$ scenario is not viable as an inflationary model. The impact of the jellium term is clearly important to the analysis of the inflationary properties in some of these scenarios. This was first studied in Ref. [33].

Here we would like to point out that the brane inflationary scenario where branes are at a small angle [2,34] remains robust because the jellium term is much smaller in this scenario. In the $(n,1)$, $(n,-1)$ wrapping scenario (which reduces to $2n$ parallel D4-Branes after inflation),

$$\eta \simeq -\frac{\theta^2}{4n} \qquad (3.2)$$

where θ is the angle between the two branes ($\theta \simeq 1/12$ and $n = 8$ are reasonable values). When the jellium contribution to $|\eta|$ is much less than $1/50$, the slow-roll

behavior of the inflaton is dictated by the other terms in the potential, in particular the quartic harmonic term as measured around the antipodal point, as studied in Ref. [2].

We would also like to point out that the $D\bar{D}$ scenario may still be possible under some special conditions. Whether that special condition on the background charge distribution is realized or not depends on the dynamics of moduli stabilization (the dilaton, the complex and Kähler structures of the compactified manifold etc.), an issue that needs better understanding [22–24].

In section 3.1.1, we give a review of the Poisson equation in compact spaces. A simple ansatz of calculating the potential energy between two charges is $q_1\Phi_2$ where Φ_2 is the potential due to the the second charge q_2, irrespective of whether the source charges in compact space add to zero or not. We shall justify this ansatz by showing that it is equivalent (up to a constant) to the potential energy between two charges (NS-NS or RR) by directly integrating the potential energy density over the compact space. This equivalence is simply illustrated in the one-dimensional case [33]. In higher dimensions, the Green's function in compact space may be represented in terms of Jacobi theta functions. In section 3.1.3, we generalize the method used in solid state physics to show how to obtain the Green's function numerically. This method should be useful in more realistic brane world models. For flat compact spaces, the Green's functions obtained by these two methods agree. In section 3.1.4, we apply the result to brane inflation in the cosmological context. As pointed out in Ref. [23], the slow-roll parameter η is too big for the brane-anti-brane scenario. On the other hand, the impact of the jellium term in the branes-at-small-angle scenario can be made negligibly small. In this sense, the branes-at-small-angle inflationary scenario remains robust. Section 3.1.8 contains

discussion.

3.1.1 Poisson Equation and Potential Energy in Compact Spaces

In non-compact space, the determination of the potential energy (Coulombic or gravitational) between two charges is well known: we treat one of the charge q_1 to be a probe charge, and the potential energy is given by $q_1\Phi_2$, where Φ_2 is the potential due to charge q_2 (even if $|q_1| > |q_2|$). Here, we argue that this simple ansatz is equally applicable in compact spaces, where Φ_2 includes the contribution of the jellium term. That is, the potential energy between two charged (Coulombic, Ramond-Ramond, gravitational or NS-NS) objects in a compact space will include the same quadratic component due to the jellium term, irrespective of whether the sum of the source charges in the compact space vanishes or not.

Consider a compact manifold M ($\partial M = \emptyset$). The Green's function is given by the Poisson equation,

$$\nabla^2 G(\mathbf{r}, \mathbf{r}') = \delta(\mathbf{r} - \mathbf{r}') - 1/\mathcal{V}$$

where $\delta(\mathbf{r} - \mathbf{r}')$ is the $d_\perp$-dimensional δ function and $\mathcal{V}$ is the volume of the compactified manifold. Integrating both sides over the $d_\perp$-dimensional compact space and using Stoke's theorem, we obtain Gauss's law. Since the compactification manifold has no boundary, this volume integral over $\nabla^2 G$ vanishes, as does the integral over the RHS of Eq.(3.3).

Consider the eigenfunctions $u_\lambda(\mathbf{r})$ of the Laplacian operator on the compact manifold with eigenvalues $\lambda \leq 0$

$$\nabla^2 u_\lambda (\mathbf{r}) = \lambda u_\lambda (\mathbf{r}).$$ (3.3)

The eigenfunctions satisfy the completeness relation:

$$\sum_\lambda u_\lambda (\mathbf{r}) u_\lambda (\mathbf{r}') = \delta (\mathbf{r} - \mathbf{r}')$$ (3.4)

Integrating both sides of Eq.(3.3) over M, we obtain $(dv = d^{d\perp} r \sqrt{-g})$,

$$\int_M dv\, u_\lambda(\mathbf{r}) = 0 \qquad \lambda \neq 0$$ (3.5)

In a compact space there is a normalizable zero mode of the Laplacian, $\nabla^2 u_0 (\mathbf{r}) = 0$, where $u_0 (\mathbf{r}) = 1/\sqrt{\mathcal{V}}$. The Green's function can be written as:

$$G (\mathbf{r}, \mathbf{r}') = \sum_{\lambda \neq 0} \frac{u_\lambda (\mathbf{r}) u_\lambda (\mathbf{r}')}{\lambda}$$ (3.6)

Note that the zero mode is absent in $G(\mathbf{r}, \mathbf{r}')$ in Eq.(3.6), thus avoiding an obvious divergence. Using Eq.(3.5) and (3.6), we have

$$\int_M dv\, G(\mathbf{r}, \mathbf{r}') = 0$$ (3.7)

Let Φ be the static potential due to a given set of charges q_i (at $\mathbf{r}_i$), $i = 1, 2, ...,$

$$\Phi(\mathbf{r}) = \sum_i q_i G(\mathbf{r}, \mathbf{r}_i)$$ (3.8)

Using Eq.(3.8) and (3.3), the total static energy due to this set of charges q_k is

$$V(\mathbf{r}_k) = \frac{1}{2} \int_M dv (\nabla \Phi)^2 = - \int_M dv\, \frac{1}{2} \Phi \nabla^2 \Phi$$
$$= -\frac{1}{2} \sum_i q_i \Phi(\mathbf{r}_i) + \frac{\sum q_i}{2\mathcal{V}} \int_M dv \Phi(\mathbf{r})$$

Using Eq.(3.7) and Eq.(3.8), we see that the last term in Eq.(3.9) vanishes. So, irrespective of whether or not the net charge vanishes,

$$V(\mathbf{r}_k) = - \sum_{i>j} q_i G(\mathbf{r}_i, \mathbf{r}_j) q_j + constant$$ (3.9)

where the constant comes from the r_i-independent self-interaction terms. When applied to the RR interaction, where $q_i = \mu_i$, we must have $\sum_i \mu_i = 0$ in our compact space. For the NS-NS interaction, q_i are the brane tensions T_i, $\sum_i T_i \neq 0$ and $V_{NS-NS}(r_i)$ has the opposite sign since same sign charges attract. Putting them together we obtain, up to a constant

$$V(\mathbf{r}_k) = + \sum_{i>j} (T_i T_j - \mu_i \mu_j) G(\mathbf{r}_i, \mathbf{r}_j) \tag{3.10}$$

where the presence of the jellium term is encoded in $G(\mathbf{r}_i, \mathbf{r}_j)$. In the two brane potential, the "Coulomb" $(1/r^{d-2})$ term and the jellium (r^2) term have the same effective strength, namely $T_1 T_2 - \mu_1 \mu_2$. This effective strength is very small for branes at a small angle. Since the constant term in the potential is linear in the brane tension T, V''/V can be made arbitrarily small.

3.1.2 One-Dimensional Example

This well-known example (given in Ref. [33]) illustrates the above result. Consider a circle of circumference L. For $0 \leq y \leq L$,

$$G(y) = -\frac{y^2}{2L} + \frac{|y|}{2} - \frac{L}{12} \tag{3.11}$$

where the constant term may be determined by the ζ-function regularization of the divergent Green's function $\hat{G}$ of the 1-dimensional lattice,

$$2\hat{G}(y) = |y| + \sum_{n=1}^{\infty} |y + nL| + |y - nL| \tag{3.12}$$

Notice that $G(y)$ satisfies Eq.(3.7).

Let us put a charge $q_1 = q$ at $y_1 = 0$ and a second charge $q_2 = -q$ at $y_2 = y$, where $0 \leq y < L$ so that the total charge in the circle is zero. Using Eq.(3.9), one

finds

$$V(y) = q^2 G(y) + \frac{q^2 L}{12} = q^2 \left(\frac{|y|}{2} - \frac{y^2}{2L} - \frac{L}{12} \right) + \frac{q^2 L}{12} \qquad (3.13)$$

where the first term is the linear potential and the quadratic term is due to the jellium effect. The last term is the self-energy term and is independent of y. As we put the charges on top of each other, $V(0) = 0$, as expected. Note that we are constraining the flux around the circle to be constant.

We may also calculate the potential at x due to these two charges ($+q$ and $-q$)

:

$$\phi_1(x) = q\frac{x}{L}(L - y) - qy + \phi_0 \qquad 0 \le x \le y$$

$$\phi_2(x) = -\frac{qxy}{L} + \phi_0 \qquad y \le x \le L$$

Note that $\phi(x)$ is continuous and piecewise linear in x, i.e., $\phi_1(0) = \phi_2(L)$ and $\phi_1(y) = \phi_2(y)$. Now we can integrate over the circle the energy density $((\nabla\phi)^2/2)$ to obtain the energy as a function of the relative position y of the charges. This exactly reproduces $V(y)$ in Eq.(3.13). In short, $\phi(x, y)$ is the potential for a probe charge at x, while $V(y)$ is what we are interested in.

For the case of two masses on a circle: m_1 at $y_1 = 0$ and m_2 at $y_2 = y$, the potential at x ($0 \le x < L$) due to these 2 masses is $\phi(x) = m_1 G(x) + m_2 G(x - y)$, where there is a jellium contribution in each Green's function. From this,

$$\nabla\phi_1(x) = -\frac{m_1 + m_2}{L}x + \frac{m_2 y}{L} + \frac{m_1 - m_2}{2} \qquad 0 \le x \le y$$

$$\nabla\phi_2(x) = -\frac{m_1 + m_2}{L}x + \frac{m_2 y}{L} + \frac{m_1 + m_2}{2} \qquad y \le x \le L$$

and, as expected, we have

$$V(y) = -\frac{1}{2} \int dx (\nabla\phi)^2 = m_1 m_2 G(y) - \frac{(m_1^2 + m_2^2)L}{24}$$

where the last constant term is the self-energy contribution.

3.1.3 Green's Function in Arbitrary Dimension

When two branes are moving in a compactified space, we need to calculate the inter-brane potential. This requires finding $\Phi(\mathbf{r}) = -G(\mathbf{r})$ that satisfies Eq.(3.3). Our main goal is to determine the Green's function around the antipodal point (the point farthest from the source). To simplify the problem, consider a square, flat d-dimensional torus of volume L^d. Using the identity

$$\frac{1}{L^2\lambda} = -\int_0^\infty e^{L^2\lambda s}ds \qquad (\lambda < 0) \tag{3.14}$$

and the eigensolutions

$$u_\mathbf{n}(\mathbf{x}) = \sqrt{L^{-d}}e^{2\pi i\mathbf{n}\cdot\mathbf{x}/L}, \qquad \lambda_\mathbf{n} = -\frac{4\pi^2 n^2}{L^2}$$

we can regularize

$$
\begin{aligned}
G(\mathbf{x}) &= -\sum_{\mathbf{n}\in\mathbb{Z}^d}(1-\delta_{\mathbf{n},0})\frac{e^{2\pi i\mathbf{n}\cdot\mathbf{x}/L}}{4\pi^2 n^2 L^{d-2}} \\
&= L^{2-d}\int_0^\infty(1-\prod_{j=1}^d\sum_{n_j\in\mathbb{Z}}e^{2\pi i n_j x_j/L-4\pi^2 n_j^2 s})ds \\
&= L^{2-d}\int_0^\infty\left[1-\prod_{j=1}^d\theta_3(\frac{\pi x_j}{L},e^{-4\pi^2 s})\right]ds
\end{aligned}
$$

Where θ_3 is a Jacobi theta function [35]

$$\theta_3\left(\frac{b}{2},e^{-a}\right) = \sum_n e^{-an^2+ibn} \tag{3.15}$$

The rapid convergence of the above expression makes the flat d-torus especially simple to numerically simulate.

When one considers compactification on a manifold (T^2, $K3$, CY_3) with a non-trivial metric, another numerical method suggests itself. Developed by Ewald and others [36], this method is suited to spaces that may be represented as a periodic

lattice (perhaps modulo some additional discrete symmetries). To illustrate the method, we proceed with a simple example, a square, flat torus. Let us again write Φ as in Eq.(3.6):

$$\Phi(\mathbf{r}) = \frac{1}{\mathcal{V}} \sum_{\mathbf{k}_j \neq 0} \frac{\exp(i\mathbf{k}_j \cdot \mathbf{r})}{k_j^2} \tag{3.16}$$

where $\mathbf{k}_j \in \frac{2\pi}{L}\mathbb{Z}^d$ is a reciprocal lattice vector and k_j its magnitude. This sum diverges for $d \geq 2$, since the number of terms grows as k_j^{d-1} (i.e., with the surface area of a d-dimensional ball). Alternatively, one may treat the torus as an infinite lattice and sum over the source and its images at the lattice points:

$$\Phi(\mathbf{r}) = \sum_{\mathbf{r}_j} \frac{\alpha}{(\mathbf{r} - \mathbf{r_j})^{d-2}} \tag{3.17}$$

where

$$\alpha = \frac{\Gamma(\frac{d-2}{2})}{4\pi^{\frac{d}{2}}}, \quad d \neq 2 \tag{3.18}$$

As we saw in the one-dimensional case, this will lead to a divergence and the need to regularize it. The answer depends on how the lattice points are summed and how the regularization is carried out.

Ewald's method is to add and subtract a diffuse charge distribution around each lattice point. The added charge makes the monopole moment of each cell zero, aiding the convergence of the real lattice sum. This additional charge (minus a jellium term) is convergently subtracted away in reciprocal space, since a reciprocal space sum converges for non-singular charge distribution. The final result is independent of the diffuse charge distribution used to regulate the sums. Details on how to implement this method in two, three and four dimensions are included in sections 3.1.10 - 3.1.12. The numerical data generated by the Ewald method

may be fit to an expression for the potential near the source of the form:

$$\Phi^{(d)}(\mathbf{r}) = \frac{\alpha}{r^{d-2}} + \frac{r^2}{2d\mathcal{V}} + \Phi^{(d)}_{harmonic}(\mathbf{r}) + constant, \quad d > 2$$

$$= -\frac{1}{2\pi}\ln\left(\frac{r}{L}\right) + \frac{r^2}{4\mathcal{V}} + \Phi^{(2)}_{harmonic}(\mathbf{r}) + constant, \quad d = 2$$

Notice that although individual terms in $\Phi^{(d)}(\mathbf{r})$ are not periodic, their sum is. The constant is fixed by requiring $\Phi^{(d)}(\mathbf{r})$ to be independent of the added and subtracted charge. The harmonic piece satisfies the Laplace equation (when restricted to the cell containing the origin):

$$\nabla^2\Phi^{(d)}_{harm} = 0 \tag{3.19}$$

For a hypercubic torus (with $\mathcal{V} = L^d$) it has the general form

$$\Phi^{(d)}_{harm}(\mathbf{r}) = \frac{C^{(d)}_s}{\mathcal{V}^{\frac{d-2}{d}}} + A^{(d)}_4 h^{(d)}_4(\mathbf{r}) + A^{(d)}_6 h^{(d)}_6(\mathbf{r}) + \ldots \tag{3.20}$$

where the $h^{(d)}_n$ are polynomials of order n with coefficients determined by Eq(3.19). For example, for a hyper-cubic lattice with coordinates x_i measured from the source (podal point) and $\mathbf{r} = (x_1, x_2, ..., x_d)$

$$h^{(d)}_4(\mathbf{r}) = \frac{1}{\mathcal{V}^{\frac{d+2}{d}}}\left[\sum_{i=1}^{d} x_i^4 - \frac{6}{d-1}\sum_{i\neq j} x_i^2 x_j^2\right]$$

$$h^{(d)}_6(\mathbf{r}) = \frac{1}{\mathcal{V}^{\frac{d+4}{d}}}\left[\sum_{i\neq j\neq k} x_i^2 x_j^2 x_k^2 + \frac{(d-2)(d-1)}{180}\sum_i x_i^6 - \frac{(d-2)}{12}\sum_{i\neq j} x_i^4 x_j^2\right]$$

In two dimensions, terms of order $4m + 2$ are not present in the harmonic piece. Beyond the sixth order terms in the hypercubic case, and for $d > 2$ for a rectangular lattice, there is more than one undetermined coefficient $A^{(d)}_{n,i}$ at each order. A two-dimensional rectangular lattice has only one parameter at any even order. At a given order n, the number of parameters for a hypercubic lattice reaches a maximum and becomes independent of dimension for $d \geq \frac{n}{2}$.

There is an expression similar to Eq.(3.19) for the potential near the antipodal point. This is the expression that is suitable for applications in brane inflation. With coordinates z_i now measured from the antipodal point ($\mathbf{z} = \mathbf{r} - (L/2, L/2, ...)$), Φ has the form

$$\Phi^{(d)}_{antipodal}(\mathbf{z}) = \frac{C^{(d)}_a}{\mathcal{V}^{\frac{d-2}{d}}} + \frac{1}{2d\mathcal{V}} \sum_{i=1}^{d} z_i^2 + B_4^{(d)} h_4^{(d)}(\mathbf{z}) + B_6^{(d)} h_6^{(d)}(\mathbf{z}) + \ldots \qquad (3.21)$$

The results for the coefficients in Eq.(3.19) and Eq.(3.21) were obtained by the method described below, and are summarized in Tables 3.1 and 3.2. The lattice spacing has been set to one. At least four terms in Φ_{harm} were kept in each dimension, but the accuracy of the numerical values could be improved by keeping more. In general, the convergence of Eq.(3.19) is somewhat better than that of Eq.(3.21).

It is easy to check that the integral of Φ over a unit cell is zero, that is, Φ satisfies Eq.(3.7). In solid state physics, the Madelung constant is found by considering the potential due to both the positive and negative ions. Since the negative ions are found at the antipodal point in a simple cubic lattice, the Madelung constant is given by $\alpha_m = C_s - C_a$. In three dimensions, our value for the Madelung constant of a simple cubic lattice agrees with Ref. [37]. The constants C_a in Table 3.2 agree with Eq.(3.15) evaluated at the antipodal point, and are four times those listed in Ref. [32].

For rectangular torus, there will be quadratic harmonic terms of the form $z_i^2 - z_j^2$. Their impact on inflation is discussed in Ref. [2]. The hypercubic way to sum the lattice generates only the harmonic terms. The numerical values of B_4 is at least a factor of 3 smaller than that given in Ref. [2]. This weakens the potential and improves the inflationary scenario.

Table 3.1: Constant, fourth order and sixth order coefficients in potential near source.

$d_\perp$	2	3	4
C_s	-0.21	-0.21	-0.17
A_4	0.12	0.44	0.34
A_6	0.00	0.0072	3.05

Table 3.2: Constant and coefficients of the fourth order and sixth order terms in the potential near the antipodal point .

$d_\perp$	2	3	4
C_a	-0.055	-0.064	-0.070
B_4	-0.62	-0.53	-2.20
B_6	0.00	0.0024	-101.5

3.1.4 Application to Brane Inflationary Scenarios

Let us consider a few brane inflationary scenarios, where the moduli stabilization effects are ignored. In order to find the potential of the inflaton as seen by a 4D observer we need to calculate the low-energy effective action for the brane system. The interaction between the branes due to the exchange of closed strings depends on their separation, so we will decompose the coordinates of the two (stacks of) branes into the center-of-mass and the relative separation.

Assuming that the branes wrap n and m times the volume $V_\parallel$, the low-energy effective action is obtained by expanding the DBI action:

$$S_{eff} = n\tau_p \int d^{p+1}\xi_1 \sqrt{1 + \partial_\mu y_1 \partial^\mu y_1} + m\tau_p \int d^{p+1}\xi_2 \sqrt{1 + \partial_\mu y_2 \partial^\mu y_2}$$

$$\simeq (m+n)\,\ell_\parallel \tau_p + n\tau_p \int d^{p+1}\xi_1 \frac{1}{2}\partial_\mu y_1 \partial^\mu y_1 + m\tau_p \int d^{p+1}\xi_2 \frac{1}{2}\partial_\mu y_2 \partial^\mu y_2$$

where τ_p is the brane tension

$$\tau_p = M_s^{p+1}/(2\pi)^p g_s \tag{3.22}$$

where M_s is the string scale and g_s the string coupling. The coordinates of the brane in the transverse directions are expressed as:

$$y_1 = y_{CM} + \frac{m}{m+n} y_r$$
$$y_2 = y_{CM} - \frac{n}{m+n} y_r$$

and substituting these into the expression for S_{eff} we obtain:

$$S_{eff} = \tau_p \frac{mn}{2(m+n)} \int d^{p-3}\xi \int d^4\xi \partial_\mu y_r \partial^\mu y_r = \int d^4\xi \frac{1}{2}\partial_\mu \psi \partial^\mu \psi \tag{3.23}$$

The relationship between y_r and ψ is given by:

$$\psi = y_r \sqrt{\frac{mn}{(m+n)}\tau_p V_\parallel} \tag{3.24}$$

where $V_\parallel = \int d^{p-3}\xi = \ell_\parallel^{p-3}$.

3.1.5   The D$\bar{\text{D}}$ Scenario

The D$\bar{\text{D}}$ potential is given in Ref. [2, 31], with $d_\perp = 9 - p$:

$$V(y) = 2\tau_p \ell_\parallel^{p-3} - \frac{\kappa^2 \beta \tau_p^2 \ell_\parallel^{p-3}}{y^{d_\perp - 2}}$$ (3.25)

where

$$\kappa^2 = 8\pi G_{10} = \frac{g_s^2 (2\pi)^7}{2 M_s^8}$$ (3.26)

and $\beta = 2\alpha$ given in Eq.(3.18). Measured relative to the antipodal point, the position of the anti-brane is given by z, which is simply y shifted by half the lattice size. The important pieces of the potential for the slow-roll condition on inflation are the constant term and the quadratic piece due to the jellium term :

$$V(z) = 2\tau_p \ell_\parallel^{p-3} - z^2 \frac{\kappa^2 \tau_p^2 \ell_\parallel^{p-3}}{d_\perp V_\perp}$$ (3.27)

where $V = V_\perp$. As pointed out in Ref. [23], the relevant slow-roll parameter η is given by:

$$\eta = M_P^2 \frac{V''}{V} \simeq -\frac{2}{d_\perp}$$ (3.28)

where the derivative is taken with respect to the scalar field ψ that appears in the low-energy effective theory, Eq.(3.24). Since $d_\perp \leq 6$, the slow-roll condition is never satisfied in this case, that is, the branes will collide far too early for any significant inflation to take place.

A priori, it is still possible that the stabilization dynamics of the extra dimensions has some unusual features that suppress η and realize the condition required for the viability of the D$\bar{\text{D}}$ inflationary scenario. One such possibility utilizes a warped geometry to suppress the inter-brane attractive potential [23].

Here, let us consider

$$\nabla^2 \Phi = \sum_i q_i \delta(\mathbf{r} - \mathbf{r}_i) - F(\mathbf{r} - (L/2, L/2, ..))$$

$$F(\mathbf{z}) = \frac{\sum_i q_i}{\mathcal{V}} + f(\mathbf{z})$$

where $f(\mathbf{z})$ is multi-periodic and consistency requires it to satisfy

$$\int_M dv f(\mathbf{z}) = 0 \tag{3.29}$$

It is not hard to imagine that $f(\mathbf{z})$ originates from the stabilization of the moduli in the extra dimensions. As one can easily see, $D\bar{D}$ inflationary scenario is viable if $F(\mathbf{z})$ vanishes at the antipodal point. To suppress the quadratic term in the inflaton potential, we need to decrease the value of $F(\mathbf{z})$ at the antipodal point so that

$$|\eta| \simeq |2\mathcal{V}F(0)/d_\perp| < 1/N_e \tag{3.30}$$

Suppose, for a torus, measured with respect to the antipodal point,

$$F(\mathbf{z}) = \frac{1 - \Pi \cos(k_j z_j)}{\mathcal{V}} \simeq \frac{\sum(k_j z_j)^2}{\mathcal{V}} \tag{3.31}$$

so that $F(0) = 0$. This implies that the inflaton potential does not have an anharmonic quadratic term around the antipodal point. Such a $D\bar{D}$ scenario will be able to give enough inflation to render the model viable. (In fact, one may choose $F(\mathbf{z})$ to reduce the contribution of the quartic term to η as well.) Among other factors, the form of $F(\mathbf{z})$ depends on the dynamics of moduli stabilization, an issue that is not fully understood [22–24]. Generically, we should consider $F(0) \ll 1/\mathcal{V}$ as a fine-tuning. Since η is generically around 1 for the $D\bar{D}$ system, we need a fine-tuning of 1 in 100 on $F(\mathbf{z})$ to suppress η. In more realistic constructions of string models, it will be very interesting to see how such a condition can be satisfied.
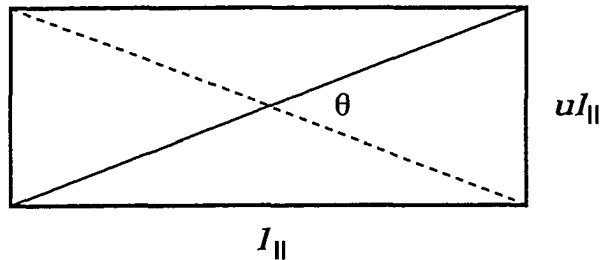
Figure 3.1: Two branes wrapping different cycles in a rectangular torus. Theangle between the branes is $\tan\theta \simeq \theta = 2u$.

3.1.6 Branes at a Small Angle

Let us consider the simple scenario [34] where $p = 4$, $d_\perp = 4$, but with different wrappings of the branes. The X^4, X^5 torus, has sides $\ell_\parallel$ and $u\ell_\parallel$ and the branes wrap one-cycles on the torus, as shown in Figure 1. These branes are separated in the X^6, X^7, X^8, X^9 directions by a distance y.

The Planck mass is given by

$$M_P^2 = \frac{M_s^8 \ell_\parallel^2 u V_\perp}{g_s^2 \pi \, (2\pi)^6} \tag{3.32}$$

We start with the example shown in Figure 3.1 where the wrapping numbers are $(1, 1)$ and $(1, -1)$. We shall consider small θ, so the angle between the branes is $\theta \simeq \tan\theta = 2u$. The constant piece of the potential is given by:

$$V_0 = \tau_p \ell_\parallel \left(2\sqrt{1 + u^2} - 2 \right) \simeq \tau_p \ell_\parallel u^2 \tag{3.33}$$

and the full potential is:

$$V(y) = \tau_4 \ell_\parallel u^2 - \frac{Q y^2}{2 d_\perp V_\perp} - \frac{\beta Q}{2 y^2} + harmonic \tag{3.34}$$

where Q includes the contributions from both the NS-NS and RR sectors.

$$Q = \frac{M_s^2}{2\pi \sin\theta} \left(1 - \frac{\sin^2\theta}{2} - \cos\theta \right) \simeq M_s^2 \theta^3 / 16\pi \simeq M_s^2 u^3 / 2\pi \tag{3.35}$$

where the $(1 - \sin^2 \theta/2)$ term comes from the NS-NS sector while the $- \cos \theta$ term comes from the RR sector. The $\sin \theta$ in the denominator comes from the length of the brane along the $\ell_\parallel$ direction. y measures the relative positions of the branes. With the above expressions for the potential and the Planck mass, we evaluate the potential $V(z)$ at the antipodal point. The relevant slow-roll parameter η there becomes:

$$\eta = M_P^2 \frac{V''}{V} = -\frac{M_S^8 \ell_\parallel^2 u V_\perp}{g_s^2 \pi (2\pi)^6 d_\perp V_\perp \tau_4 \ell_\parallel u^2} Q \left(\frac{\partial y}{\partial \psi}\right)^2 = -\frac{4u^2}{d_\perp} = -\frac{\theta^2}{4} \qquad (3.36)$$

For $u \simeq 1/M_s \ell_\parallel \simeq \alpha_{GUT} \simeq 1/25$ (a reasonable choice, where α_{GUT} is the standard model coupling at the GUT scale), the slow-roll condition is easily satisfied, and it is possible to obtain more than 60 e-foldings of inflation since $N_e \sim 1/\eta$.

A few comments are in order. As the jellium term contribution to η is very small, the number of e-foldings is dictated by the first non-zero harmonic term. Here it is the quartic term with strength B_4 given in Table 3.2. As we pointed out earlier, the B_4 obtained here are at least a factor of three smaller than those used in Ref. [2]. Thus the inter-brane potential is weaker than Ref. [2] uses, and so it is much easier to get sufficient inflation than they indicate.

The Madelung term C_a will shift the vacuum energy of the inflaton potential. As is clear from Eq.(3.34) and Table 3.2, this shift is positive, that is, it increases the vacuum energy term in the inflaton potential. Its contribution tends to decrease the magnitude of η.

After collision, the two branes at a small angle reduce to two parallel branes (horizontal in Fig.(3.1)) with zero vacuum energy. In an orientifold, the tension and RR charge of these two branes are canceled by the presence of orientifold planes. This implies that during inflation, the branes at angle will have a non-zero force with the remaining branes and orientifold planes. For example, the interaction

between the $(1, -1)$ D4-Brane and a $(1, 0)$ D4-Brane is proportional to

$$Q_{(1,0)} = -\frac{M_s^2}{2\pi \sin\theta} \left(1 - \frac{\sin^2(\theta/2)}{2} - \cos(\theta/2)\right) \simeq \frac{Q}{16} \qquad (3.37)$$

and its interaction with orientifold planes is also suppressed by the same factor of 16, but with opposite sign. These contribute a small correction to the interaction between the $(1, -1)$ and the $(1, 1)$-branes. One can always place the $(1, 1)$-brane, the $(1, -1)$-brane, and the $(1, 0)$-branes at initial positions that are favorable to inflation.

3.1.7 Other Branes at a Small Angle Scenarios

Next we consider branes wrapping the long dimension of the torus more than once. Suppose one branes has $(n, 1)$ wrapping and the other has $(n, -1)$ wrapping. After collision, we are left with $2n$ parallel branes. In this case the angle between the branes is $\theta = 2u/n$ and the constant piece of the potential is:

$$V_0 = 2\tau_p \ell_{\parallel} \left(\sqrt{n^2 + u^2} - n\right) \simeq \tau_p \ell_{\parallel} \frac{u^2}{n} \qquad (3.38)$$

The branes now intersect in n^2 points, so the charge Q is given by:

$$Q = n^2 \frac{M_s^2}{2\pi} \frac{u^3}{n^3} = \frac{M_s^2}{2\pi} \frac{u^3}{n} \qquad (3.39)$$

The relationship between ψ and y becomes:

$$\psi = y\sqrt{\tau_p \ell_{\parallel} \frac{n}{2}} \qquad (3.40)$$

and the slow-roll parameter η becomes:

$$\eta \simeq -\frac{u^2}{n} \qquad (3.41)$$

For small u and large n, the slow-roll condition is easily satisfied, and it is possible to obtain many more than 60 e-foldings of inflation since $N_e \sim 1/|\eta|$. The other

slow-roll parameter $\epsilon = 0$ at the antipodal point. In the actual case, the slow-roll parameters are dictated by the quartic harmonic term where ϵ is negligibly small. For a reasonable choice $n = 8$, we see that the number of e-foldings that can be obtained for inflation is further improved. In fact, the quadratic term is negligible in this case and the inflaton rolling is dictated by the quartic harmonic term discussed in Ref. [2].

We may also consider branes with dimensionalities other than $p = 4$. In the $p = 6$, $d_\perp = 2$ case the D6-Branes span the X^4, X^5 torus and wrap different cycles of the X^6, X^7 torus. They are localized in the X^8, X^9 torus and the interaction potential is logarithmic. The potential and the Planck mass are given by:

$$M_P^2 = \frac{M_S^8 V_{45} \ell_{\parallel}^2 \theta V_\perp}{g_s^2 \pi \, (2\pi)^6}$$

$$V(y) = \frac{\tau_6 V_{45} \ell_{\parallel} \tan^2 \theta}{4} - \frac{Qy^2}{2 d_\perp V_\perp} - \beta Q \log(M_s y)$$

where $Q \simeq M_s^4 \theta^3 / 16\pi$. Again, in the small angle approximation, the relevant slow-roll parameter becomes:

$$\eta \simeq -\frac{(2\pi)^2 \theta^2}{\left(M_s r_{\parallel}\right)^2} \tag{3.42}$$

The slow-roll parameter is again small in this case, and the end of the slow-roll is determined by the attractive logarithmic potential. The region yielding enough slow-roll is reasonably large and there is no need to fine-tune the initial conditions.

It will be interesting to work out the situation of other brane inflationary scenarios [38–40].

3.1.8 Discussions

In the simplified scenario discussed here, the $D\bar{D}$ inflationary scenario is not viable. On the other hand, the branes at a small angle scenario remains a viable model

for inflation. Cosmic strings are generically produced at the end of the brane inflationary epoch. Using the temperature fluctuation in the cosmic microwave background radiation to fix the superstring scale, the cosmic string tension arising from the brane recombination in the branes at a small angle inflation happens to be much bigger than that in the $D\bar{D}$ scenario [2,3]. If branes-at-a-small-angle scenario is preferred, one consequence is that the cosmic string tension will be on the high side, up to values just below the present experimental bounds. This enhances the hope to test the brane inflationary scenario via the search of signatures of cosmic strings.

As is clear from the analysis, the brane inflationary scenario depends on the dynamics of moduli stabilization. Presumably compactification moduli are stabilized by some strong dynamics, or effective potential. The minimum of such an effective potential measures the cosmological constant. Understanding the moduli stabilization problem implies some understanding of the cosmological constant problem, or in a less ambitious framework, moduli stabilization must accommodate the smallness of the observed dark energy [22]. Hopefully, brane inflation in string theory allows us to address this important issue.

3.1.9 Ewald's Method

Here we will detail Ewald's technique and extend it to suit our purpose. Consider the d-dimensional torus as an infinite lattice and let $\Phi(\mathbf{r})$ satisfy

$$\nabla^2 \Phi(\mathbf{r}) = \sum_j -\delta(\Delta \mathbf{r_j}) + \frac{1}{\mathcal{V}}$$

$$\Phi(\mathbf{r}) = \Phi_1(\mathbf{r}) + \Phi_2(\mathbf{r}) + constant$$

$$\nabla^2 \Phi_1(\mathbf{r}) = \sum_j -P(\Delta r_j) \exp(-\epsilon^2 \Delta r_j^2) + 1/\mathcal{V}$$

$$\nabla^2 \Phi_2(\mathbf{r}) = \sum_j \left[-\delta(\Delta \mathbf{r_j}) + P(\Delta r_j) \exp(-\epsilon^2 \Delta r_j^2) \right]$$

Where $\Delta \mathbf{r_j} = \mathbf{r} - \mathbf{r_j}$, and $\mathbf{r_j}$ is the jth lattice vector. Here $P(\Delta r_j) \exp(-\epsilon^2 \Delta r_j^2)$ can be thought of as a charge distribution inserted at the jth lattice site, normalized so that

$$\int_{\mathbb{R}^d} P(r) \exp(-\epsilon^2 r^2) dv = 1 \tag{3.43}$$

The charge distribution may extend outside the unit cell, but integrating one distribution over all space is identical to integrating all distributions over the unit cell. The effect of adding and subtracting a diffuse charge distribution is to regularize the summation over the lattice. The full potential $\Phi(\mathbf{r})$ is the sum of $\Phi_2(\mathbf{r})$ (the real-space sum) and $\Phi_1(\mathbf{r})$ (the reciprocal lattice sum). For a good choice of $P(r)$ the sums are separately convergent, and together reproduce $\Phi(\mathbf{r})$ for the original point-charge distribution. Clearly, $\Phi(\mathbf{r})$ should be independent of $P(r)$ and ϵ, which are chosen to enhance the convergence of the sums. There is a range of choices of ϵ (for our calculation $18 \leq \epsilon \leq 24$) for which the results of Eq.(3.43) are independent of ϵ. Other crucial conditions are listed and demonstrated in the next section. This procedure is well tested since it is widely used in solid state physics to compute the Madelung constant.

3.1.10 Three Dimensions

In three dimensions, a simple choice is to add and subtract a Gaussian charge distribution at each lattice site. This gives $P(r) = \epsilon^3 \pi^{-3/2}$. Then we have

$$\Phi_1^{(3)}(\mathbf{r}) = \frac{1}{\mathcal{V}} \sum_{\mathbf{k}_j \neq 0} \frac{\exp(-k_j^2/4\epsilon^2)\exp(i\mathbf{k}_j \cdot \mathbf{r})}{k_j^2}$$

$$\Phi_2^{(3)}(\mathbf{r}) = \frac{1}{4\pi} \sum_{\Delta r_j} \frac{1 - \mathrm{erf}(\epsilon\Delta r_j)}{\Delta r_j}$$

where $\mathbf{k_j}$ is the jth reciprocal lattice vector. Note that the following necessary conditions are satisfied:

1) The terms in Φ_1 converge faster than k_j^{-3}.

2) Φ_1 reduces to Eq(3.16) when $\epsilon \to \infty$.

3) The terms in Φ_2 converge faster than Δr_j^{-3}.

4) Φ_2 goes to zero as $\epsilon \to \infty$.

5) Φ_2 reduces to $\sum_j \Delta r_j^{-1}$ as $\Delta r_j \to 0$.

Any other choice for $P(r)$ must lead to potentials that satisfy these same limits for the method to work.

In principle there is also an arbitrary constant of integration, but the requirement that Φ be independent of ϵ yields

$$\Phi^{(3)}(\mathbf{r}) = \Phi_1^{(3)}(\mathbf{r}) + \Phi_2^{(3)}(\mathbf{r}) - \frac{1}{4\mathcal{V}\epsilon^2} \tag{3.44}$$

The ϵ-dependent term comes from the missing zero mode in $\Phi_1(r)$, as can be seen by differentiating with respect to ϵ. The constant vanishes as $\epsilon \to \infty$, so that Eq.(3.44) recovers Eq.(3.16). This also satisfies Eq.(3.7). In practice, a suitable choice of ϵ increases the convergence of the calculation. In condensed matter a jellium is always used to make the lattice neutral, but a more general term can be easily incorporated into this technique by including the appropriate Fourier

expansion in Φ_1.

The numerical potential generated by summing Eq.(3.44) over the lattice can be fit to a potential of the form given in Eq.(3.19)

$$\Phi^{(3)}(\mathbf{r}) = \frac{1}{4\pi r} + \frac{r^2}{6\mathcal{V}} + \frac{C_s^{(3)}}{\mathcal{V}^{\frac{1}{3}}} + A_4^{(3)} h_4^{(3)}(x_i) + A_6^{(3)} h_6^{(3)}(x_i) + \cdots$$

where the quadratic piece comes from the jellium, and the constant is related to the Madelung energy of the lattice. The data generated by the Ewald method can also be used to fit the potential near the antipodal point. We expect this expansion to be harmonic, except for the r^2 term. With coordinates now measured from the center of each cube, this is

$$\Phi_{antipodal}^{(3)}(\mathbf{z}) = \frac{C_a^{(3)}}{\mathcal{V}^{\frac{1}{3}}} + \frac{1}{6\mathcal{V}} \sum_{i=1}^{3} z_i^2 + B_4^{(3)} h_4^{(3)}(z_i) + B_6^{(3)} h_6^{(3)}(z_i) + \cdots$$

Of course, if the expression near the podal point is known exactly, Eq(3.45) can be obtained algebraically using $z_1 = x_1 - \frac{L}{2}$, etc. Generally, though, the higher order coefficients $A_{10}, A_{12}, \ldots$ will not be small, so it is best to use a numerical fit.

3.1.11 Four Dimensions

To implement the same procedure in dimensions other than three, we first need to choose a suitable form for $P(r)$. We will need the Laplacian in d dimensions:

$$\nabla^2 \varphi(r) = \frac{1}{r^{d-1}} \frac{\partial}{\partial r} \left[r^{d-1} \frac{\partial}{\partial r} \varphi \right] \tag{3.45}$$

The choice for $P(r)$ is guided by the behavior of Φ_1 and Φ_2 in the limits mentioned below Eq(3.44). In particular, each should converge at least faster than $\frac{1}{r^{d-2}}$ or $\frac{1}{k^{d-2}}$ since the number of points in the sums over the lattice grow as the $(d-1)$ power of r or k. Also, $\Phi_2(\mathbf{r})$ should reduce to the usual Coulomb potential as $r \rightarrow 0$. Taking

$\epsilon \to \infty$, which amounts to eliminating the added charge distributions, recovers Eq(3.16). In four dimensions, a simple choice is [36]:

$$\Phi_2^{(4)}(\mathbf{r}) = \frac{1}{4\pi^2} \sum_{\Delta r_j} \exp(-\epsilon^2 \Delta r_j^2) \left(\frac{1}{\Delta r_j^2} + a\epsilon^2 + b\epsilon^4 \Delta r_j^2 + ... \right) \tag{3.46}$$

The coefficients $(a, b, ..)$ can be adjusted to give a single term in the charge distribution $P(r) \propto r^n$. The choice of how many higher powers of r to include in the above equation is a matter of taste and simply changes n. Consider $a = \frac{1}{2}, b = 0$. Then

$$P^{(4)}(r) = \frac{\epsilon^6 r^2}{2\pi^2}$$

$$\Phi_1^{(4)}(\mathbf{r}) = \frac{1}{\mathcal{V}} \sum_{\mathbf{k}_j \neq 0} \frac{\exp(-k_j^2/4\epsilon^2) \exp(i\mathbf{k}_j \cdot \mathbf{r})}{k_j^2} \left(1 - \frac{k_j^2}{8\epsilon^2} \right)$$

$$\Phi^{(4)}(\mathbf{r}) = \Phi_1^{(4)}(\mathbf{r}) + \Phi_2^{(4)}(\mathbf{r}) - \frac{3}{8\mathcal{V}\epsilon^2}$$

The constant in the last expression above guarantees that Φ is independent of ϵ.

3.1.12 Two Dimensions

In 2 dimensions, a useful form for the real-space part is

$$\Phi_2^{(2)}(\mathbf{r}) = \frac{1}{2\pi} \sum_{\Delta r_j} \int_{\Delta r_j}^{\infty} \exp(-\epsilon^2 r'^2) \left(\frac{1}{r'} + a\epsilon^2 r' + b\epsilon^4 r'^3 + ... \right) dr' \tag{3.47}$$

To evaluate Φ_2 in the Ewald sum, note that some convenient expressions for the exponential integral are:

$$\int_t^{\infty} \frac{\exp(-u)}{u} du = -\gamma_E - \log(t) - \sum_{n=1}^{\infty} \frac{(-1)^n t^n}{n \cdot n!}$$

$$= \exp(-t) \frac{1}{1 + t - \frac{1}{3+t-\frac{4}{5+t-...}}}$$

For the simplest choice $a = b = 0$, we have

$$P^{(2)}(r) = \frac{\epsilon^2}{\pi}$$

$$\Phi_1^{(2)}(\mathbf{r}) = \frac{1}{\mathcal{V}} \sum_{\mathbf{k}_j \neq 0} \frac{\exp(-k_j^2/4\epsilon^2)\exp(i\mathbf{k}_j \cdot \mathbf{r})}{k_j^2}$$

$$\Phi^{(2)}(\mathbf{r}) = \Phi_1^{(2)}(\mathbf{r}) + \Phi_2^{(2)}(\mathbf{r}) - \frac{1}{4\mathcal{V}\epsilon^2}$$

Extending the techniques from the previous three sections, we now have a well-defined way to evaluate the potential numerically for general dimension, charge configuration, and metric.

3.2 Return of Cosmic Strings

An exciting feature of Brane Inflation is found in the dynamics of brane antibrane annihilation. As the branes approach each other, the open string modes stretched between them become lighter, and eventually tachyonic. The existence of this complex tachyon triggers the dissolution of the branes into lower dimensional degrees of freedom, most notably $D(p - 2)$ branes. Because of the large expansion rate, the tachyon must be uncorrelated over distances larger than the Hubble radius [41] (and possible much smaller). This guarantees the production of co-dimension two defects which must extend in the expanding (non-compact) directions at a density of at least one per Hubble volume. [3, 4]. Thus the question remaining is what impact, if any, these cosmic strings have on today's universe.

CHAPTER 4

THE ORIENTIFOLD FORMALISM

In order to find solutions to string theory which describe our universe, one must compactify the six extra dimensions in a way which does not conflict with particle phenomenology or cosmology. The simplest way to compactify would be toroidal, with six mutually orthogonal circles. The high degree of (holonomy) symmetry in such a compactification manifold would manifest itself as $D = 4, \mathcal{N} = 4$ supersymmetry, which is incompatible with the chiral standard model. Since chiral theories have at most $\mathcal{N} = 1$ SUSY, the task at hand is how to break most, but not all of the underlying ten dimensional supersymmetry. (Compactifications which preserve $\mathcal{N} = 1$ SUSY can have light fermions.) A powerful technique known as orbifolding is able to do just this. Geometrically, such a compactification can be thought of as a simple limit of some Calabi-Yau three-fold, albeit with singular points. Surprisingly, these singularities are completely smooth and well-behaved as a background on which strings can propagate. The string states which appear on these singularities parameterize the geometric moduli smoothly, and allow for continuous transitions between singular and non-singular versions of the geometry. An algebraic way to view such a background is as a projection onto invariant states and inclusion of new "twisted" sectors which live at, and smooth out the singularities. An attractive generalization of the orbifold construction would be to allow for D-branes and other objects to be introduced. Simply adding them by hand is not guaranteed to be a consistent solution of string theory, and will generically introduce anomalies. An alternative which guarantees wold sheet consistency is the orientifold construction. This is mathematically very similar to orbifold constructions, but projects and twists more general world-sheet symmetries. While this

48

is very powerful as a model building tool and can generate semi-realistic versions of the standard model, we would like to take it one step further by introducing anti-branes. By choosing a model with stacks of branes and anti-branes separated in the compact directions, we can realize brane inflation in a realistic context. The orientifold formalism is naturally able to generate string backgrounds which are consistent, phenomenologically interesting, and possess an inflationary era which ends with brane annihilation.

4.1 Discrete Symmetries

The GSO projection of the type II string theories may be thought of as *gauging* the discreet symmetry $(-1)^F$ where F is the world-sheet fermion number. Gauging, in this sense refers to two actions: a projections onto invariant states, and (to preserve modular invariance) adding new "twisted" (Ramond) sectors whereby states are only required to be single valued modulo the action of $(-1)^F$. Thus, the modular invariant superstring theories come in $0A/B$ and IIA/B varieties depending whether odd/even states are kept, and whether the left and right moving sectors are given the same/opposite GSO projection [42]. This practice of projecting and twisting can be used with any world-sheet symmetry, including spacetime isometries (toroidal compactification, orbifolding) and world-sheet parity (orientifolding). The most general orientifolds [43–46] combine spacetime and world-sheet (e.g. Ω) symmetries. The consistency of orientifolds always guarantees both tadpole and anomaly cancellation. Tadpole cancellation is accomplished through a balancing of the number of D-Branes with the orientifold planes present. Orientifold planes are non-dynamical *negative tension* charged branes which cancel the R-R and (often) NS-NS tadpoles from D-Branes. Consistency still allows for

non-vanishing NS-NS tadpoles. The field content of many orientifold models can often be uniquely fixed by anomaly cancellation. For six dimensional supersymmetric theories, the field content must obey

$$n_H - n_V = 244 - 29 n_T \tag{4.1}$$

where n_H, n_V, and $n_T + 1$ correspond to the number of hypermultiplets, vector-multiplets, and tensormultiplets in the $D = 6 \, \mathcal{N} = 1$ supergravity [47]. Of course, a four dimensional compactification is also required to have no six-dimensional (or ten-dimensional, for that matter) gravitational anomaly, but this consistency condition is not manifest in four dimensional calculations. For this reason, four dimensional orientifolds often require more careful consistency checks.

We interpret twisting by Ω as identical to the open string doubling trick [48]. Hence Ω-twisting, while not related to modular invariance, introduces open strings for the world-sheet consistency of the theory.

4.2   Application to Brane Inflation

Sugimoto [49] generalized the supersymmetric orientifold by adding $D\bar{D}$ pairs to the simplest type IIB orientifold. This has several interesting effects. The gauge content is enlarged due to the existence of new open string sectors, and supersymmetry is broken via the large cosmological constant $2n_9\tau_9$. In effect, this can be thought of adding $D9\bar{D}9$ pairs to the ten dimensional type I theory. No inflaton field is present in this theory, but a similar construction can be done with more general IIB orientifold compactifications involving D5 or D3 branes. In this case, a consistent compactification can give rise to both a realization of brane inflation, and reduce to a phenomenologically interesting vacuum afterward.

Below, we consider two D5-Branes at two angles. If the angles are the same, the two D5-Branes are BPS with respect to each other. This is the case in conventional orientifold models like $T^6/\mathbb{Z}_3$, $T^6/\mathbb{Z}_4$, $T^6/\mathbb{Z}_6$, and $T^6/\mathbb{Z}_{12}$ [50]. These models have a single Kähler modulus. However $T^6/\mathbb{Z}_2$ has more than one Kähler modulus. By varying them, an attractive potential between the angled D5-branes appears. In the construction below, the angles between D-branes will be equal and *opposite*, producing an attractive force which can be tuned with the Kähler moduli.

4.3 Model

We construct a model by compactifying the Type I theory on T^6. We choose all tori to be orthogonal and all radii to be equal. This is motivated by our desire to lift this model to an orientifold, such as type IIB modulo $\mathbb{Z}_2$ and/or $\mathbb{Z}_3$ groups [47]. We include $5_1 - \bar{5}_1$ pairs [49]. The subscript signifies the chosen orientation of wrapping the 4-5 plane (the first of three tori). We calculate the partition function for this model in section 4.10, including the generalization to arbitrary additional $5 - \bar{5}$ and $9 - \bar{9}$ pairs. The added five branes are co-dimension four objects in the nine branes and as such contribute bi-fundamental $\mathcal{N} = 2$ hyper multiplets to our 4-D theory. In section 4.5 we include the generalized Gimon-Polchinski spectrum, although for simplicity we will focus on the non-orbifolded theory described above.

4.4 The Massless Spectrum

The gauge group is

$$SO(32 + n_{\bar{9}}) \times SO(n_{\bar{9}}) \times U(n_5) \times U(n_5). \tag{4.2}$$

We expect the $9 - 9$ sector to produce a $(D = 4)$ $\mathcal{N} = 4$ VSF and the $5 - 5$ and $\bar{5} - \bar{5}$ sectors to each produce $\mathcal{N} = 2$ $VSFs$.

Following Sugimoto, we find that the $\bar{9} - \bar{9}$ sector yields fermions in the symmetric representation. In four dimensions this corresponds to a pair of Dirac fermions. The $9 - \bar{9}$ sector, in addition to the bifundamental tachyon, has massless fermions. Counting degrees of freedom yields four Dirac fermions in the bifundamental. This is the case for the $5 - \bar{5}$ sector, as well.

The $9 - 5$, $9 - \bar{5}$, $\bar{9} - 5$ and $\bar{9} - \bar{5}$ sectors each produce $\mathcal{N} = 2$ hypermultiplets (in the bi-fundamental representation). The spectrum of this model is illustrated in Table 4.1.

Table 4.1: Massless fermion multiplets in the modified Type I

$$SO(32 + n_{\bar{9}}) \times SO(n_{\bar{9}}) \times U(n_5) \times U(n_5)$$

(Adj., 1, 1, 1)	$\mathcal{N} = 4$ VSF	
(1,1,Adj., 1)	$\mathcal{N} = 2$ VSF	
(1,$\boxplus$, 1, 1)	$\mathcal{N} = 0$ fermion	
($\underline{1,\square,1,\bar{\square}}$)	$\mathcal{N} = 2$ Hyp. Mult.	
($\square$, $\square$, 1, 1)	$\mathcal{N} = 0$ fermion	4 Dirac
(1, 1, $\square$, $\square$)	$\mathcal{N} = 0$ fermion	4 Dirac

4.5 Gimon Polchinski with $5_2 - \bar{5}_2$ pairs

Now we consider adding 5-branes to the $\mathbb{R}^4 \times T^2 \times T^4/\mathbb{Z}_2$ Orientifold of Gimon and Polchinski. We place the branes perpendicular to the orientifold 5-planes. The orientation is given in Table 4.2

Table 4.2: New 5-branes

$X^\mu =$	2	3	4	5	6	7	8	9
Original 9	x	x	x	x	x	x	x	x
Original 5	x	x	x	x				
New $5 - \bar{5}$	x	x			x	x		

The new gauge group is $U(16) \times U(16) \times U(n_5) \times U(n_5)$. With the exception of the $5 - \bar{5}$ sector, the six dimensional supersymmetry imposes $D = 4, \mathcal{N} = 2$ SUSY on the entire spectrum, summarized in Table 4.3.

Table 4.3: Massless fermion multiplets in the modified $T^2 \times T^4/\mathbb{Z}_2$

$$U(16) \times U(16) \times U(n_5) \times U(n_5)$$

(Adj., 1, 1, 1)	$\mathcal{N} = 2$ VSF
$2(\boxminus, 1, 1, 1)$	$\mathcal{N} = 2$ Hyp. Mult.
$(\square, \square\ 1, 1)$	$\mathcal{N} = 2$ Hyp. Mult.
$(\square, 1, \square, 1)$	$\mathcal{N} = 2$ Hyp. Mult.
$(1, 1, \square, \square)$	$\mathcal{N} = 0$

4.6 Configuration

The non-orientifold configuration described above may be T_{4589} dualized to leave 5-branes in the 0123 and 67 or 89 directions as can be seen in Table 4.4.

We thus have 16 D5-Branes and 16 O5 planes in the (0123 and) 67 directions and n_5 D5 and $D\bar{5}$-Brane pairs in the 89 directions. In the 45 plane (T_1^2) we see

Table 4.4: Making orthogonal 5-branes

$X^\mu =$	2	3	4	5	6	7	8	9
9	x	x	x	x	x	x	x	x
$5 - \bar{5}$	x	x	x	x	.	.	.	.
T_{4589}-Dual	↓	↓	↓	↓	↓	↓	↓	↓
New 5	x	x	.	.	x	x	.	.
New $5 - \bar{5}$	x	x	.	.	.	.	x	x

two stacks of branes, namely the $D5_3$ and $D\bar{5}_3$ stacks. The original 16 $D5_2$ are divided among these two locations as well, and the interstack separation y_I will be the inflaton. For simplicity we may take there to be only a single $D5_3 - D\bar{5}_3$ pair. Now we split-join the $D\bar{5}_3$ with one of the original 5-Branes, and do the same with the partner $D5_3$ and an original 5-brane. This is illustrated in Figure 4.1. Topologically, the new "joined" 5-branes go from being $\mathbb{R}^4 \times T^2$ to $\mathbb{R}^4 \times T_2$ where T_2 is the genus two Riemann surface. The appearance of T_2 may be seen as the unique way to split-join two stable tori which intersect transversally at a single point. Consequently, the new D5-branes cannot be everywhere Ricci flat. It is interesting to note that the pairs we have joined were BPS with respect to each other, being orthogonal in both the 68 and 79 planes. This process thus corresponds to motion along a flat direction of moduli space. After split-joining, the two genus-two Riemann surfaces are not BPS since the two angles between them are *opposite*. One key feature in this construction is the equal (but opposite) footing between the 68-plane and 79-plane. As can be seen in the illustration below, the new 5-branes (which are still separated in T_1^2 by a distance y_I) will feel a strong force between each (other unless the Kähler moduli are fine-tuned), since the angle
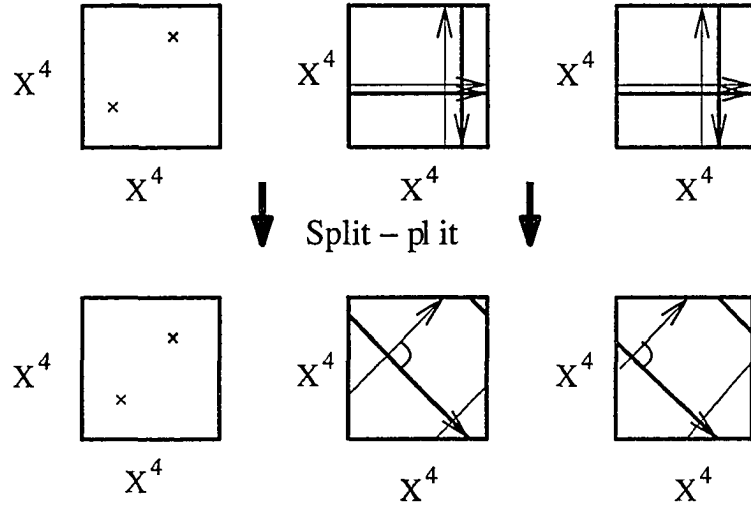
Figure 4.1: Creating our branes at angles from orthogonal D5 pairs: Line thickness is indicative of location in 4-5 plane.

between the branes in the 68-plane is opposite to that in the 79-plane. In other words, we have taken a $D\bar{D}$ configuration to a branes-at-angles configuration. By modifying the appropriate Kähler moduli, we can tune the angles to be arbitrarily small (but still opposite). On the other hand, we could introduce BPS 5-branes (and additional O5 planes) to create branes at equal (not opposite) angles.

4.7 Branes at Angles and BPS Intersections

A striking result in string theory is the preservation of half of the remaining supersymmetry (i.e. eight supercharges) when two D4-branes are rotated with respect to each other by an SU(2) rotation. [42]. Albeit with fewer available parameters, this result applies to D5-branes. Such is the case when the only two non-zero relative angles are equal. This implies that the inter-brane potential is equal to a constant. Such a 'branes at angles' inflation scenario is not new [40]. Not surprisingly, the zero force result applies to the low energy effective action, as well. Because we build our model out of a brane anti-brane scenario, it is not surprising that the

angles produced in Figure 4.1 are not BPS.

4.8 Classical Action

Let us calculate the interaction potential between two Dp branes oriented at angles θ_1 and θ_2 in two 2-planes. The positions of the branes are described by the coordinates:

$$\left\{ \begin{array}{ll} X^\mu = \xi^\mu & \mu \leq p \\ X^\mu = 0 & \mu > p \end{array} \right. \quad \left\{ \begin{array}{ll} X^\mu = \xi^\mu & \mu \leq p \\ X^{p-1} = \xi^{p-1} \cos \theta_1 \\ X^p = \xi^p \cos \theta_2 \\ X^{p+1} = \xi^{p-1} \sin \theta_1 \\ X^{p+2} = \xi^p \sin \theta_2 \\ X^I = y^I (\xi^\mu) & I \geq p+3 \end{array} \right. \tag{4.3}$$

The background generated by one brane is (in the string frame):

$$ds^2_{string} = H_p^{-\frac{1}{2}} (x_\perp) \, ds^2_{p+1} + H_p^{\frac{1}{2}} (x_\perp) \, ds^2_\perp$$

$$e^{-\phi} = H_p^{\frac{3-p}{4}} (x_\perp)$$

$$A_{0\cdots p} = 1 - H_p^{-1} (x_\perp)$$

In the probe brane approximation we use the string-frame BI + WZ actions for one brane in the background created by the other brane. The action is:

$$S_p = S_{BI} + S_{WZ}$$

$$S_{BI} = -T_p \int d^{p+1}\xi \, e^{-\phi} \sqrt{-\det \left(G_{MN} (X) \, \partial_\mu X^M \partial_\nu X^N \right)}$$

$$S_{WZ} = -T_p \int A_p$$

We proceed to calculate the pull-back of the $p + 1$ form field in the world-volume of the second brane. The field is given by: $A_p = A_{0\cdots p} dX^0 \wedge \cdots \wedge dX^p$ such that

S_{WZ} becomes:

$$S_{WZ} = -T_p \int A_{0\cdots p} J\left(\frac{X^0,\cdots,X^p}{\xi^0,\cdots,\xi^p}\right) d\xi^0 \wedge \cdots \wedge d\xi^p =$$

$$-T_p \cos\theta_1 \cos\theta_2 \int d^{p-1}X d\xi^{p-1} d\xi^p \left(1 - H_p^{-1}(x_\perp)\right)$$

We now calculate the pull-back of the metric in the probe brane worldvolume. We use the indices i,j if $\mu,\nu \le p-1$.

$$g_{ij} = G_{IJ}\partial_i y^I(\xi^\mu)\partial_j y^J(\xi^\mu) = H_p^{-\frac{1}{2}}\left(\eta_{ij} + H_p\partial_i y^I(\xi^\mu)\partial_j y_I(\xi^\mu)\right)$$

$$g_{p-1,p-1} = G_{p-1,p-1}\left(\frac{\partial X^{p-1}}{\partial\xi^{p-1}}\right)^2 + G_{p+1,p+1}\left(\frac{\partial X^{p+1}}{\partial\xi^{p-1}}\right)^2$$

$$= H_p^{-\frac{1}{2}}\left[\cos^2\theta_1 + H_p\sin^2\theta_1\right]$$

$$g_{p,p} = G_{p,p}\left(\frac{\partial X^p}{\partial\xi^p}\right)^2 + G_{p+1,p+1}\left(\frac{\partial X^{p+2}}{\partial\xi^p}\right)^2 = H_p^{-\frac{1}{2}}\left[\cos^2\theta_2 + H_p\sin^2\theta_2\right]$$

$$g_{p-1,p} = 0$$

Using these results in the expression for the BI action we obtain:

$$S_{BI} = -T_p \int d^{p-1}X d\xi^{p-1} d\xi^p H_p^{\frac{p-3}{4}} \cos\theta_1 \cos\theta_2 \sqrt{1 + H_p\tan^2\theta_1} \times$$

$$\sqrt{1 + H_p\tan^2\theta_2} \times H_p^{-\frac{1+p}{4}} \sqrt{-\det\left(\eta_{ij} + \partial_i y^I(\xi^\mu)\partial_j y_I(\xi^\mu)\right)}$$

The distance between the branes now depends on the position along the brane:

$$x_\perp^2 = X_{p-1}^2 + \xi^{p-1}\sin^2\theta_1 + \xi^p\sin^2\theta_2 \tag{4.4}$$

If we choose the two angles to be equal, $\theta_1 = \theta_2 = \theta$ and assume the branes to be straight and not moving, $\partial_i y_I(\xi^\mu) = 0$, we obtain:

$$S_{BI} + S_{WZ} = -T_p\cos^2\theta \int d^{p-1}X d\xi^{p-1} d\xi^p \left[\frac{H_p-1}{H_p} + \frac{1+H_p\tan^2\theta}{H_p}\right]$$

$$= -T_p \int d^{p+1}\xi$$

which is completely independent of the separation between the branes. The interaction force is zero, in accord with the string theory calculation. Since no cosmological constant is present, no inflation can take place in such a scenario.

4.9 F-Theory Connections

F-theory is a non-perturbative generalization of the Type IIB string theory and its orientifold descendants. Specifically, F-theory accurately describes the orientifold theories even when their moduli are taken outside of the perturbative region in which the orientifold is defined [51]. (Example: Up to T-duality, orientifold planes on which no D-branes sit are seen to be bound states of four (p,q) sevenbranes [52].) For this reason, F-theory is a bridge between otherwise disconnected perturbative IIB orientifolds.

Our model has been constructed to easily mature to the Gimon-Polchinski orientifold [46]. There are in fact many six dimensional orientifold models, all of which represent different limits of the K3 (D-)manifold. It can be shown that K3 is the unique Calabi-Yau 2-fold which permits compactification of $D = 10$ $\mathcal{N} = 1 \rightarrow D = 6 \, \mathcal{N} = 1$ models. All of these K3 orientifolds are conjectured to be different D-manifold limits of F-theory on an elliptically fibered $\mathbb{C}P^1 \times \mathbb{C}P^1$ [53]. In a sense, this bridges two six dimensional theories which resemble our model, namely $T^4/\mathbb{Z}_2$ and $T^4/\mathbb{Z}_3$. The $\mathbb{Z}_3$ model is a natural place in moduli space for our theory to grow all of its compact radii to be of equal size. This is evident when one tries to impose a $\mathbb{Z}_3$ global $\rightarrow$ gauged symmetry on a (spacetime) torus. The $\mathbb{C}/(\mathbb{Z} \oplus \tau\mathbb{Z})$ identification is compatible with the $\mathbb{Z}_3$ identification only for $\tau = e^{i\pi/3}$. When we look at the $\mathbb{Z}_2$ model, we notice no such restriction, i.e. $\tau = e^{i\pi/2}$ is only one point on a moduli space $Im[\tau] \in [1, \infty)$. In fact it is logical

that the $\mathbb{Z}_2$ model has more (all 80) gravitational moduli available to it, since the GP spectrum comes with twenty additional neutral hypermultiplets, each with four real scalar degrees of freedom.

4.10 The Partition Function

Our partition function may be broken up into four topologies T^2, K_2, M_2, and C_2. The 5-brane sector will only contribute to C_2, whereas additional $9\bar{9}$ pairs contribute to both M_2 and C_2. Each topology can be factored into a bosonic and a fermionic part.

$$Z = Z_{T^2} + Z_{K_2} + Z_{C_2} + Z_{M_2}$$

$$Z_\mathcal{M} = Z_\mathcal{M}^X Z_\mathcal{M}^\psi$$

For simplicity, we assume the compactified tori to be orthogonal, and that all are of radius R. Compactification has two effects, namely a discretization of momentum and additional nontrivial winding sectors. Then

$$Z_{T^2} = \frac{1}{2} \int_{F_0} \frac{d^2\tau}{4\pi^2\tau_2} iV_4 (2\pi R)^6 (\eta\bar{\eta}(\tau))^{-8} (4\pi^2\tau_2\alpha')^{-5} \left(\sum_{m,n\in Z} e^{-\frac{\pi R^2}{\tau_2\alpha'}|m+n\tau|^2} \right)^6 Z_{T^2}^\psi(\tau)$$

$$(4.5)$$

The initial factor of $\frac{1}{2}$ is due to the Ω-projection. The Klein Bottle is a trace over states with identical left and right moving quantum numbers and thus has no winding states:

$$Z_{K_2} = \frac{1}{2} \int_0^\infty \frac{dt}{2\pi t} iV_4 (2\pi R)^6 (\eta(2it))^{-8} (4\pi^2 t\alpha')^{-5} \left(\sum_{m\in Z} e^{-\frac{\pi R^2}{t\alpha'}m^2} \right)^6 Z_{K_2}^\psi(2it) \quad (4.6)$$

The Cylinder may be broken into terms coming from all pairings of $\{9, \bar{9}, 5, \bar{5}\}$. We orient all 5-branes to wrap the 8th and 9th dimensions only. A simple prescription for determining the contribution from $D\bar{D}$ cylinders is to perform an opposite

GSO projection (i.e. flip the sign of the R-R exchange). As can be seen below, the

bosonic modes are only trivially modified in $D\bar{D}$ cylinders.

$$Z_{C_2}^{9-9} = \frac{n_9^2}{2} \int_0^\infty \frac{dt}{2\pi t} i V_4 (2\pi R)^6 \eta(it)^{-8} (8\pi^2 \alpha' t)^{-5} \left(\sum_{m \in Z} e^{-\frac{\pi R^2 m^2}{2t\alpha'}} \right)^6 Z_{C_2}^\psi(it)$$

$$Z_{C_2}^{\bar{9}-\bar{9}} = \frac{n_{\bar{9}}^2}{2} \int_0^\infty \frac{dt}{2\pi t} i V_4 (2\pi R)^6 \eta(it)^{-8} (8\pi^2 \alpha' t)^{-5} \left(\sum_{m \in Z} e^{-\frac{\pi R^2 m^2}{2t\alpha'}} \right)^6 Z_{C_2}^\psi$$

$$Z_{C_2}^{9-\bar{9}} = \frac{2 n_9 n_{\bar{9}}}{2} \int_0^\infty \frac{dt}{2\pi t} i V_4 (2\pi R)^6 \eta(it)^{-8} (8\pi^2 \alpha' t)^{-5} \left(\sum_{m \in Z} e^{-\frac{\pi R^2 m^2}{2t\alpha'}} \right)^6 Z_{C_2}^{\psi 9-\bar{9}}$$

$$Z_{C_2}^{5-5} = n_5^2 \int_0^\infty \frac{dt}{2\pi t} i V_4 (2\pi R)^2 \eta(it)^{-8} (8\pi^2 \alpha' t)^{-3} \sum_{\tilde{m} \in Z^2, \tilde{n} \in Z^4} e^{-\frac{\pi R^2 \tilde{m}^2}{2t\alpha'} - \frac{t 4\pi^2 R^2 \tilde{n}^2}{2\pi\alpha'}} Z_{C_2}^{\psi 5-5}$$

$$Z_{C_2}^{\bar{5}-\bar{5}} = n_{\bar{5}}^2 \int_0^\infty \frac{dt}{2\pi t} i V_4 (2\pi R)^2 \eta(it)^{-8} (8\pi^2 \alpha' t)^{-3} \sum_{\tilde{m} \in Z^2, \tilde{n} \in Z^4} e^{-\frac{\pi R^2 \tilde{m}^2}{2t\alpha'} - \frac{t 4\pi^2 R^2 \tilde{n}^2}{2\pi\alpha'}} Z_{C_2}^{\psi \bar{5}-\bar{5}}$$

$$Z_{C_2}^{5-\bar{5}} = 2 n_5 n_{\bar{5}} \int_0^\infty \frac{dt}{2\pi t} i V_4 (2\pi R)^2 \eta(it)^{-8} (8\pi^2 \alpha' t)^{-3} \sum_{\tilde{m} \in Z^2, \tilde{n} \in Z^4} e^{-\frac{\pi R^2 \tilde{m}^2}{2t\alpha'} - \frac{t 4\pi^2 R^2 \tilde{n}^2}{2\pi\alpha'}} Z_{C_2}^{\psi 5-\bar{5}}$$

As expected, the 5-Branes display V_4 from the non-compact integration, and

$4\pi^2 R^2$ from the two Neumann directions of discrete momentum. The four Dirich-

let directions allow winding sectors, and no momentum. The 9-5 cylinders will

have four Neumann-Dirichlet directions, which are half-odd-integer moded. The

corresponding Ramond fermions must then be half-odd-integer moded, and the NS

fermions integer moded.

$$Z_{C_2}^{9-5} = 2 n_9 n_5 \int_0^\infty \frac{dt}{2\pi t} i V_4 (2\pi R)^2 \eta(it)^{-4} (8\pi^2 \alpha' t)^{-3} \left(\sum_{m \in Z} e^{-\frac{\pi R^2 m^2}{2t\alpha'}} \right)^2 Z_1^0(it)^{-2} Z_{C_2}^{\psi 9-5}$$

$$(4.7)$$

Because a 5-brane and a $\bar{5}$-brane are identical when embedded in a 9-brane,

the $9 - \bar{5}$, $\bar{9} - 5$, and $\bar{9} - \bar{5}$ cylinders differ only by the combinatoric coefficient.

Since the 5-Branes we are inserting into the Type I theory are Ω-invariant, they

make no contribution to the Möbius Strip vacuum amplitude. A prescription for

$Z_{M_2\bar{9}}$ is simply to flip the sign of the R-R contribution (i.e. opposite Ω-projection

in the R-R sector).

$$Z^9_{M_2} = \frac{n_9}{2} \int_0^\infty \frac{dt}{2\pi t} iV_4(2\pi R)^6 \eta(2it)^{-8} Z^0_0(2it)^{-4}(8\pi^2\alpha't)^{-5} \left(\sum_{m\in Z} e^{-\frac{\pi R^2 m^2}{2t\alpha'}}\right)^6 Z^{\psi 9}_{M_2}$$

$$Z^{\bar{9}}_{M_2} = \frac{n_{\bar{9}}}{2} \int_0^\infty \frac{dt}{2\pi t} iV_4(2\pi R)^6 \eta(2it)^{-8} Z^0_0(2it)^{-4}(8\pi^2\alpha't)^{-5} \left(\sum_{m\in Z} e^{-\frac{\pi R^2 m^2}{2t\alpha'}}\right)^6 Z^{\psi\bar{9}}_{M_2}$$

The explicit fermionic contributions are based on the Jacobi θ and Dedekind η functions via

$$Z^\alpha_\beta(\tau) = \frac{1}{\eta(\tau)}\theta[{\alpha/2 \atop \beta/2}](0,\tau) \tag{4.8}$$

$$Z^\psi(\tau) = \frac{1}{2}[Z^0_0(\tau)^4 - Z^0_1(\tau)^4 - Z^1_0(\tau)^4 - Z^1_1(\tau)^4] \tag{4.9}$$

Then

$$Z^\psi_{T^2}(\tau) = \mid Z^\psi(\tau) \mid^2$$

$$Z^\psi_{K_2}(2it) = Z^\psi(2it)$$

$$Z^\psi_{C_{2p-p}}(it) = Z^\psi(it)$$

$$Z^\psi_{C_{2p-\bar{p}}}(it) = \frac{1}{2}[Z^0_0(it)^4 + Z^0_1(it)^4 - Z^1_0(it)^4 + Z^1_1(it)^4]$$

Notice that the signs of the $\beta = 1$ terms (R-R exchange) has been flipped in the $p-\bar{p}$ term. The dimensionality of the Dp-Branes does not affect $Z^\psi_{C_{2p-p}}$ since Dirichlet-Dirichlet strings are moded like Neumann-Neumann strings with no momentum. Finally,

$$Z^\psi_{M_2} = \frac{(1_{RR} - 1_{NSNS})}{2}[Z^0_1(2it)^4 Z^1_0(2it)^4] \tag{4.10}$$

For the 9-5 cylinder, we take the fermionic partition function for four dimensions to be the usual Z^ψ terms for four dimensions, and then flip the spacial periodicity for the four Neumann-Dirichlet directions (i.e. $\alpha \to \alpha + 1(\mathrm{mod}\ 2)$).

$$Z^\psi_{C_{29-5}}(it) = \frac{1}{2}[Z^0_0(it)^2 Z^1_0(it)^2 - Z^0_1(it)^2 Z^1_1(it)^2 - Z^1_0(it)^2 Z^0_0(it)^2 - Z^1_1(it)^2 Z^0_1(it)^2]$$

$$\tag{4.11}$$

Notice that both the NS-NS (first and third) term and R-R (second and fourth) term are each separately zero. This means that the net R-R tadpole is unaffected by the 9-5 sector. If we use the Poisson resummation formula and modular transformation properties of the partition function, we can deduce the vanishing R-R tadpole conditions:

$$n_9 = 32 + n_{\bar{9}}$$

$$n_5 = n_{\bar{5}}$$

4.11 Summary

We have used a toy model to demonstrate how the orientifold construction can be used to realize brane inflation. Key features of these orientifolds are encoded in the partition function, which determines both the vacuum energy (inflationary potential) and consistency of the model. The massless spectrum and gauge group structure reveal consistency through the vanishing of gravitational and non-abelian anomalies. The existence of stable defects is determined by K-theoretic analysis of the gauge symmetry breaking, and (seemingly) anomalous $U(1)$ symmetries (cancelled by the Green-Schwartz mechanism) give cosmic string candidates in four dimensions. To decipher the gauge symmetry breaking, one simply sets $n_{\bar{9}}$ and $n_{\bar{5}}$ to zero everywhere.

A more realistic attempt to realize brane inflation would include moduli stabilization, as in the KKLMMT scenario of flux compactification. The presence of fluxes is also favorable due to the generic warping they induce. Since worldsheet calculations are extremely difficult in these more complicated backgrounds,

attempts to build the standard model (or its extension to SUSY GUTs) are quite limited. This is not disastrous for brane inflation (which benefits dramatically from warping), since much progress can be made using both low-energy supergravity and the AdS/CFT correspondence.

CHAPTER 5

COSMIC STRINGS

5.1 Dynamics and Description

The simplest cosmic strings is described by the Nambu-Goto action

$$S_{NG} = -\mu \int_{\mathcal{M}^2} \sqrt{-|g|}. \tag{5.1}$$

This string has no structure or thickness, and is characterized entirely by it's tension μ and embedding. The Polyakov action, used to quantize the Bosonic string is a slight improvement because it carries an independent world sheet metric, whose equations of motion equate it with the pull back metric used in S_{NG}, *provided this pull back is non-singular*. Although this is almost never the case, it can be arranged e.g. by a rectangular loop initially at rest. For such a string loop, the corners eventually will contain a finite amount of energy despite being points. This means that the stress-tensor cannot be completely specified by the embedding, and thus represents a failure of S_{NG}. The independent world sheet metric can represent this missing degree of freedom, much in the same way a massless point particle cannot be completely described by it's embedding, but rather needs an independent world-line metric to characterize its energy [48]. The equations of motion for a Nambu (or Polyakov) string in flat space is

$$\ddot{\mathbf{x}}(\sigma, t) - \mathbf{x}''(\sigma, t) = 0 \tag{5.2}$$

in a gauge where $\dot{\mathbf{x}} \cdot \mathbf{x}' = 0$ and $\dot{x}^2 + x'^2 = 1$.

The general solution for a cosmic string loop can be obtained formally, c.f. Eq.(6.17), although inverse functions are used. For strings in an FRW spacetime, see [54,55].

In field theory, the simplest cosmic string is given by the Abelian Higgs model. Abelian Higgs strings are topologically stable, and the arguments for this may be carried over to certain string theoretic cosmic strings [56]. However, it is possible to destabilize these vortices by expanding the field content via the introduction of magnetic monopoles. For example, if a symmetry is sequentially broken via: $SU(2) \to U(1) \to \emptyset$, monopoles are produced under the first breaking, and strings under the second. But since $\pi_1(SU(2)) = 0 = \pi_2(SU(2))$ no topologically stable strings or monopoles exist. Instead, meta-stable strings can break by monopole pair nucleation. The topological stability then becomes only a dynamical (meta)stability. Polchinski has conjectured [57] that all cosmic strings in string theory are topologically stable if and only if an Aharanov-Bohm phase exists for some (otherwise neutral) particle which can be scattered off the string. This is motivated by the fact that string theories seem to saturate the Dirac quantization condition. It is easy to show that a non-trivial Aharanov-Bohm phase indicates that string breakage would violate the Dirac quantization condition. Several instabilities seem to plague stringy cosmic strings. The first, pointed out by Witten [58] assumed that cosmic strings were fundamental strings. In the type I background, an F-string is not BPS. Such a string lacks a two-form field (electrically sourced by strings) and is thus unstable to breakage. If such a source did exist, then in four dimensions this field would be associated with a massless axion via Hodge duality: $d\phi = *_4 dB_2$. It is well known that any axion not protected by a symmetry must develops a potential from instanton effects. This would force all BPS cosmic strings to bound domain walls, whose tension would prevent any long-lived cosmic strings. While this seems to rule out cosmic strings, a third mechanism [56,59,60] is able skirt both issues. If the classically massless axion is "eaten" by a gauge field, it is

protected (by gauge invariance) from non-perturbative corrections. At the same time, the existence of an axion gives the string a conserved charge (flux) which forbids breakage except on monopoles of the same charge as the flux contained within the string. The breakage rate per unit length per unit time would be exponentially suppressed by the monopole mass via the factor $e^{-\pi m^2/\mu}$. It is easy to find models where this renders strings stable over cosmological length and time scales. From a stringy perspective, the various $U(1)$s of some six-dimensional compactification can be Higgsed via the four dimensional Green-Schwartz mechanism. This means that a stringy cosmic string parallel to the non-compact directions will appear as an abelian Higgs-like vortex. Monopole-antimonople formation can occur when the string breaks on D-branes or orientifold planes. If stringy monopoles are sufficiently massive, stringy cosmic strings produced via brane-antibrane annihilation will survive as long-lived cosmic strings in the Brane World.

5.1.1 History

Cosmic strings have drawn interest for many years, and are cosmologically relevant for a variety of reasons. The attention given to them throughout the past two decades was based on the prospect that cosmic strings formed in the early universe during a second order phase transition (like GUT symmetry breaking) could be responsible for the density perturbations leading to large scale structure seen in the universe today [41]. This has been successfully ruled out by observations of the CMB, which strongly support inflation as the seed of structure formation. But string theoretic investigations of inflation lead again to the rise of cosmic strings, this time in the form of much lower tension strings which are left behind at the end of inflation [3,4]. This is due to the most successful model of inflation within

string theory: Brane Inflation [2]. A generic prediction of Brane Inflation is that cosmic strings are left behind after the phase transition which triggers the end of inflation. In a wide variety of models these cosmic strings are predicted to be soft enough to avoid conflict with current cosmological observations, and yet are not so soft as to be out of reach of near future cosmological experiments. Because of this, string cosmology has become the most likely field to find empirical evidence in favor of string theory.

Brane Inflation is attractive because it has a natural place in the most elegant and simple model of our universe in string theory: The Brane World. The Brane World scenario describes the Standard Model of particle physics living on a stack of fundamental objects in string theory called D-Branes. The ten dimensions of string theory are compactified on four large dimensions (our universe) with the remaining six very small (giving rise to internal degrees of freedom). Dp-Branes are $(p + 1)$ dimensional membranes spanning our four large dimensions, and are carriers of all charged particles in string theory (open strings), while closed strings (gravitons) are free to propagate throughout the bulk. The bulk volume, which in many models is highly warped by RR fluxes, dilutes the strength of gravitational interaction and determines the relationship between the fundamental (string) scale, the Planck scale, and the electroweak scale. The simplest Brane World scenario involves a stack of D3-Branes (3+1 dimensional planes localized at points in the six-dimensional bulk) on which the $SU(3) \times SU(2) \times U(1)$ standard model lives. Inflation is realized by including a D3 anti D3 pair (anti D-Branes have negative charge, but positive tension) separated a distance away in the six-dimensional extra dimensions. The (internal) distance between the standard model and the anti-D3 is the 4-D inflaton field, and its potential is generated by the attraction between D3

and anti-D3 Branes. The universe inflates while the branes approach each other, and when the separation becomes of order the string length, the open strings connecting the D3 and anti-D3 become tachyonic. This (complex) tachyon rolls to its minimum, annihilating the anti-D3 and one D3. Because regions that are separated by distances larger than the Hubble length are uncorrelated, the complex tachyon will necessarily form co-dimension two defects in our universe with an initial number density greater than or equal to one per Hubble volume. The fact that the defect is co-dimension two is guaranteed by the complex tachyon vacuum manifold (S^1). The Hubble length argument (Kibble mechanism) guarantees that the defect is extended in our universe.

The energy of annihilation of the D-Branes leads to a hot big bang, and a radiation dominated universe containing cosmic strings. Because cosmic strings are linearly extended, their number density should naively scale like $1/a^2$, which would lead them to dominate the universe very quickly. However, because cosmic strings are two dimensional objects propagating in effectively four dimensions, one can show that they will generically intersect. When two string segments intersect, a topology change can occur in order to minimize the cosmic string length. This nonzero intercommutation probability causes the cosmic string network to break off loops which loose energy to gravitational radiation. Like all radiation, this scales as $1/a^4$. As expected, the rate of cosmic string intercommutation depends on the density of strings, the expansion rate, and the probability of nontrivial interaction. These factors combine in a remarkable way, leading to the so called scaling solution of cosmic strings [9]. It is a generic feature of cosmic string networks and the simplest simulations lead to a predicted number density of approximately ten or twenty long strings per Hubble volume, along with many small loops [61].

In string theory, the aforementioned cosmic strings are fundamental objects (D1-branes or F-strings), although the field theory description of these is very much akin to the well known abelian Higgs model. String theory is not the only theory to predict cosmic strings, and the features that distinguish competing theories are worth studying. The most striking feature of string theory cosmic strings is the possibility of multi-tension networks formed by three way junctions of so-called (p,q) strings whose spectrum of tensions is rich and model dependent [62]. Field theory cosmic strings would generically not bind into such networks, and the intercommutation probability cannot be less than one in four dimensional field theories such as Abelian Higgs under normal conditions [12,17].

5.1.2   General Relativity and Cosmic Strings

The most direct detection of a cosmic string would be a lensing event. The geometry of a cosmic string is crucial for this prediction. For simplicity, we can source Einstein's equations with a static cosmic string. One could start with the abelian Higgs model and compute the components of the energy-momentum tensor. One finds that in the limit of thin vortex core diameter that the string is characterized by a single parameter, the tension μ. This means that the string has no substructure (like matter density) that could give rise to a natural rest frame, and so not only is the string uniform along its axis, but boost-invariant as well (the string is "slippery"). (Dynamically, the string is expected to be endowed with an effective matter density due to wiggles propagating along the string.) The thin string source is described by the Nambu action which sources the Einstein-Hilbert action via the pullback of the metric onto the string's world sheet. As desired, this gives the string's potential energy as tension $\times$ length. The complete action and

equations of motion are

$$S = \frac{1}{16\pi G} \int d^4 x \sqrt{-det[g]} R - \mu \int dt dz \sqrt{-det[x_*(g)]}$$

$$\Rightarrow R_{\mu\nu} - \frac{1}{2} R g_{\mu\nu} = 8\pi G \mu \delta^{(2)}(x, y) x_*(g)_{\mu\nu}$$

We can find the metric by solving the above Einstein equations for an axially symmetric, translation invariant, boost invariant, time independent spacetime. These symmetries are characterized by the following equation for the metric:

$$\frac{\partial}{\partial x^i} g_{\mu\nu} = 0 \qquad x^i \in \{t, z, \varphi\}$$

$$(t\frac{\partial}{\partial z} + z\frac{\partial}{\partial t}) g_{\mu\nu} = 0$$

This is satisfied by the following ansatz.

$$ds^2 = -dt^2 + d\rho^2 + \rho^2 (1 - \frac{\delta_0}{2\pi}) d\varphi^2 + dz^2 \qquad (5.3)$$

The parameter δ_0 in the above solution is the so called deficit angle. The metric describes the geometry of a cone. The space is everywhere flat except at the vertex, where the cosmic string sits. If we examine the solution near the core we should regulate the singularity by substituting a smoothed out Heaviside function in place of δ_0 via (say) $\delta_0 \to \delta_0 \tanh(+\infty\rho)$ then we find

$$\delta_0 = 8\pi G\mu. \qquad (5.4)$$

Light passing on one side of the cosmic string will thus be uniformly deflected by δ_0 relative to the light going around the opposite side. The two images are thus undistorted and identical as in Figures 5.2.a, separated by an angular deviation $\delta\varphi$ given by

$$\delta\varphi = \frac{D_{s,cs}}{D_{O,cs} + D_{s,cs}} \delta_0 \sin(\theta) = \frac{D_{s,cs}}{D_{s,O}} \delta_0 \qquad (5.5)$$
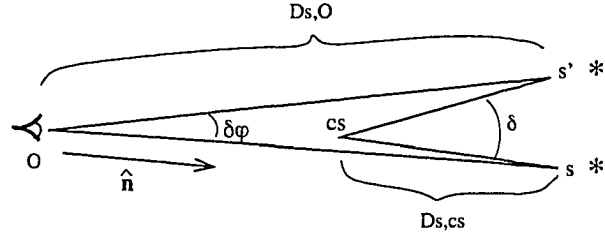
Figure 5.1: A straight cosmic string introduces a deficit angle δ. Here, the sources s and s' are to be identified.

where θ is the relative angle between the cosmic string and the line of sight, and $D_{x,cs}$ is the *normal* distance between x and the cosmic string. This is illustrated in Figure 5.1.

One can show that the geometry due to a straight cosmic string is equivalent to that of a point particle in 2+1 dimensions, where the Ricci tensor completely and locally determines the Riemann curvature tensor. Thus regions with vanishing $T^{\mu\nu}$ are flat. This is why straight cosmic strings produce such simple images. Because there are no forces between local cosmic strings we can solve the lensing problem for very complicated networks of cosmic strings, including three-way junction lensing events which produce an image as seen in the far right of Figure (5.2.b) [63].

We can calculate the effects of a moving string by appealing to Lorentz invariance with the result that the effective deficit angle δ is given by [64]

$$\delta = \delta_0 \gamma (1 + \hat{n} \cdot \mathbf{v}) \tag{5.6}$$

with $\hat{n}$ the outward pointing unit vector. The most general case is discussed in section 5.2.1.
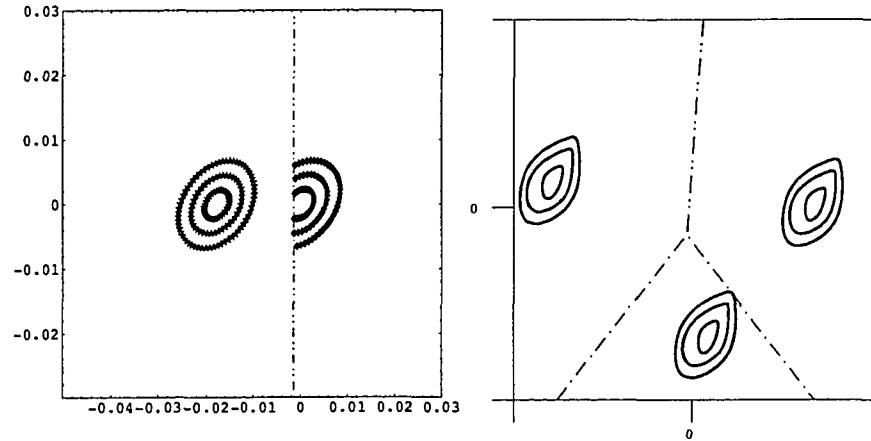
Figure 5.2.a: Images from a single string.

Figure 5.2.b: Three way lensing. The pairwise compatibility of the images is equivalent to the equilibrium condition.

5.1.3 Observables

A potential string candidate is thought to be responsible for the anomalous brightness fluctuation in the lensing system Q0957+561A,B [65]. A foreground galaxy lenses the quasar in a way that results in a 417 day difference in arrival time. Brightness fluctuations with much smaller delay must therefore be due to an oscillating object in the foreground. A cosmic string loop is the most likely candidate, although more information would be needed to confirm or reject this hypothesis.

The cosmic microwave background provides several opportunities to detect cosmic strings. They include

- A linear discontinuity in the CMB temperature due to moving cosmic strings between us and the last scattering surface.

- Density perturbations caused by the wakes of moving cosmic strings at the last scattering surface
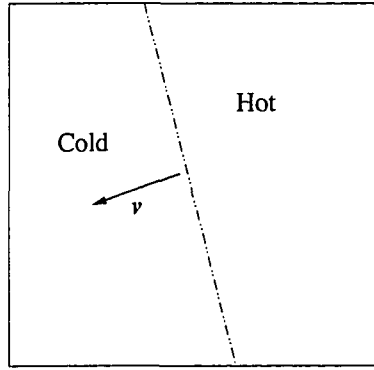
Figure 5.3: The sky is warmer behind a moving string.

- B-mode polarization in the CMB from vector and tensor perturbations due to cosmic strings

Figure 5.3 illustrates the most direct and dramatic of these signatures: a linear step discontinuity in the observed CMB temperature (Kaiser-Stebbins discontinuity). One can calculate the blue-shift due to a moving cosmic string to be [16]

$$\frac{\delta T}{T} = 8\pi G\mu \frac{v\sin(\alpha)}{\sqrt{1-v^2}} \tag{5.7}$$

where α is the relative angle between the cosmic string velocity and the outward pointing unit vector. The WMAP bound on such a discontinuity places an upper bound on $G\mu <= 3.3 \times 10^{-7}$ [61].

Another striking imprint on the CMB could be found in the power spectrum. One can examine both C_ℓ^{TT} and C_ℓ^{BB} to bound the tension of cosmic strings. The bottom line [66] is that C_ℓ^{BB} will peak at much smaller angular scales ($700 \lesssim \ell \lesssim 1000$) due to cosmic strings than it will for adiabatic perturbations, which peak around $\ell \lesssim 100$. Current data places a bound of $G\mu <= 1.3 \times 10^{-6}\sqrt{\frac{Bp}{0.1}}$ where $p \leq 1$ is the intercommutation probability and $B \lesssim 0.1$ is the fractional contribution to perturbations due to cosmic strings. Jackson, Jones, and Polchinski find that $10^{-3} \lesssim p \lesssim 1$ for F-strings, and $0.1 \lesssim p \lesssim 1$ for D-strings [12,17].
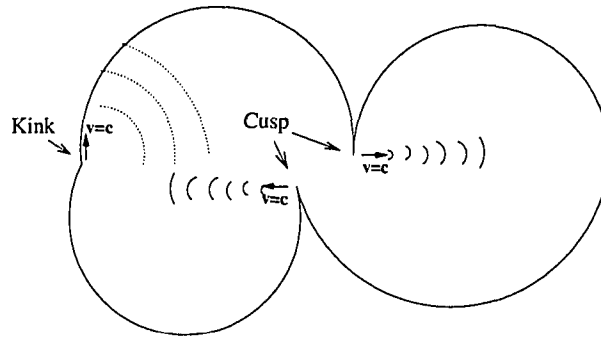
Figure 5.4: A smooth cosmic string containing only first and third harmonic excitations develops cusps for much of its evolution. A kink has been added for comparison.

Lastly, the CMB polarization measurements will be sensitive to the gravitational radiation emitted by oscillating cosmic strings. All in all, current CMB data suggest $G\mu \leq 2.7 \times 10^{-7}$ [18].

Gravitational radiation is the dominant source of energy loss of the cosmic string network. One expects a stochastic background supplemented with stark bursts from so called cusps and kinks. Cosmic string loops lose energy to gravity at a rate of $\dot{E} = \Gamma G\mu^2$ where $\Gamma \approx 100$ is a pretty standard prediction for most simulations. The majority of this radiation is in the form of Gaussian "confusion noise" generated by the large oscillations of characteristic frequency R^{-1} where R is the size of the loop, as well as from kinks and wiggles. A kink is a discontinuity in the direction of a cosmic string, and results from the intercommutation of long strings, or self intersection of loops. Any point on the string that is not smooth (finite second derivative) must move at the speed of light. These produce a fan shaped burst of gravitational radiation loosely directed along the plane of motion of the kink. A cusp is a sharp discontinuity with characteristic shape $y = x^{2/3}$ that generically appear on *smooth* cosmic string loops [67]. Figure 5.4 illustrates both a kink and a cusp radiating gravitationally.

Turok [68] developed an analytic solution to the cosmic string equations of motion by expanding the left and right moving waves in their Fourier modes. Interestingly, the non-linearity in gauge fixing limits this method to the first and third harmonics only. Nevertheless a rich class of string loops emerged from this which often possessed cusps (at least two per period) and rarely self intersected. Cusps produce highly focused bursts of gravitational radiation in the direction that the cusp moves. Fine scale wigglyness tends to smooth these cusps, and causes the cusps to launch away very tiny closed loops [69]. The smoothing of the cusps also widens the forward cone of gravitational radiation to subtend an angle $\theta \lesssim \sqrt{1 - v_{cusp}^2}$. Notice that a pure cusp (no wiggles or gravitational back-reaction) has $v_{cusp} = 1$. The focused burst of gravitational radiation is in stark contrast to the Gaussian "confusion noise," and could be detected much more easily. Damour and Vilenkin predict that tensions as low as $G\mu \approx 10^{-13}$ could be detectable by LIGO/VIRGO and LISA [70]. (But see also [71].) Their predictions for gravitational wave amplitudes (in the frequency band appropriate for the various experiments) is plotted in Figures 5.5.a - 5.6.b. Pulsar timing observations do not benefit from these extremely intense cusp events because they are too focused (rare) to affect pulsar experiments over the course of only a few tens of years. The current bound from gravitational wave detection is $c^{3/2}G\mu < 10^{-7}$ where c is the average number of cusp appearances per string oscillation period.

One may divide the gravitational radiation spectrum into three scales, all of which are relevant to cosmic string detection. Those with wavelength much greater than one light-year will leave an imprint on the CMB polarization measurements. Those with wavelength much shorter than one light-year can be observed directly with experiments such as LIGO, VIRGO, and highly tuned solid state devices.
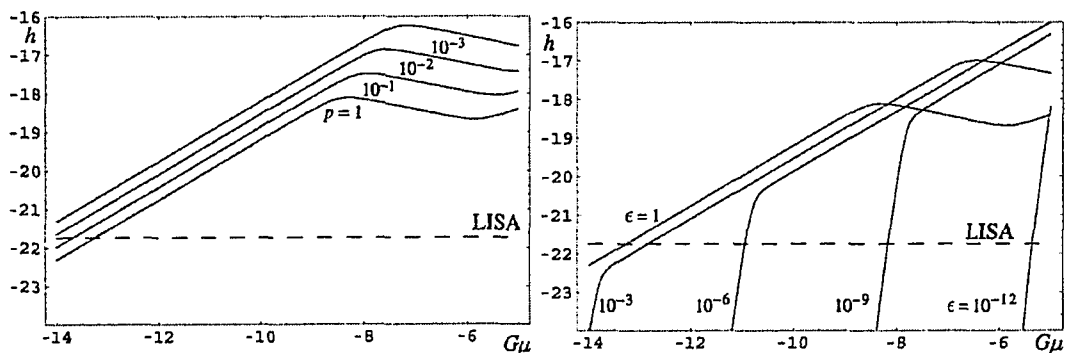
Figure 5.5.a: Fixing $c = 1$ and varying the recombination probability p. x-axis is $\log_{10}(G\mu)$.

Figure 5.5.b: Fixed $p = 1$ and varying the loop-length parameter $\epsilon = \alpha/\Gamma G\mu$. The x-axis is $\log_{10}(G\mu)$.
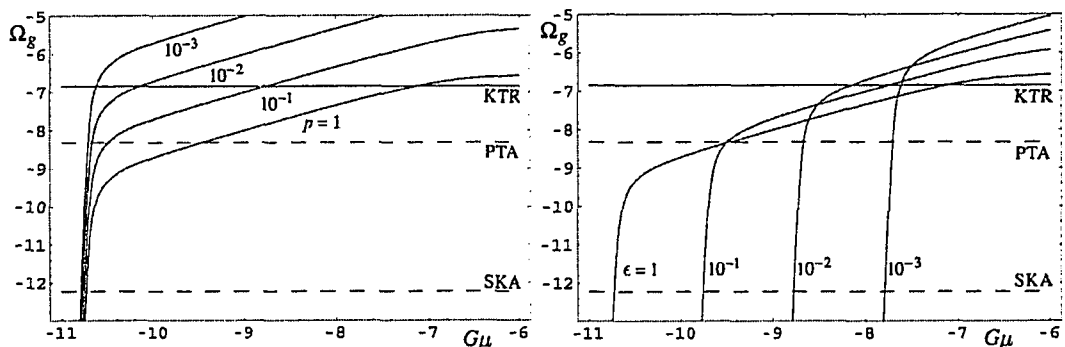
Figure 5.6.a: Constraints on $G\mu$ for various intercommutation probabilities p. The KTR line is from eight years of timing millisecond pulsars PSR 1855+09 and PSR 1937+21. The PTA line represents (disputed) sensitivity from a seventeen year timing of PSR 1855+09. The SKA line represents expected sensitivity from pulsar detection from the square kilometer array of radio telescopes.

Figure 5.6.b: Constraints on $G\mu$ for various loop size parameter ϵ. The KTR line is from eight years of timing millisecond pulsars PSR 1855+09 and PSR 1937+21. The PTA line represents (disputed) sensitivity from a seventeen year timing of PSR 1855+09. The SKA line represents expected sensitivity from pulsar detection from the square kilometer array of radio telescopes.
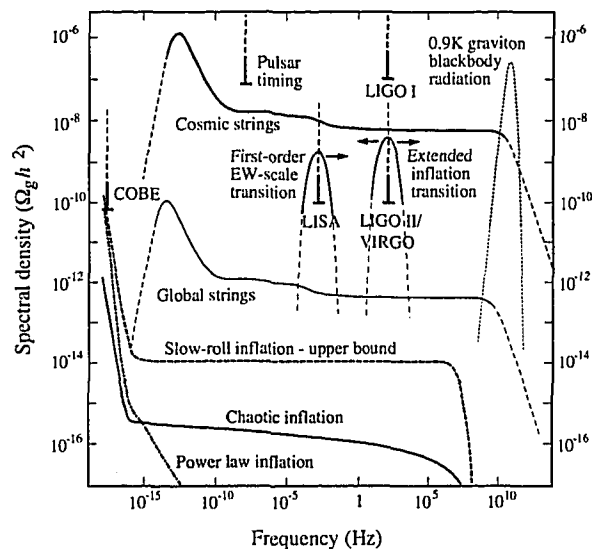
Figure 5.7: An amplitude^2 vs. frequency plot for gravitational waves from cosmic strings and other sources. Included is the detection windows of various experiments. (taken from [72]).

The space based LISA will measure such frequencies as well. Wavelengths of order one light-year can be measured using long term observation of millisecond pulsar timing. Passing gravitational waves momentarily lengthen and shorten directions perpendicular to the direction of propagation. LIGO/VIRGO can detect this with extremely precise interferometers.

Cosmic strings are not the only source of gravitational radiation in the universe. A potentially strong source is accreting neutron stars, which reach an equilibrium state around 300 Hz at which point all in falling angular momentum is radiated away as gravitational waves [73]. The electron capture rate is temperature dependent, which leads to density variations large enough to supply adequate quadrupole moment for radiation amplitude of $h_c \sim 10^{-26}$. LIGO/VIRGO are most suited to detect this radiation. A summary of gravitational wave amplitudes expected at various frequencies is represented in Figure 5.7.

There is an interesting puzzle called Olber's Paradox regarding radiation sources. The stochastic gravitational radiation power measured from each source (cosmic string loop, accreting neutron star) decreases as the inverse square of the distance from the source to the observer. However, since the universe is homogeneous on large scales we know that the number of sources at a given distance increases quadratically with the distance, η. This seems to imply that the total luminosity of (gravitational) radiation for any co-moving observer is the divergent integral $\int \eta^2 \frac{1}{\eta^2} d\eta$, that is, the contribution from each shell of radius η and thickness $d\eta$ does not depend on η! The resolution of this paradox comes from the finite age of our universe. The total power integral has a natural cutoff of $\eta_{max} = \eta_0 - \eta_i$, the amount of time since such sources were first created. This means that despite the potentially infinite volume of our universe, only a finite power is incident upon us because only sources closer than the age of the universe can contribute.

5.1.4 Summary

Table 5.1 illustrates various bounds on cosmic strings in our universe. As a reference, the KKLMMT framework predicts models with [23, 74].

$$4 \times 10^{-10} \leq G\mu \leq 5 \times 10^{-7}. \tag{5.8}$$

Near future experiments, including LISA, LIGO II & VIRGO, SKA, PTA, Planck, QUIET, and pCMBR data will be able to test the KKLMMT Brane Inflation paradigm.

Table 5.1: Bounds on Cosmic String Tension

PSRs J1713+0747, B1855+09, B1937+21 [75]	$G\mu \leq 2 \times 10^{-7}$
WMAP non-gaussianity (Kaiser-Stebbins) [61]	$G\mu \leq 3.3 \times 10^{-7}$
WMAP & SDSS [8,18]	$G\mu \leq 2.7 \times 10^{-7}$
WMAP & 2dFGRS [66]	$G\mu \leq 1.3 \times 10^{-6}\sqrt{\frac{Bp}{0.1}}$
7 yr. obs. PSRs B1885+09, B1937 +21 [76]	$G\mu \leq 6 \times 10^{-6}$
WMAP Anisotropy (statistical) [77]	$G\mu \leq 8.2 \times 10^{-6}$
LIGO I burst detection [70]	$G\mu \leq 10^{-6}$
WMAP Anisotropy (patern search) [77]	$G\mu \leq 1.54 \times 10^{-5}$

5.2 Lensing by (p,q) Strings

Some time after the existence of cosmic strings was proposed [41], several researchers recognized that the conical spacetime generated by cosmic strings leads to a unique gravitational lensing signature: undistorted double images [78, 79]; the discovery ofeven a single such gravitational lensing event would be seen as irrefutable evidence for the existence of cosmic strings. Previous detailed studies of string lensing phenomena have focused on infinite strings and string loops, whether straight or wiggly [64, 80-85]. For standard, abelian Higgs strings, these are the only lensing effects that one would expect to find.

But string theory's enriched cosmic string phenomenology includes the existence of two basic cosmic string types: fundamental, or F-strings, and Dirichlet one-branes, or D-strings. These two kinds of strings are able to interact and form bound states. These bound states are known as (p, q) strings, as they are composed of p F-strings and q D-strings [12, 86]. String binding allowsfor a variety of new

observational phenomena, yet does not cause any cosmological catastrophes [11]. In particular, the existence of string binding interactions generically implies that there will be Y-shaped junctions of three strings that form each time there is a string binding event. These Y-shaped junctions give rise to lensing phenomena that are qualitatively distinct from anything abelian Higgs models can produce.

Since cosmic strings are perhaps the only directly observable remnant of brane inflation, it is vital that we identify any distinctive effects that are peculiar to the cosmic "superstrings" that are produced in brane-collision reheating. Cosmic superstrings may be our best hope for directly observing some aspects of string theory. The observation of even a single distinctive lensing event – one that could not be explained in an abelian Higgs model – would be a "smoking gun" for the existence of a non-trivial cosmic string network that is the hallmark of cosmic superstring models. We note, however, that similar junctions are found in non-abelian string networks as well (e.g., the S_3 networks studied in ref. [87, 88]).

Here, we describe the principal novel phenomena arising from the binding junctions that characterize non-trivial networks of cosmic superstrings. In §5.2.1, we review lensing by a straight cosmic string, writing down some general formulae that have not previously appeared in the literature.

In Figure 5.8 we illustrate the quintessential signature of a (p, q) network junction. This is an imaginative construction of what the galaxy NGC 2997 [1] might look like if it were lensed by a Y-shaped string junction. In §5.2.2, we derive the simple procedure used to generate this image.

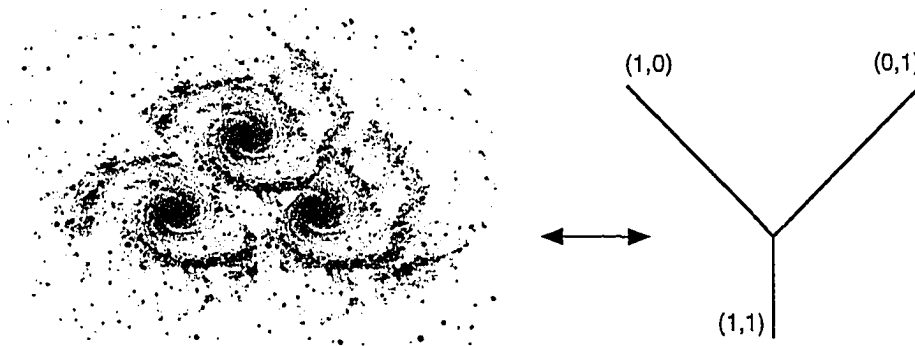[1]Anglo-Australian Observatory/David Malin Images

Figure 5.8: Illustration of lensing of a single galaxy by a (p, q) network junction. Note that each image is partially obscured, which is a generic feature of cosmic string lensing events [89]. This is not an actual observation.

5.2.1 Review of Straight String Lensing

The lensing due to a straight string is surprisingly simple; this comes about because the surrounding spacetime is locally flat. Many details of this lensing can nevertheless be quite subtle, and so here we correct two errors found in the literature, namely the angular separation formula and the orthogonality of the image pairs with respect to the observed cosmic string. A string oriented in a direction $\hat{s}$ produces two images on opposite sides of the string separated by an "angular separation vector" $\vec{\delta\varphi}$ of magnitude

$$|\vec{\delta\varphi}| = 8\pi G\mu\sqrt{\gamma^2(1 + \hat{n} \cdot \mathbf{v})^2 - \cos^2\theta}\frac{D_{s,cs}}{D_{s,o}}. \tag{5.9}$$

In our notation, bold face variables represent 3-vectors, bold hatted variables are unit 3-vectors, and over-arrows signify 2-vectors which live in the plane orthogonal to the direction of sight. Here $G\mu$ is the dimensionless string tension, $\gamma = 1/\sqrt{1 - \mathbf{v}^2}$, $\mathbf{v}$ is the string velocity, $\hat{n}$ is the unit vector directed along the line of sight, θ is the angle between the cosmic string and $\hat{n}$ (i.e., it is defined

by $\hat{n} \cdot \hat{s} = \cos\theta$), $D_{s,cs}$ is the distance from the source to the cosmic string, and $D_{s,o}$ is the distance from the source to the observer. The distances should be interpreted as the light travel distances in the observer's reference frame. Because cosmic strings are boost invariant along their axis, we will always work in the gauge where $\mathbf{v}$ satisfies $\mathbf{v} \cdot \hat{s} = 0$. Equation 5.9 can be derived by working in the cosmic string rest frame, where light rays will be deflected by a fixed angle $8\pi G\mu$, and then rotating and boosting the string to give it the desired $\mathbf{v}$ and θ. Since the scalar product $k^\mu k'_\mu$ is invariant under such a boost, and must equal the rest frame value of $\omega\omega'(1 - \cos(8\pi G\mu))$, we can extract the angular separation in any reference frame. We only keep the lowest order in $G\mu$. Vilenkin [78, 79] pointed out that a straight cosmic string in motion will appear curved, like a large hyperbola in the sky; we note that, as expected, the apparent vanishing point of the hyperbola corresponds to the point where the magnitude of the angular separation vector goes to zero ($\vec{\delta\varphi} \to 0$). This is an important consistency check. The reason for the apparent curvature is because what we see is the cosmic string world sheet intersected with our past light cone, which we mentally project onto the $t = 0$ hyper-plane. The cosmic string equations of motion are solved by

$$\mathbf{x}(\sigma, t) = \hat{s}\sigma/\gamma + \mathbf{v}t + \mathbf{b} \tag{5.10}$$

with impact parameter $\mathbf{b}$ (with respect to the origin/observer) orthogonal to both $\hat{s}$ and $\mathbf{v}$. The *observed* cosmic string is described by the illusory embedding

$$\mathbf{y}(\sigma, t) = \mathbf{x}(\sigma, t - |\mathbf{y}(\sigma, t)|). \tag{5.11}$$

This equation simply states that the *apparent* location of any point on the string is given by the *actual* location at an earlier time. This amount of time is given precisely by the time it took the light to travel from that *perceived* location to our

eye. Solving for **y** yields

$$\mathbf{y}(\sigma, t) = \hat{\mathbf{s}}\sigma/\gamma + \mathbf{v}(\gamma^2 t - \sqrt{\mathbf{b}^2\gamma^2 + \sigma^2 + \mathbf{v}^2\gamma^4 t^2}) + \mathbf{b}. \tag{5.12}$$

The apparent string then has orientation given by $\hat{\mathbf{s}}_{apparent} = \mathbf{y}'(\sigma, t)/|\mathbf{y}'|$, which is in general not equal to $\hat{\mathbf{s}}$. These string orientation vectors may be projected onto the sky via

$$\vec{s} = \hat{\mathbf{s}} - (\hat{\mathbf{n}} \cdot \hat{\mathbf{s}})\hat{\mathbf{n}} \tag{5.13}$$

$$\vec{s}_{apparent} = \hat{\mathbf{s}}_{apparent} - (\hat{\mathbf{n}} \cdot \hat{\mathbf{s}}_{apparent})\hat{\mathbf{n}}. \tag{5.14}$$

The difference between apparent and actual string orientation can then be characterized by the angle between these two 2-vectors:

$$\cos\beta = \frac{\vec{s} \cdot \vec{s}_{apparent}}{|\vec{s}||\vec{s}_{apparent}|} = \frac{\cos\theta\mathbf{v} \cdot (\hat{\mathbf{n}} \times \hat{\mathbf{s}})\gamma}{\sin\theta\sqrt{\gamma^2(1 + \hat{\mathbf{n}} \cdot \mathbf{v})^2 - \cos^2\theta}}. \tag{5.15}$$

Interestingly, the relative angle between $\vec{\delta\varphi}$ and $\vec{s}$ can be shown to be $\pi/2 + \beta$ which implies that the angular separation vector is always orthogonal to the *apparent* cosmic string as in Figure 5.9.

$$\vec{\delta\varphi} \cdot \vec{s}_{apparent} = 0 \tag{5.16}$$

One might wonder how it is possible for a cosmic string that appears to be bent in the shape of a hyperbola to produce an undistorted image. Indeed since the lensed images appear perpendicular to the *bent* string, the image pairs must differ by a very slight distortion. This is not in contradiction with the fact that the spacetime surrounding the string is flat: The images are moving at slightly different velocities, which gives rise to both the Kaiser-Stebbins (blue-shift) effect, as well as a relative "hyperbolic distortion" due to the finite travel time of light. So the distortion induced by an extremely relativistic string is none other than the distortion that all moving bodies appear to have; c.f. Eqn. (5.11).
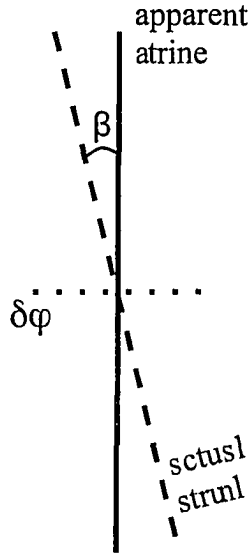
Figure 5.9: A schematic view of the lensing due to a single string in the most general case; when the string's velocity is non-zero, the angular separation vector is perpendicular to the apparent string, rather than to the actual string.

5.2.2 Lensing by Y-Junctions

A feature of superstring networks is that they are composed of at least two distinct string species: so-called fundamental or F-strings as well as D1-branes, or D-strings. These different types of strings can mutually interact via binding, creating (p, q) bound states composed of p F-strings and q D-strings [12,59,86]. The tension of such strings is given by

$$\mu_{p,q} = \sqrt{p^2 \mu_F^2 + q^2 \mu_D^2}$$ (5.17)

Networks of such strings are cosmologically safe, as they are expected readily to go to scaling [11].

It is in the region near the Y-shaped junctions formed after collisions that the new string lensing effects are seen. In Figure 5.8, we showed an image as it might actually appear, with the invisible strings and angular separation vectors
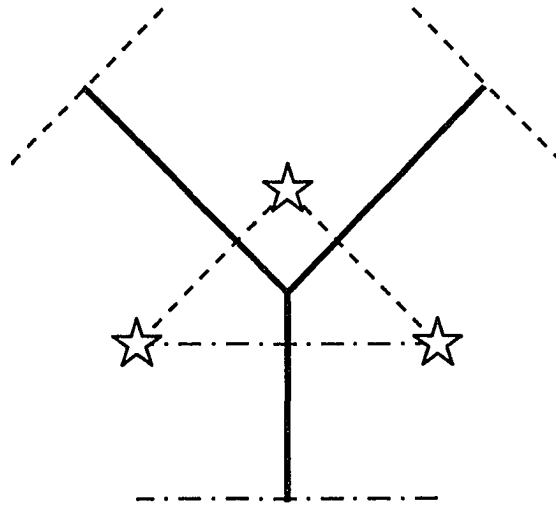
Figure 5.10: The imaging pattern of a three-way junction. The dark lines represent the force-balanced string junction; in reality, strings themselves are invisible. The dotted and dot-dashed lines represent, schematically, the angular separation vectors associated with the strings. We suppress the heads of the vectors, since their orientation is arbitrary. For string tensions in the upper range allowed by observations – that is, $G\mu \sim 10^{-7}$ [8,66,90–92] – the size of the angular separation vectors would be of order 1 arc-second. The stars represent the lensed images, with the angular separation vectors drawn in for illustrative purposes.
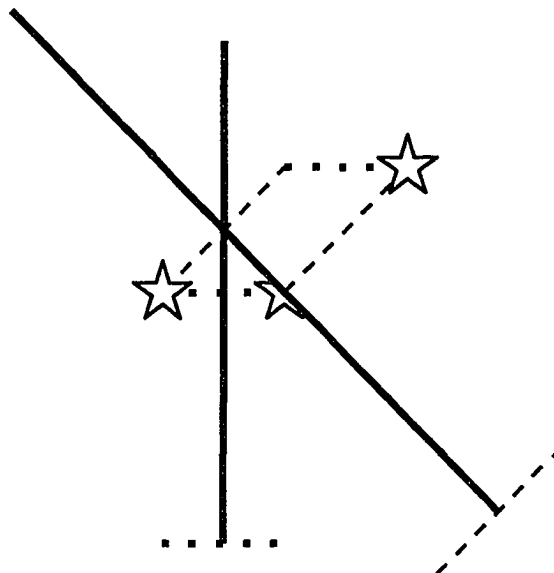
Figure 5.11: The imaging pattern is shown for two overlapping cosmic strings. The dotted and dot-dashed lines represent, schematically, the angular separation vector associated with the strings. Notice that only the object and two of the three images are visible.

suppressed. In Figure 5.10, we show a mock-up of the triple image formed in the vicinity of a Y-junction together with the strings that produce the image. In brief, each leg of the Y-junction lenses exactly like an infinite straight string.

To motivate the above result, let us begin by considering a source simultaneously imaged by two long strings.

For two overlapping strings, it is straightforward to construct a set of rules for the multiple imaging of a single source. Each straight cosmic string has an associated two dimensional "angular separation vector" the length of which is given by Eqn. (5.9). For string tensions in the upper range allowed by observations [8,66,90–92], the magnitudes of these angular separation vectors are of order 1 arcsecond. The orientation of the angular separation vector is perpendicular to the associated cosmic string.

1. Begin with an original image (i.e. the object); the choice of which image to begin with is arbitrary.

2. Construct a parallelogram originating at the object and generated by the angular separation vectors associated with each cosmic string; each corner represents a new image.

   (a) Each image (except the object) will be associated with the set of cosmic strings whose angular separation vectors were used to create it.

   (b) If exactly those strings that are associated with an image – and no others – lie between the object and that image, then that image will be visible; otherwise, that image will be invisible.

3. Thus, given the existence of one visible image (the object), the location and status – visible or invisible – of the other three images is known. An example of this is shown in Figure 5.11.

4. This procedure is consistent with the fact that a visible image is made invisible when and only when any cosmic string moves across it, and an invisible image is made visible only when a cosmic string moves across it.

For three overlapping strings, we follow the same procedure as before, with the same rules. The only difference is that rather than forming a parallelogram, three angular separation vectors lead to a parallelepiped. We show an example of this sort of diagram in Figure 5.12.

Finally, let us stipulate that the three strings are coplanar and intersect at one point. If they are to be in force balance, then their orientation unit vectors must
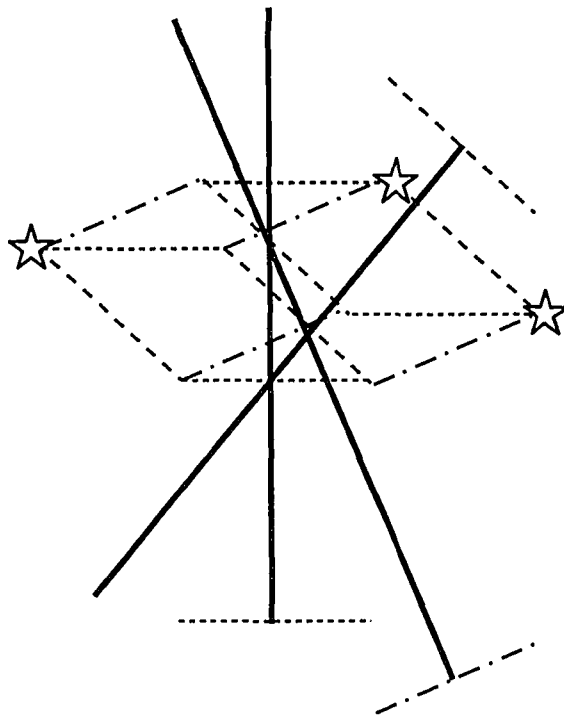
Figure 5.12: The imaging pattern for three overlapping cosmic strings is shown. Only the object and two of the seven images are visible.

obey

$$\sum_{i=1}^{3} \mu_i \gamma_i \hat{s} = 0. \tag{5.18}$$

The γ-factors correct for the Lorentz contraction caused by boosting in a direction not perpendicular to all three strings.

If the three infinite strings satisfy Eqn. (5.18) then one may "cut-and-paste" them into two Y-junctions without changing the energy-momentum tensor. One of the Y-junctions can then be pulled away to reveal a single junction and its lensed images.

When cosmic strings intersect at a three-way junction, the background metric is solvable if and only if [93] the strings obey the force balance equation. Dynamically, however, the force balance equation is always satisfied since the neighborhood of the junction point can be taken to have an arbitrarily small mass, thus allowing it to respond instantaneously to any net force. This would not be the case if the vertex had a large mass (e.g., if it were a monopole). Thus there is a consistency check that must be performed for lensing by Y-junctions: each string lenses the two images surrounding it, and so the picture is over determined. In other words, each object has two images which must also satisfy the lensing equation of the string separating them. This means we must check that the angular separation vector triangle closes:

$$\sum_{i=1}^{3} \delta\vec{\varphi}_i = 0. \tag{5.19}$$

In fact, we find that the force balance Eqn. (5.18) is a sufficient condition for Eqn. (5.19) to be satisfied. This could be inferred from the first claim of this paragraph, but is also possible to verify directly using the equations found in §5.2.1.

5.2.3 Conclusion

We have presented an exact solution for both the lensing of three-string junctions and for multiple overlapping strings. We do not yet know how prevalent such junctions would be in realistic networks of (p,q) strings. Since they are expected to be somewhat rare, however, our chief hope for locating such a junction would be, first, to locate an actively lensing cosmic string. Ira Wasserman has pointed out that the multi-image signature of crossing or bound strings is much less ambiguous than two images with identical spectra, since galaxy collisions cannot simulate such an image. As of now, no astronomical observations have yielded unambiguous evidence for a string lensing event, In passing, we note that, since high velocities generally enhance lensing (see Eqn. 5.9), there cannot be a firm lower bound placed on the tension of the inferred string from a single lensing event. Should such an event be found, we might hope to track it across the sky by interpolation between further lensing events or through the Kaiser-Stebbins effect [16, 77, 94, 95] until a junction could be located along its length. If it so happens that a single cosmic string lensing event is discovered, an eager modern-style search would doubtless ensue in hopes of tracking down further such events; in such a scenario, the sort of cross-sky tracking suggested above might become possible. Within any such search, the discovery of even one triple imaging event as described in this paper would be an unmistakable indicator of the existence of a cosmic string network with non-trivial interactions, the very kind predicted in brane inflationary models. Finding this sort of smoking gun – so rare as to be invisible to serendipitous discovery – might be possible in such a scenario, giving us hope for an experimental examination of string theory unthinkable even a few years ago.

THE IMPOSSIBILITY OF CLOSED TIME-LIKE CURVES FROM COSMIC STRINGS

6.1 Introduction

Although cosmic strings as the seed of structure formation [96] has been ruled out by observations of large scale structure and the cosmic microwave background, their presence at a lower level is still possible. Indeed, cosmic strings are generically present in brane inflation in superstring theory, and their properties are close to, but within all observational bounds [2, 7, 23, 59, 66, 97]. This is exciting for many reasons since current and near future cosmological experiments/observations will be able to confirm or rule out this explicit stringy prediction. If detected, the rich properties of cosmic strings as well as their inflationary signatures provide a window to both the superstring theory and our pre-inflationary universe. The cosmic strings are expected to evolve to a scaling string network with a spectrum of tensions. Roughly speaking, the physics and the cosmological implications are entirely dictated by the ground state cosmic string tension μ, or the dimensionless number $G\mu$, where G is the Newton's constant [96]. The present observational bound is around $G\mu \lesssim 2 \times 10^{-7}$. Recently, it was shown [7] that the cosmic string tension can easily saturate this bound in the simplest scenario in string theory, namely, the realistic $D3 - \bar{D}3$-brane inflationary scenario [23]. This means gravitational lensing by such cosmic strings, providing image separation of order of an arc second or less, is an excellent way to search for cosmic strings. Generic features of cosmic strings include a conical "deficit angle" geometry, so a straight string provides the very distinct signature of an undistorted double image. Cosmic

91

string lensing has been extensively studied [79, 83, 98, 99].

In the string network, some segments of cosmic strings will move at relativistic speeds. It is therefore reasonable to consider the gravitational lensing by highly relativistic cosmic strings. We also confront another interesting feature of cosmic strings, first realized by Gott [100]: the possible appearance of closed time-like curves (CTCs) from two parallel cosmic strings moving relativistically past each other. As the strings approach each other fast enough in Minkowski spacetime, the path encircling the strings in the sense opposite to their motion becomes a CTC. This is sometimes called the Gott spacetime or Gott time machine.

Although there is no proof that a time machine cannot exist in our world [101, 102], their puzzling causal nature leads many physicists to believe that CTCs cannot be formed. This skepticism has been encoded in Hawking's Chronology Protection Conjecture (CPC) [103]. However, CPC as proposed is not very precise; even if we assume CPC is correct, it is not clear exactly what law of physics will prevent the specific Gott spacetime. There are a number of interesting and insightful studies attempting to apply CPC against the Gott's spacetime :

- Recall that the original Chronology Protection Conjecture [103] is motivated by two results. The more general of the two is the semi-classical divergence of the renormalized stress-energy tensor near the "chronology horizon," or Cauchy surface separating the regions of spacetime containing CTCs from those without. These (vacuum)"polarized" hypersurfaces led Hawking to conjecture that *any* classical spacetime containing a chronology horizon will be excluded from the quantum theory of gravity. However, a recent paper [104] found an example where this chronology horizon is well defined in the background of a string theory (to all orders in α'). So, in superstring

theory, the CPC is not generically true: the Taub-NUT geometry receives corrections that preserve the travsersibility of the chronology horizon. Unlike classical Taub-NUT, stringy Taub-Nut contains time-like singularities, although they are far from the regions containing CTCs. The second hint that CPC is true is the theorem proved by Hawking and Tipler [103, 105] that spacetimes obeying the weak energy condition with regular initial data and whose chronology horizon is compactly generated cannot exist. These theorem depends crucially on the absence of a singularity, and so Hawking's claim that finite lengths of cosmic string cannot produce CTCs is only true if one rejects the possibility of a singularity being present somewhere on the chronology horizon [106].

- When we consider possible formation of CTCs coming from cosmic string loops (though this is not necessary for our general argument), Tipler and Hawking make use of the null energy condition and smoothness to argue against CTCs. The null energy condition can be satisfied even when one smooths out the conical singularity (with a field theory model) at the core of the cosmic strings. However, in superstring theory, such a procedure is not permitted. The cosmic strings are either D1-strings or fundamental strings. Classically, the core is a δ-function with no internal structure (e.g., energy distribution) in the string cross-sections, so the string has only transverse excitation modes. Suppose we smooth out the δ-function. Then one can rotate the string around its axis and endow it with longitudinal modes. The presence of such longitudinal modes violate the unitarity property of the superstring theory. (In fact, in the presence of such longitudinal modes, general relativity is no longer assured in superstring theory.) In this sense, the

string geometry is not differentiable, and one must generalize the appropriate theorems before they may be applied.

- Cutler [107] has shown that the Gott spacetime contains regions free of CTCs, that the chronology horizon is classically well defined, and that Gott spacetime contains no closed (as opposed to just self-intersecting) null geodesics. Hawking points out that this last feature must be discarded for bounded versions of Gott (and similar) spacetimes. This means that if one can avoid the Tipler and Hawking theorems (by including singularities), a cosmic string loop could create a local version of Gott spacetime *with* closed null-geodesics. Cutler found a global picture of the Gott spacetime very much in agreement with general arguments made by Hawking regarding the instability of Cauchy horizons, specifically the blue-shifting of particles in CTCs. Here, we find a concrete example of this phenomenon using a lensing perspective.

- As parallel strings move relativistically past each other to create CTCs, a black hole may be formed by the strings before the CTC appears, thus preventing CTCs. If this happens, one can consider the formation of a black hole as a realization of CPC. However, it is easy to see that, using Thorne's hoop conjecture, there is a range of string speed where the CTCs appear, but no black hole is formed. The results of Tipler and Hawking suggest that either the strings are slowed to prevent CTCs, or a singularity forms somewhere else in the geometry. We will argue that the strings are slowed, and no CTC forms.

- Tipler [105] proved that whenever a CTC is produced in a finite region of spacetime, a singularity must necessarily accompany the CTC. This singular-

ity does not represent a no-go theorem, since the CTC and its sources need not encounter the singularity. In fact Tipler's physical argument against the creation of CTCs is the unfeasibility of creating singularities. However, it is well-known that singularities such as orbifold fixed points and conifolds are perfectly fine in superstring theory, where Einstein gravity is recovered as a low energy effective theory. Furthermore, under the appropriate circumstances, topology changes are perfectly sensible. This consistency is due to the extended nature of string modes.

- One may consider the Gott spacetime in 2+1 dimensions. The 2+1 dimensional gravity relevant for the problem has been studied by Deser, Jackiw and 't Hooft [108]. For a closed universe, 't Hooft [109] argues that the universe will shrink to zero volume before any CTCs can be formed. For an open universe, Carroll, Farhi, Guth and Olum (CFGO) [106] show that it will take infinite energy to reach Gott's two-particle system which has space-like total momentum. However, the argument depends crucially on the dimensionality of spacetime. We argue that this last property is quite specific to 2+1 dimensions. In 3+1 dimensions, we show that it is easy to realize Gott's two-string system. For example, a long elliptical string with slowly moving sides will collapse to two nearly parallel segments at high velocity, and can do so without forming a black hole. So CTC formation from the evolution of cosmic string loops seems quite easy to construct. This feature is purely 3+1 dimensional.

If none of the above arguments against CTCs are fully applicable to the Gott 3+1 spacetime, does this mean CPC fails and Gott spacetime can be realized in the real universe? Or are there other mechanisms which prevent the formation of

CTCs?

In this paper, we use a lensing framework to demonstrate the classical instability near the Cauchy horizon which we argue will prevent the formation of cosmic string CTCs in any realistic situation. To be specific, our argument goes as follows :

- A particle or a photon gets a positive kick in its momentum in the plane orthogonal to the strings each time it goes around a CTC [16, 106, 110].

- Once inside the chronology horizon, such a particle is generically attracted to a CTC; that is, a worldline in the vicinity of the CTC will coalesce with the CTC. This is our main observation.

- The particle will go through the CTC numerous times (actually an infinite number of times) instantaneously; that is, the particle will be instantaneously infinitely blue-shifted.

- It follows that the back-reaction must be important; conservation of angular momentum and energy implies that the cosmic strings will slow down, or, more likely, bend; this in turn prevents the formation of CTCs. Note that this back reaction must disrupt the closed time-like curve, otherwise the infinite blue-shift can not be prevented. Thus a single particle, say a graviton or photon, no matter how soft, will bend the cosmic strings so that CTC cannot be formed. The following picture seems reasonable: as the two segments of cosmic strings move toward each other, they are bent and so radiate gravitationally. This slows them down to below the critical value for CTC formation. We expect no singularity/divergence to appear.

- Since there is a cosmic microwave background radiation in our universe, these photons preclude the existence of CTCs. Of course, the cosmic microwave

background radiation is not the only wrench in the machine. Gravitons or some other particles can be emitted by the moving strings, either classically or via quantum fluctuation. In particular, gravitons must be present in spacetimes of dimensions 3+1 or greater. A single graviton, no matter how soft, will lead to the above effect. We argue this is how the chronology protection conjecture works in the Gott spacetime.

This result is not too surprising in light of the likely (blue-shift) instability of Cauchy horizons discussed by Hawking and others, although a counter example was found by Li and Gott [111] while analyzing possible vacua of Misner space, whose Cauchy horizon can be free of instability. As in our example, a divergence occurs only in the presence of particles, although we find that blue-shifting (and not particle number) is the cause.

The blue-shift instability is well studied in the literature [112]. The strong cosmic censorship conjecture predicts that a Cauchy horizon is, in general unstable (e.g. that of a Reisner-Nordström black hole in asymptotically flat spacetime), and that this instability is the result of the infinite blue shift of in falling perturbations. This must be similar to the instability we describe, but our picture is resolved differently. We find that the CTC never forms because surrounding particles scatter off the cosmic strings, bending and slowing them. Hence no Cauchy horizon (stable or not) ever forms.

't Hooft [113] argues that, since the local equations of motion for a cosmic string are well-defined, one should be able to list the Cauchy data at any particular time, and demand the Laws of Nature to be applied in a strictly causal order. If one phrases the logic this way, there are no CTCs by construction, in agreement with the chronology protection conjecture and strong cosmic censorship. So the question

is: what is wrong with Gott spacetime? His answer to this question is that the Cauchy planes become unstable: in terms of these, the Universe shrinks to a line in 3+1 dimensions. The moment a disturbance from any tiny particle is added somewhere in the past, it generates so much curvature that the inhabitants of this universe are killed by it. In our scenario, we give a specific mechanism with more details: a single graviton or photon, even a very soft one, will suffice. An infinitely blue-shifted photon (or any particle) will cause so much curvature that 't Hooft's collapsing scenario occurs. Here, we agree with the chronology protection principle and 't Hooft that a CTC is not formed. However, we believe that, due to the energy-momentum-angular momentum conservations, the back-reaction will bend the cosmic strings and induce gravitational radiation so that the CTC is never formed. Neither the curvature nor the energy of the photon blows up. Note that the bending of the strings can not happen in 2+1 dimensions.

In this paper, the motion of a photon/graviton around the cosmic strings is a crucial ingredient of the analysis. We shall start with a review of the gravitational lensing by a straight moving cosmic string. Here we correct a mistake lensing formula mistake in the literature (see Appendix A). Next we review the evolution of a simple string loop to a loop with two long segments that are moving past each other at ultra-relativistic speed. Far away from the ends, we treat the two long segments as if they were two infinite parallel strings. Next we review Gott spacetime. Finally we show that the CTCs encircling the two strings are attractors for particles. Our analysis ends here. Supplemented with plausible reasonings, we argue that the above mechanism is a way to prevent CTCs in the real universe. Throughout, we shall assume $\delta_0 = 8\pi G\mu$ to be very small (say, less than 10^{-5}).
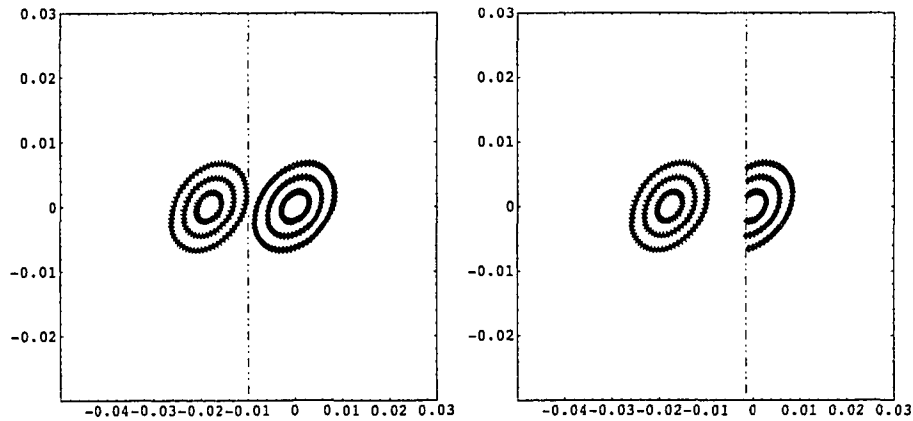
Figure 6.1.a: A Cosmic String near a galaxy

Figure 6.1.b: The images must lie on opposite sides of the string.

6.2 Cosmic String Lensing

One may calculate the observational signatures of rapidly moving cosmic strings (straight and loops), in particular their lensing effects on distant galaxies and the CMB. The simplest case of a straight, nearly static cosmic string has the distinctive signature of producing two identical images, each being undistorted and equidistant from the observer.

Above is pictured a cosmic string moving to the right across a distant galaxy. We call the angular separation of the images $\delta\varphi$, and the photon deflection angle δ, as in the diagram below. Although the double images on the left picture of Fig. 1 may be due to two almost identical galaxies (a rare but not impossible scenario), the picture on the right will be a much cleaner signature of cosmic string lensing. If one sees a double image candidate, one expects to see other candidates nearby. Searching for incomplete images will be important.

This leads to the well known result $\delta\varphi = \frac{D_{s,cs}}{D_{s,O}}\delta$. The spacetime around a static cosmic string is Minkowski space with the identification of two semi-infinite
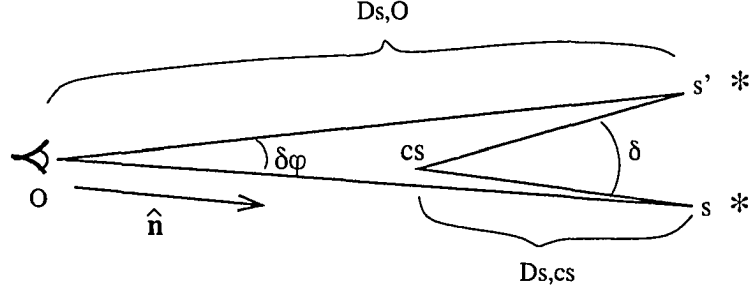
Figure 6.2: A straight cosmic string introduces a deficit angle δ. Here, the sources s and s' are to be identified.

hyperplanes whose intersection is the cosmic string world sheet. This is equivalent to identifying every event s in space time with a dual s' where the relation between s and s' with a static cosmic string located at r_{cs} is

$$s' = R_{\delta_0}(s - r_{cs}) + r_{cs}. \tag{6.1}$$

Here R_{δ_0} is a pure rotation (counter clockwise). (Notice r_{cs} can be any point on the cosmic string world-sheet.) It should be noted that s is visible only when it appears to the right of the cosmic string, and s' is visible only when to the left.

The general case involves a cosmic string moving at some four-velocity v_{cs}. We will always take v_{cs} to be perpendicular to the cosmic string world sheet, since any parallel component is unphysical (assuming a pure tension string). Interestingly, this velocity is only well defined in combination with a "branch cut". This is related to the fact that a passing cosmic string will induce a relative velocity between originally static points in space, so a constant velocity field will not be everywhere single valued. More physically, parallel geodesics moving past a cosmic string will be bent toward each other, provided they pass the string on opposite sides. Specifying a branch cut enables the conical geometry to be mapped to Minkowski space (minus a wedge), where things are simpler. The pure rotation identification is valid only in the center of mass frame of the cosmic string, so in
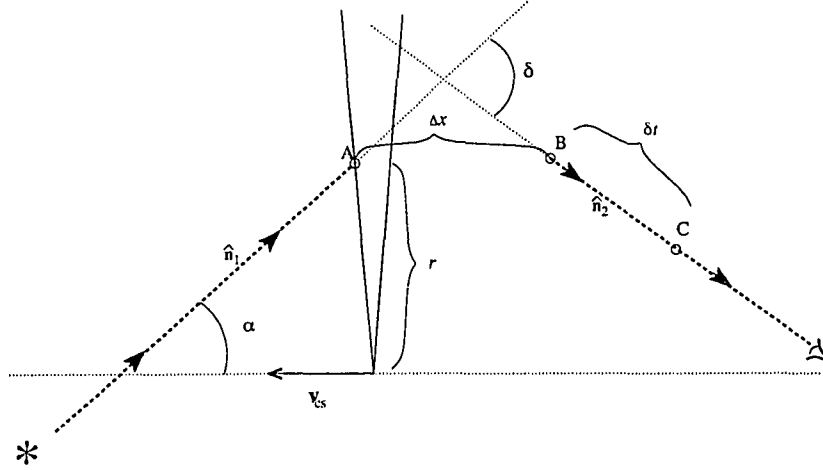
Figure 6.3: The path of a photon coming from the source at the lower left and reaching the observer at the right. The straight cosmic string is moving with speed v_{cs} to the left. The photon's initial velocity $\hat{n}_1$ makes an angle α with respect to $-\mathbf{v}_{cs}$. At A the photon strikes the leading edge of the deficit wedge (a distance r from the position of the cosmic string).

general

$$s' = \Lambda_{v_{cs}} R_{\delta_0} \Lambda_{-v_{cs}}(s - r_{cs}) + r_{cs} \qquad (6.2)$$

where $\Lambda_{v_{cs}}$ is a pure boost such that $\Lambda_{-v_{cs}} v_{cs} = (1, 0, 0, 0)$. We have simply boosted into the strings reference frame and then performed the rotation-identification. Then we boost back.

Here we investigate the lensing due to nearly straight segments moving at arbitrarily relativistic speeds. We consider the interaction of a photon with a cosmic string's deficit angle. In Figure 6.3, a photon is crossing the deficit angle at a distance r from the string vertex. The photon is re-directed by an angle δ and makes a spacial and temporal jump. This jump $(s' - s)$ is found using the coordinate identification in Eq. (2), where $s =$A is the photon striking the deficit angle and $s' =$B is its emergence from the deficit angle. If we choose the deficit angle to be perpendicular to $\mathbf{v}_{cs}$, the spacial jump is parallel to $\mathbf{v}_{cs}$, and is given

by

$$\Delta x = 2r \tan(\delta_0/2)\gamma_{cs} \qquad \Delta t = -2r \tan(\delta_0/2)\gamma_{cs} v_{cs}. \qquad (6.3)$$

where $\gamma_{cs} = 1/\sqrt{1 - v_{cs}^2}$. In Figure 6.3, events A and B are identified, while events A and C are simultaneous. If the photon strikes the leading edge of the deficit angle, the jump is behind the cosmic string and backward in time. If the photon strikes the trailing edge, the jump is in front of the cosmic string and forward in time. For ultra relativistic cosmic strings, only photons traveling almost exactly parallel to the string's velocity will strike the trailing edge of the deficit angle.

We will calculate the change in momentum of a particle interacting with the cosmic string. In the string rest frame, we know that

$$k_{final} = R_{\delta_0} k_{initial} \qquad (6.4)$$

so we simply boost the above equation into the frame where the string is moving at velocity v_{cs}. Then

$$k_{final} = \Lambda_{v_{cs}} R_{\delta_0} \Lambda_{-v_{cs}} k_{initial}. \qquad (6.5)$$

To calculate the directional change in a photon's velocity, we take the above formula with $k^2 = -m^2 = 0$ and for simplicity we take the photon to travel in a plane perpendicular to the cosmic string. Then we find (dropping the cs subscript)

$$\cos(\delta) = \frac{((A - B)\cos(\alpha) + \sin(\alpha)(v\sin(\delta_0) - \cos(\delta_0)\sin(\alpha)/\gamma))}{\sqrt{(\sin(\delta_0)(v + \cos(\alpha)) - \cos(\delta_0)\sin(\alpha)/\gamma)^2 + (B - A + \sin(\alpha)\sin(\delta_0))^2}}$$

where

$$A = \gamma\cos(\alpha)(v^2 - \cos(\delta_0)) \qquad B = \gamma(v\cos(\delta_0) - 1).$$

The blue-shift can be calculated as well, yielding

$$\frac{\omega_{final}}{\omega_{initial}} = \gamma\sin(\alpha)\sin(\delta_0) + \gamma^2(1 + v\cos(\alpha) - v\cos(\alpha)\cos(\delta_0) - v^2\cos(\delta_0)). \qquad (6.6)$$

Straight portions of a cosmic string moving at ultra relativistic speeds produce photon deflection of order π in conjunction with severe blue-shift. Slower moving cosmic strings will obey the Kaiser-Stebbins formula [16] and cause the sky behind the moving string to be blue shifted relative to the sky in front of the string.

With the exception of loops, we expect cosmic strings to move moderately relativistically, but with $\gamma \delta_0 \ll 1$. In this limit, the above formula reduces to

$$
\begin{aligned}
\delta &= \delta_0 \gamma (1 + v \cos(\alpha)) \quad \rightarrow \\
\delta\varphi &= \frac{D_{s,cs}}{D_{s,O}} \times \frac{8\pi G\mu}{\sqrt{1 - v^2}} \times (1 + \hat{n} \cdot \mathbf{v}).
\end{aligned}
$$

The first factor $D_{s,cs}/D_{s,O}$ is a plane-geometric coefficient for $8\pi G\mu\gamma$, which is the relativistic energy of the string. The third term is the result of the finite travel time of light, and does not represent the coordinate locations of the images in the observer's frame. Notice that a moving string (except one moving toward the observer) has a stronger lensing effect. This result disagrees with that given in Ref. [79], which has the γ factor in the denominator. To see this difference more clearly, we give in Appendix A the simple derivation of Ref. [79] and point out where the error occurs. Recall that the typical speed of the cosmic strings in the network is rather large, $v \sim 2/3$ [9,10,114]. There will be segments of strings that have $\gamma \gg 1$ and they have the best chance to be detected via lensing.

The above formula only applies to cosmic strings perpendicular to the line of sight. For the most general lensing due to straight cosmic strings, see section 5.2.1.

6.2.1 Alternate Derivation of Lensing by a Moving Cosmic String

The approximate results of the above section for the lensing due to a moving cosmic string is derivable using an elegant argument due to Vilenkin [79]. Here we begin with the cosmic string tension being very small, and we point out where the error in Ref. [79] is. Vilenkin argues that the angular deflection of light by a cosmic string may be calculated by appealing to Lorentz invariance. For a string at rest, the angular separation is given by

$$\delta\varphi = \frac{D_{s,cs}}{D_{s,O}}\delta_0,\tag{6.7}$$

where for simplicity we have assumed the string lies orthogonal to the line of sight. We may consider two light waves, one from each image, k and k'. Their scalar product is given by

$$k^\mu k'_\mu = \omega\omega'(1 - \cos(\delta\varphi)) \approx \frac{1}{2}\omega\omega'(\delta\varphi)^2.\tag{6.8}$$

We may assume that the two light waves have the same frequency: $\omega = \omega'$. (This can be true in all reference frames since we are expanding to first order in δ_0.) We can then relate the angular separation in any two reference frames by the frequency of the light waves:

$$\omega_0\delta\varphi_0 = \omega\delta\varphi\tag{6.9}$$

i.e., the higher the observed frequency, the lower the observed angular separation. The frequency in a reference frame where the string moves at velocity $\mathbf{v}$ relative to the observer is given by

$$\omega = \frac{\omega_0}{\gamma(1 + \hat{\mathbf{n}} \cdot \mathbf{v})}\tag{6.10}$$

where $\hat{n}$ is the direction from the observer to the source (and thus string), and hence

$$\delta\varphi = \gamma(1 + \hat{n} \cdot \mathbf{v})\delta\varphi_0. \tag{6.11}$$

The roles of ω and ω_0 are erroneously swapped in Ref. [79], which thus agrees with ours only for $\hat{n} \propto \mathbf{v}$. Physically, a traveler moving transverse to the light we observe should measure a higher frequency than we do (i.e. $\omega < \omega_0$ for $\hat{n} \cdot \mathbf{v} = 0$). It should also be pointed out that a string moving across the sky will blueshift the CMB behind it by an amount

$$\frac{\omega_{back}}{\omega_{front}} = 1 + |\mathbf{v} \times \hat{n}|\gamma\delta_0, \tag{6.12}$$

that is, the sky becomes hotter after a cosmic string passes.

6.3 The Evolution of a Simple String Loop

Naively, ultra-relativistic straight strings are rather unlikely, and two parallel ultra-relativistic straight strings passing each other with such a large kinetic energy density must take some arrangement. It is along this line of reasoning that CFGO [106] argues against the formation of Gott spacetime in 2+1 dimensions. In 3+1 dimensions, the situation is much more relaxed. String loops provide ultra relativistic speeds that long cosmic strings rarely obtain. This is favorable for the possibility of closed time-like curve formation. Here we demonstrate how a cosmic string loop can evolve to long, nearly parallel segments moving ultra-relativistically toward each other at arbitrarily small impact parameter but without touching. In accordance with the hoop conjecture, the loop avoids collapsing to a black hole, seemingly allowing the formation of a Gott spacetime with CTCs. Such a spacetime contains closed null geodesics. We will argue that, unlike in $2 + 1$ dimensions

the gravitational radiation present is enough to preclude the formation of CTCs. In agreement with Tipler and Hawking, the loop must slow down.

The classical string equation of motion is

$$\ddot{\mathbf{r}}(\sigma, \tau) - \mathbf{r}''(\sigma, \tau) = 0 \tag{6.13}$$

with the constraint equations $\dot{\mathbf{r}} \cdot \mathbf{r}' = 0$ and $\dot{r}^2 + r'^2 = R_0^2$. We'll see that $2\pi R_0 \mu$ is the total energy of the loop. A dot symbolizes differentiation with respect to $\tau = t/R_0$, and a prime denotes differentiation with respect to σ. The general solution $\mathbf{r}(\sigma, \tau)$ can be written as a linear combination of periodic left- and right-moving waves,

$$\mathbf{r}(\sigma, \tau) = \frac{R_0}{2}[\mathbf{a}(\sigma - \tau) + \mathbf{b}(\sigma + \tau)] \tag{6.14}$$

where $(a')^2 = (b')^2 = 1$. Consider a set of initial data

$$\mathbf{r}(\sigma, 0) = \mathbf{r}_0(\theta), \qquad \dot{\mathbf{r}}(\sigma, 0) = \mathbf{v}_0(\theta)R_0 \tag{6.15}$$

where the unit circle bijection $\theta(\sigma)$ is used to parametrize the initial data and $\mathbf{v}_0 \cdot \mathbf{r}_0 = 0$. The gauge conditions imply

$$\sigma(\theta) = \int_0^{\sigma(\theta)} d\sigma' = \frac{1}{R_0} \int_0^\theta \frac{|\mathbf{r}_0'(\theta')|}{\sqrt{1 - v_0^2(\theta')}} d\theta'. \tag{6.16}$$

We require $\sigma(2\pi) = 2\pi$. The inverse $\theta(\sigma)$ may then be found, as well as the general solution

$$\mathbf{r}(\sigma, \tau) = \frac{1}{2} \left[\mathbf{r}_0(\theta(\sigma + \tau)) + \mathbf{r}_0(\theta(\sigma - \tau)) + R_0 \int_{\sigma - \tau}^{\sigma + \tau} \mathbf{v}_0(\theta(\sigma')) d\sigma' \right]. \tag{6.17}$$

We can apply this formula to the Gott initial data, namely two parallel segments of length $l_0 = \pi R_0 \sqrt{1 - v_0^2} = \pi R_0/\gamma_0$ passing arbitrarily close, each with speed v_0 in opposite directions:

$$\mathbf{r}_0(\theta) = \frac{R_0}{\gamma_0}(0, \Delta(\theta), \epsilon \cos(\theta))$$

$$\mathbf{v}_0(\theta) = -\frac{\sqrt{\gamma_0^2 - 1}}{\gamma_0}(\Delta'(\theta), 0, 0)$$
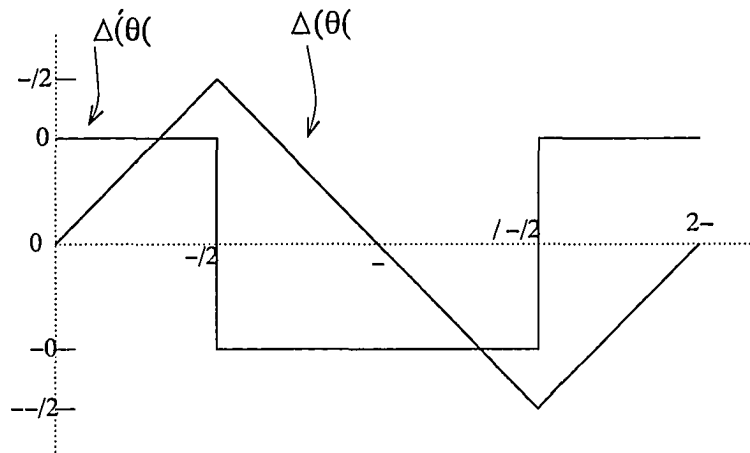
Figure 6.4: The triangle function $\Delta(\theta)$ and its derivative $\Delta'(\theta)$.

with $\epsilon \ll 1$ (head on collision of the two string segments is avoided with a non-zero ϵ.) Illustrated below are $\Delta(\theta)$ and $\Delta'(\theta)$.

Using Eq.(6.16) we find $\sigma(\theta) = \theta + O(\epsilon^2)$, and

$$
\begin{aligned}
\mathbf{r}(\sigma, \tau) = \frac{R_0}{2\gamma_0}[\quad &(\sqrt{\gamma_0^2 - 1})[\Delta(\sigma + \tau) \quad - \quad \Delta(\sigma - \tau)], \\
&\Delta(\sigma + \tau) \quad + \quad \Delta(\sigma - \tau), \\
&\epsilon\cos(\sigma + \tau) \quad + \quad \epsilon\cos(\sigma - \tau) \quad].
\end{aligned}
$$

A multi-image snapshot is pictured below.

The first possible obstacle to CTC formation that we consider is Thorne's hoop conjecture. This states that an event horizon will form (and shroud any CTCs) when and only when a region of a given circumference C contains more rest energy than the critical energy $C/4\pi G$. We need the loop to collapse to an object with length greater than a critical length $\ell_{crit} = \delta_0 R_0$. We immediately see that no event horizon forms for the above solution with $\gamma_0 \delta_0 < \pi$. This allows for the Gott case $\gamma \delta_0 > 2$.

One can estimate the lifetime of a cosmic string loop to be of order $100 R_0$ where R_0 is the maximum size of the loop ($2\pi R_0 = Energy/tension$) [99]. Gravitational
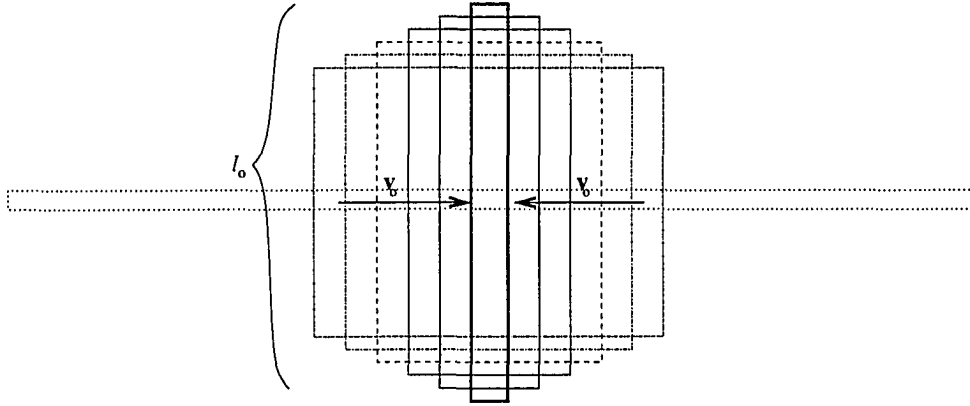
Figure 6.5: The Gott-loop has maximum minor and major axes given by l_0 and $l_0 v_0 \gamma_0$,respectively. The speed of the vertical and horizontal loop sides is given by v_0 and $\sqrt{1 - v_0^2}$, respectively.

radiation carries away the otherwise conserved energy

$$E = \oint \frac{\mu |dr|}{\sqrt{1 - v_\perp^2}}. \tag{6.18}$$

The time scale of decay is much longer than the time scale of evolution, so one may ignore the gravitational radiation. Naively, the inclusion of gravitational radiation may only require some minor adjustment of the original string loop. In reality, the gravitational radiation plays a role in slowing down the loop sides, preventing CTC formation.

Implicit in this discussion is the assumption that a small region containing parallel segments of cosmic string loops will have the geometry of infinite strings moving similarly. This is a reasonable assumption for the following reason. Einstein's equations are local and cannot depend on distant sources (or the lack thereof). Even if CTCs were to form, they do so in a bounded region of spacetime (unlike the 2+1 case), and thus can be considered a local feature which does not reflect upon distant (spatially or temporally) regions. One could imagine adding a small cosmological constant to the 2+1 dimensional Gott spacetime to match up with an

asymptoticly flat universe far from the strings. Such a geometry would be sensible for a string loop in our universe: Gott spacetime near the loop, yet asymptotically flat. One would expect that any process of embedding Gott spacetime in a bounded region would necessarily introduce closed null geodesics. In Gott spacetime, null geodesics only close asymptotically as one moves toward space-like infinity.

Recent brane inflation models have proposed having the inflationary branes located in the tip of a Klebanov-Strassler throat of a Calabi-Yau 3-fold [23]. In some scenarios, the standard model branes are in a different throat. One feature of this construction is that cosmic strings produced after inflation are meta stable, and will not be able to decay via open string interaction with the standard model branes [59]. It should be pointed out that extra dimensions have no effect on Gott's construction of CTCs, provided that the radii of the extra dimensions are small compared to the radius of the CTC. This can be seen as follows. A cosmic string in our universe is an object extended in one non-compact direction, and zero or more compact directions. The four dimensional effective theory will always have a conical singularity on the location of the string, and any corrections to this will be due to massive axion and (KK) modes of the metric– particles whose range is limited to sizes of order the radii of the extra dimensions. Thus as long as we don't probe distances so near the string that these corrections are significant, the conical geometry is valid and Gott's construction is meaningful. In fact, the CTCs in Gott's construction exist at large radii from the cosmic strings, and so one never needs to probe the near-string geometry.

Lensing due to entire cosmic string loops has been analyzed in Ref. [83].

6.4 Gott's Construction of CTCs

Here we give a brief review of Gott's original construction. The key feature is the conical deficit angle ($\delta_0 = 8\pi G\mu$) around a cosmic string. This results in a "cosmic shortcut," since two geodesics passing on opposite sides of the string will differ in length. This shortcut, like a wormhole, leads to apparent superluminal travel. Under boost, "superluminal" travel becomes "instantaneous" travel. Gott realized that this "instantaneous" travel could be performed in one direction, and then back again when two cosmic strings approach each other at very high speed. The actual trajectory is time-like, i.e. performed by a massive body, and resembles an orbit around the center of mass of the cosmic string system (in a direction with opposite angular momentum as the cosmic strings). Below we illustrate the geometry with two strings at rest.

In Figure 6.6, there are three (geodesic) paths from A to B. The central path is not necessarily the shortest, in fact it can be seen that

$$w = x\cos(\frac{\delta_0}{2}) + d\sin(\frac{\delta_0}{2}). \tag{6.19}$$

Thus although $A \rightarrow B$ is traversed by a particle on a time-like trajectory above or below the cosmic strings, the departure and arrival events may have space-like separation in the $y = 0$ hyperplane which extends between the two strings. In this hyperplane, the average velocity of this particle can be calculated as

$$v \leq \frac{2x}{2w} = \frac{1}{\cos(\delta_0/2) + \frac{d}{x}\sin(\delta_0/2)}. \tag{6.20}$$

(In our analysis, we focus on light-like motion since time-like motion is, in a sense bounded by this case.) For large enough x, this velocity is greater than that of light and so we may boost to a frame where the departure and arrival events are

simultaneous. This is true for any d. In the above picture, we will sever the spacetime at the $(y = 0)$-hyperplane and boost such that the top string is moving to the left at speed $v_{cs} > \cos(\delta_0/2)$ and the bottom string is moving to the right at the same speed. This means that we can take $A \to B$ on the upper path and $B \to A$ on the lower path, and in both directions the elapsed time is zero. This is possible when

$$2 < 2\gamma \sin(\delta_0/2) \approx \gamma\delta_0. \qquad (6.21)$$

It is sufficient that the $y = 0$ hyperplane has vanishing intrinsic and extrinsic curvature for us to consistently sew the two halves together. Notice that the limiting case of $\gamma\delta_0 = 2$ corresponds to closed light-like curves. (We will assume that $\frac{d}{x} \to 0$ for simplicity.)

The (two-fold) boosted version of the above setup is pictured below. The events are numbered in "proper" chronological order (that is, the order in which they occur on the particle worldline), but the center of mass coordinate frame chronological order needs to be explained. Event 1 is the light ray initially traveling up to meet the rapidly moving deficit angle, which happens at event 2. This meeting is identified (under Eq.2) with event 3, although in center-of-mass coordinates event 3 happens before the previous events occur. Events 1, 4, and 7 are cm-simultaneous at $t = 0$ while events 2 and 5 occur at $t_{cm} = +1$, and events 3 and 6 at $t_{cm} = -1$. Notice that $\delta = \pi$.

We would like to apply our understanding of ultra relativistic cosmic strings to Gott spacetime. We can use the jumps in location, time and direction (Δt, Δx, and δ) to construct all photon paths around a cosmic string system and determine the complete lensing behavior. Below is a graph of δ for several values of $\gamma\delta_0$, as given by Eq.(6.6).
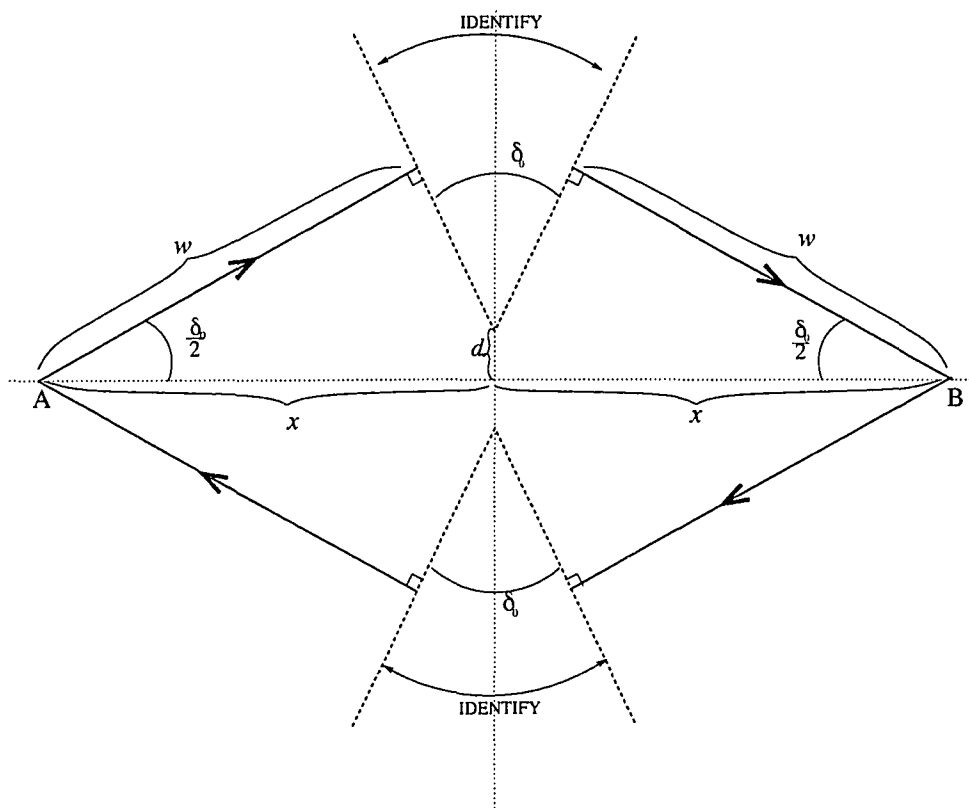
Figure 6.6: The Gott spacetime, before the strings are moving. This space-time will be severed at the $y = 0$ hyperplane (line AB), boosted, and then smoothly glued together again. A and B are separated by a distance of $2x$, while the cosmic strings are separated by a distance of $2d$.
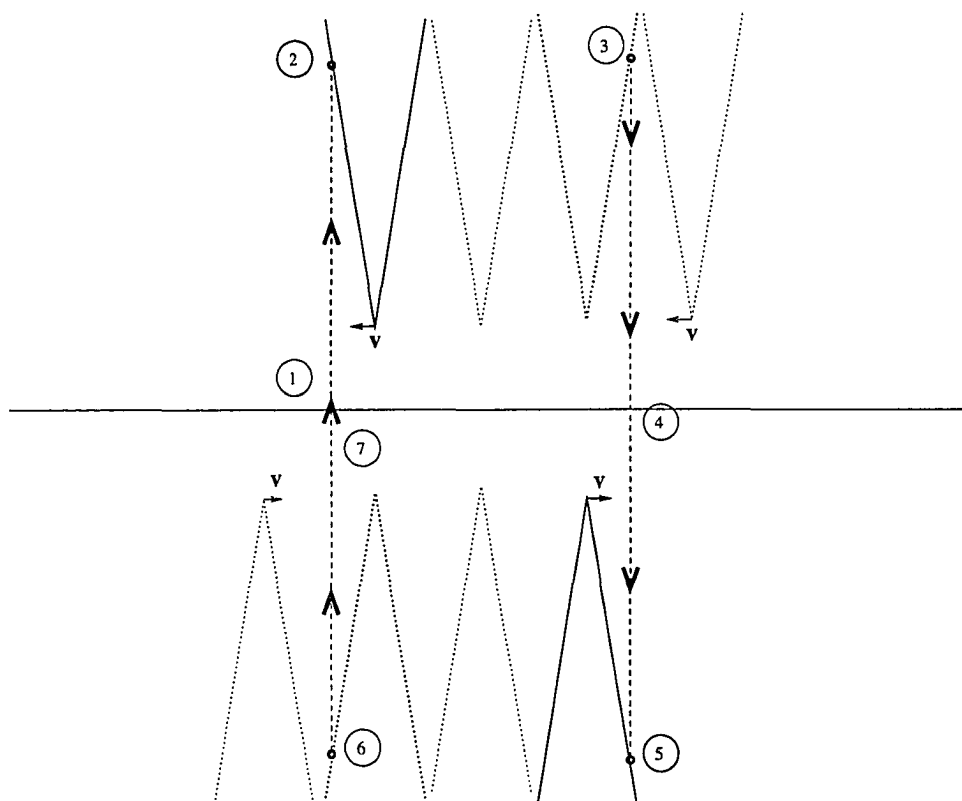
Figure 6.7: This is the critical case where $\gamma\delta_0 = 2$. The deflection angleis calculated using Eq.(6.6) and the discontinuity in the world line using Eq.(6.3). We have drawn $d > 0$ for clarity. The particle travels along the path labeled 1 to 7 and back to 1, arriving at the same point in space and time, i.e., a closed time-like curve. In this case, the particle is neither blue- nor red-shifted.
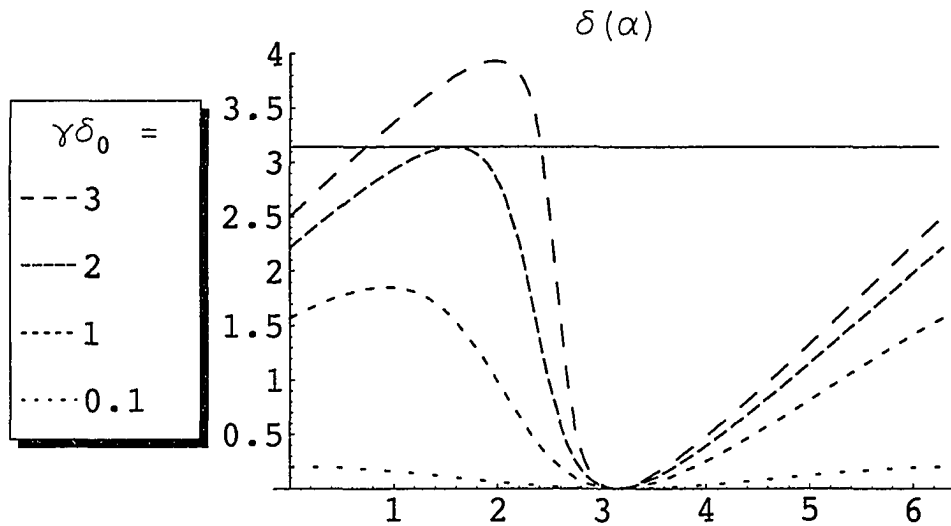
Figure 6.8: This plot derives entirely from Eq.(6.6). Here, $\delta(\alpha)$ is the deflection angle of the photon as a function of the angle α between the photon direction and (minus) the cosmic string velocity (see Figure 6.3). $\gamma\delta_0 = 2$ is the critical case, when the peak of $\delta(\alpha)$ touches the value π (the solid horizontal line).A $\gamma\delta_0 > 2$ curve crosses $\delta(\alpha) = \pi$ at 2 points. Notable is where $\delta(\alpha)$ crosses π (see e.g. the $\gamma\delta_0 = 3$ curve) with positive slope at α_s. A positive slope crossing implies a stable fixed point. Photons with different initial α not far from α_s will follow closed time-like paths and approach $\alpha = \alpha_s$. Photons are blue-shifted at all positive slope crossings. The amount of blue-shift each time is given by Eq.(6.6).

Of importance is where the graphs take the value π. Because the two cosmic string velocities differ in direction by π, $\delta = \pi$ is a fixed point of photon direction. As Cutler showed, a crossing with positive slope is stable and blue-shifted, while the one with negative slope is unstable and red-shifted. The stable blue-shifted fixed point will always exist for $\gamma\delta_0 > 2$ (super-critical case) and thus represents a catastrophic divergence. This is because a particle in the presence of this geometry will fall into a stable orbit with exponentially diverging energy. The above graph is accurate for massless particles, but massive particles (equivalently: particles with nonzero momentum along the strings) will behave similarly once they become blue-shifted. In total, we find

- particle trajectories in the vicinity of a $\gamma\delta_0 > 2$ pair of cosmic strings will be attracted to the stable orientation $\delta(\alpha) = \pi$, $\delta'(\alpha) > 0$ (see Fig. 8). This is because the two cosmic strings velocities are equal and opposite, that is, when a particle incident at angle α_n is deflected by an angle δ_n, $\alpha_{n+1} = \alpha_n + \pi - \delta_n$. Thus not only is $\alpha = \pi$ a 'fixed point' of incidence angle, but it is a stable one if $\delta'(\alpha) > 0$, since then a slight increase in α will cause a slight increase in δ. A slight increase in δ will then decrease the next α, and return the system to equilibrium. (This assumes $\delta'(\alpha) < 1$, which is always the case.) Figure 6.9 illustrates the attractor in action.

- photon momentum in the plane perpendicular to the strings will be blue-shifted as given by Eq.(6.6). This formula applies to any relativistic particle. The blue shift occurs twice for each revolution, once from each string;

- since momenta along the string lengths are not blue-shifted, non-relativistic particles and particles with velocities along the length of the cosmic strings
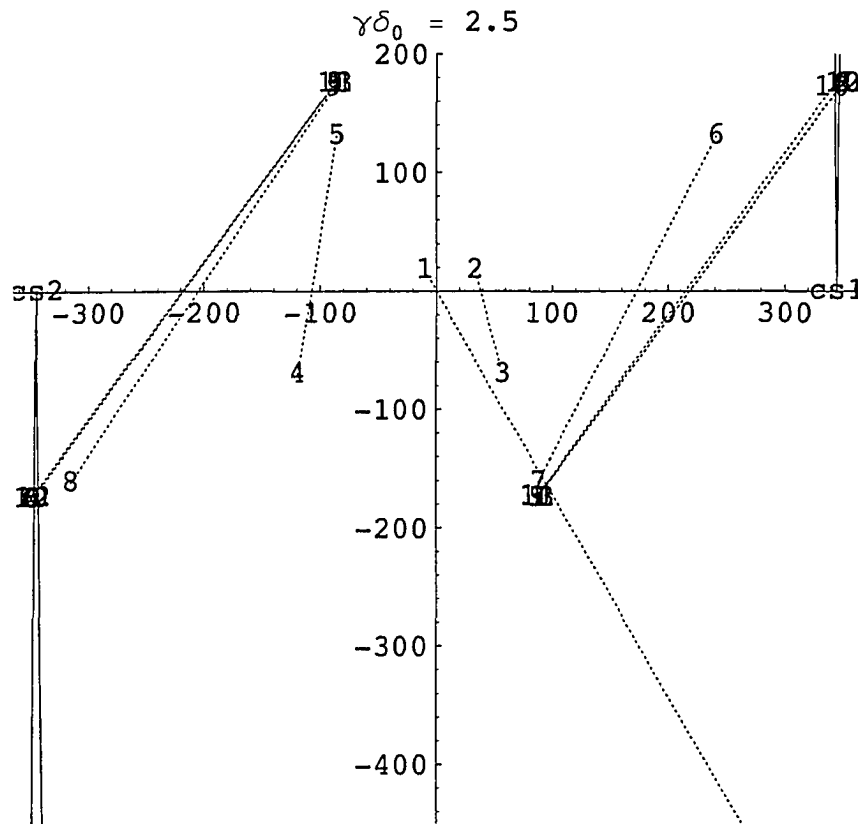
Figure 6.9: The supercritical case: Cosmic string #1 (cs1) is moving to the left and cosmic string #2 is moving to the right. The particle enters from the bottom right and reaches cs1's deficit angle at 1. Its world line appears to jump to the right to 2, now directed down and slightly to the right. This process continues indefinitely, 3, 4, ...∞, the world line spiraling clockwise outward as it falls into a stable orbit (the two long, outermost parallel segments). The coordinate discontinuity seen here does not reflect any actual discontinuity. The numbers on the world line satisfy $2n+1 \equiv 2n+2$ where the equivalence is identification via Eq.(2). The coordinate discontinuities plotted here are calculated with Eq.(6.3), and the trajectory angle is determined by Eq.(6.6). The initial conditions of the above trajectory are not tuned, but rather generic. Approximately half of all initial particle trajectories will end up in a CTC.

will be attracted to relativistic trajectories perpendicular to the string length;

- In the limit of small d the average distance to the core of the CTC will not vary. This means that the orbits will close, rather than shrink;

- the energy of each particle in the CTC will diverge exponentially as a function of number of cycles taken; since it takes no time to travel any number of cycles, infinite blue shift takes place;

- therefore, $\gamma\delta_0 > 2$ implies a catastrophic divergence in the presence of even a single particle.

It should be noted that the exponential divergence in energy is kinematic, and has nothing to do with particle number. Below is pictured the trajectory of a photon in a supercritical Gott space. The photon enters from the lower right, and then spirals clockwise outward into a stable, blue-shifted orbit. The upper and lower deficit angle wedges are moving to the left and right, respectively.

We thus may conclude that although closed light-like curves may exist ($\gamma\delta_0 = 2$), a purely classical divergence destroys the Gott solution of closed time-like curves ($\gamma\delta_0 > 2$) in the presence of a dynamical field (e.g. gravitons or photons). Cosmic string loops cannot produce closed time-like curves. This is in agreement with Li and Gott [111] which finds Misner space (and by implication Grant space and Gott space) to suffer from a classical instability similar to the one found here. It should be noted that the hoop conjecture is not involved in this breakdown. Even the 2+1 dimensional Gott space, where the hoop conjecture is not applicable, is unstable in the presence of dynamical fields.

6.5 Comments

6.5.1 General Discussions

Semi-classical gravity raises an objection to the existence of CTCs, or at least to spacetimes that contain both regions with CTCs and regions out of causal contact with them. The boundary between such regions is called the "chronology horizon," and in known examples this horizon coincides with a divergence of the renormalized energy-momentum tensor. This led Hawking to pose the "chronology protection conjecture," in which he proposes that any classical examples of spacetimes containing CTCs will be excluded by a quantum theory of gravity. Thorne and Kim disagreed [115] on the grounds that the divergence of $< T_{\mu\nu} >_{ren}$ is so weak that a full quantum gravity will remedy the semi-classical pathology. Grant found that the divergence on a set of polarized hypersurfaces is much larger than that on the chronology horizon. String theory can directly address the conjectures made using semi-classical arguments. Recent papers have evoked an Enhançon-like mechanism as a stringy method to forbid the formation of CTCs in some spacetimes [116]. On the other hand, a recent paper by Svendsen and Johnson demonstrated the existence of a fully string theoretic background (exact to all orders in α') containing CTCs and a chronology horizon, namely the Taub-NUT spacetime. It is not clear if g_s corrections destroy this result once matter is introduced, but the empty background is an exact result. This seems to provide a counterexample to the Chronology Protection conjecture.

It is easy to see that a cosmic string with only the lowest mode will start as a circle and collapse to a point. Before it reaches that limit, a black hole is formed. An elliptic or rectangular loop can be made to collapse to parallel, relativistic

segments without forming a black hole. Although we argue that potential CTCs will be disrupted by the presence of photons (or any other mode), it is also possible that the huge blue-shift will cause the formation of a black hole, resulting in a black hole with cosmic string loops protruding. In this case, the presence of CTCs inside the black hole is acceptable, since they are not observable. More analysis is needed to fully address this issue.

6.5.2 Specific Discussions on 2 + 1 Dimensions

A simpler scenario with CTCs was found by van Stockum [117] and Deser, Jackiw and 't Hooft (DJtH) [108] whereby a single stationary cosmic string is given angular momentum about its axis. The resulting background is given by

$$ds^2 = -(dt + Jd\theta)^2 + dz^2 + dr^2 + (1 - 4G\mu)^2 r^2 d\theta^2. \qquad (6.22)$$

It seems unlikely for such a cosmic string to exist in string theory (at least as fundamental objects [118]), since the cosmic strings in superstring theory lack the internal degree of freedom "spin". DJtH noticed an unusual feature of the Gott spacetime. They classified the energy momentum of Gott's solution in terms of the Lorentz transformations encountered under parallel transport (PT) around the strings (holonomy). It is well known that the PT transformations around a single cosmic string is rotation-like, i.e. can be expressed as

$$\Xi = \Lambda_\beta R_{\delta_0} \Lambda_{-\beta} \qquad (6.23)$$

where Λ_β is a pure boost with rapidity β and R_{δ_0} is a pure rotation about the angle δ_0. One may calculate the holonomy of a Gott pair via

$$\Xi = \Lambda_\beta R_{\delta_0} \Lambda_{-\beta} \Lambda_{-\beta} R_{\delta_0} \Lambda_\beta, \qquad (6.24)$$

and it is found that Ξ is boost-like, i.e. $\Xi = \Lambda_\beta \Lambda_\zeta \Lambda_{-\xi}$. DJtH regarded the energy momentum of a Gott pair to be unphysical on the grounds that its holonomy matches that of a tachyon (boost-like). It is an unusual feature of spacetimes that are not asymptotically flat that $T^{\mu\nu}$ can be space-like (tachyonic) despite the fact that it is made up of terms that are time-like.

Headrick and Gott [119] refuted this criticism by showing that the Gott pair geometry was quite unlike the tachyon geometry both because a tachyon does not yield CTCs and because the holonomy definition of $\overline{T^{\mu\nu}}$ was incomplete. Later, Carroll, Farhi, Guth and Olum (CFGO) [106] and 't Hooft [109] gave more convincing arguments against CTCs. CFGO and Gott and Headrick found that the PT transformation of a spinor distinguished between tachyon and Gott pair geometries. A more complete description of geometry would include not just the PT transformation, but the homotopy class of the PT transformation as well. Equivalently, one should extend $SO(2,1)$ to its universal covering group.

One may interpret the "boost-like" holonomy as boost identification, as was done by Grant [120]. This makes the Gott spacetime akin to a generalized Misner space. Grant was able to show that the Gott/Misner spacetime suffers from large quantum mechanical divergences on an infinite family of polarized light-like hypersurfaces. This divergence is stronger than that at the chronology horizon [120].

Regardless of whether the Gott spacetime is physical or not, it can be shown that the Gott spacetime in 2+1 dimensions cannot evolve from cosmic strings initially at rest [106]. This is quite different from the 3+1 dimensional case.

6.5.3   The Instability in 3 + 1 Dimensions

Recent realization of the inflationary scenario in superstring theory strongly suggests that cosmic superstrings were indeed produced toward the end of the inflationary epoch. With this possibility, the issue has renewed urgency. In the above discussions, we argue that the reasoning against the Gott spacetime in 2+1 dimensions does not apply to the 3+1 dimensional case. In short, the Gott spacetime is entirely possible in an ideal classical situation. However, we argue that instability set in if there is a quanta/particle nearby. The particle will be attracted to the closed time-like curve and is infinitely blue-shifted instantly. Of course, back reaction takes place before this happens. This back reaction must disrupt the closed time-like curve, otherwise the infinite blue-shift will not be prevented. In an ideal situation where there is no quanta nearby, one still expects particles like (very soft) gravitons/photons can emerge due to quantum fluctuation. In fact, quantum fluctuation of the cosmic strings themselves as they move rapidly toward each other will produce graviton radiations. One graviton, no matter how soft, is sufficient to cause the instability. So we believe that the Gott spacetime is unstable under tiny perturbations and so cannot be formed in any realistic situation.

6.6   Conclusion

Recent implementation of the inflationary scenario into superstring theory led to the possibility that cosmic strings were produced toward the end of brane inflation in the brane world. This possibility leads us to re-examine the Gott spacetime, where closed time-like curves appear as two cosmic strings move ultra-relativistically pass each other. In an ideal situation, the Gott spacetime is an exact

solution to Einstein equation, with a well-defined chronology horizon. It does not collapse into a black hole and can be readily reached. So it seems perfectly sensible that such a spacetime can be present in a universe that contains cosmic strings. In this chapter, we find that nearby photons and gravitons will be attracted to the closed time-like curves, resulting in an instantaneous infinite blue-shift. This really implies that the back-reaction must be large enough to disrupt the formation of such closed time-like curves. We interpret this as a realization of the chronology protection conjecture in the case of the $3+1$ dimensional Gott spacetime.

APPENDIX A

THE GEOMETRIC DELTA FUNCTION

A.1 Definition

On a D dimensional oriented manifold $\mathcal{M}^D$ with $\mathcal{M}^p \subseteq \mathcal{M}^D$ an oriented sub-manifold of dimension p we define the "Dirac delta $(D-p)$-form" $\delta_{D-p}(\mathcal{M}^p)$ as follows:

$$\int_{\mathcal{M}^D} C_p \wedge \delta_{D-p}(\mathcal{M}^p) := \int_{\mathcal{M}^D \cap \mathcal{M}^p} C_p \tag{A.1}$$

where the pullback is implicit on the RHS. The subscripts denote the order (for differential forms), and superscripts denote the dimension (for manifolds, immersions, and chains). Stokes' theorem then implies

$$
\begin{aligned}
\int_{\partial \mathcal{M}^D} C_{p-1} \wedge \delta_{D-p}(\mathcal{M}^p) &= \int_{\mathcal{M}^D} dC_{p-1} \wedge \delta_{D-p}(\mathcal{M}^p) + (-1)^{p-1} C_{p-1} \wedge d\delta_{D-p}(\mathcal{M}^p) \\
&= \int_{\partial(\mathcal{M}^D \cap \mathcal{M}^p)} C_{p-1} + (-1)^{p-1} \int_{\mathcal{M}^D} C_{p-1} \wedge d\delta_{D-p}(\mathcal{M}^p)
\end{aligned}
$$

and so

$$d\delta_{D-p}(\mathcal{M}^p) = (-1)^p \delta_{D-p+1}(\partial \mathcal{M}^p), \tag{A.2}$$

where we have used the fact that $\partial(\mathcal{M}^p \cap \mathcal{M}^q) = (\partial \mathcal{M}^p \cap \mathcal{M}^q) \cup (-1)^{D-p}(\mathcal{M}^p \cap \partial \mathcal{M}^q)$. Here $\cup$ is essentially the group sum of r-chains in $\mathcal{M}^D$. This definition of $\cup$ is equivalent to

$$\delta_{D-p}(\mathcal{M}^p \cup \mathcal{M}^{p'}) = \delta_{D-p}(\mathcal{M}^p) + \delta_{D-p}(\mathcal{M}^{p'}). \tag{A.3}$$

Also, following the definition we find

$$
\begin{aligned}
\int_{\mathcal{M}^D} C_{p+q-D} \wedge \delta_{D-p}(\mathcal{M}^p) \wedge \delta_{D-q}(\mathcal{M}^q) &= \int_{\mathcal{M}^D \cap \mathcal{M}^q} C_{p+q-D} \wedge \delta_{D-p}(\mathcal{M}^p) \\
&= \int_{\mathcal{M}^D \cap \mathcal{M}^q \cap \mathcal{M}^p} C_{p+q-D}
\end{aligned}
$$

123

which leads to the relation

$$\delta_{D-p}(\mathcal{M}^p) \wedge \delta_{D-q}(\mathcal{M}^q) = \delta_{2D-p-q}(\mathcal{M}^q \cap \mathcal{M}^p) \qquad \text{(A.4)}$$

This identity illuminates some generic features of submanifolds.

- The intersection of a p and a q dimensional submanifold in D dimensions will generally be of dimension $p + q - D$.

- When the previous statement does not hold, integration on the intersection must vanish. This is because the intersection is not stable under infinitesimal perturbation (and not transversal). Consider the case where $\mathcal{M}^p \cap \mathcal{M}^q$ is tuned to be of dimension $p + q - D + n$. If $n > 0$, then an infinitesimal perturbation of either manifold will break up the intersection into an n-dimensional array of $p + q - D$ dimensional manifolds, but with alternating orientations. The alternating orientations cause the integral to vanish. If $n < 0$ then the infinitesimal perturbation blows the intersection up into a manifold of the proper dimension, but one of measure zero (from Sard's theorem).

- For example, consider two 2-planes in three dimensions which are tuned to be tangent over some (two dimensional) region. After infinitesimal perturbation, the intersection would look like a map of a coastline with many "lakes" and "islands" and lakes on the islands etc. But each shore has opposite orientation with respect to that of its neighbors, and so the *oriented intersection* vanishes.

- Now consider two cosmic strings tuned to be completely coincident in four dimensional spacetime. Under perturbation this becomes a two-dimensional

array of points (events). The orientation (sign) of each point is determined by the relative velocity and angle between the strings at the points of intersection: the sign of $(\hat{s}_1 \times \hat{s}_2) \cdot (v_1 - v_2)$ determines the sign of the intersection event. This will alternate like a checkerboard, and so again the (oriented) intersection is actually empty. (Here, $\hat{s}$ is tangent to the string in the direction of its orientation, and v is the string's transverse velocity.)

- When two submanifolds each have odd co-dimension, the orientation of their intersection flips when the order of the manifolds is reversed. This is consistent with the Leibniz rule for the boundary operator given below Eqn.(A.2). As an example of this, consider two 2-planes in three dimensions, whose intersection is a line. The orientation of each plane is characterized by a normal vector, and the anti-symmetric cross product of these is used to determine the orientation of the line of intersection.

- We will think of $\cap$ as being the sort of oriented intersection operation from intersection homology which makes the above properties automatic (i.e. it is stable under infinitesimal perturbation of either submanifold).

A.2 Coordinate Representation

The coordinate representation of $\delta_{D-p}(\mathcal{M}^p)$ is straightforward in coordinates where the submanifold is defined by the $D - p$ scalar constraint equations

$$q \in \mathcal{M}^p \quad \Longrightarrow \quad \lambda^i(x^1[q], ..., x^D[q]) = 0 \qquad i = 1...D - p \qquad \text{(A.5)}$$

via

$$\delta_{D-p}(\mathcal{M}^p) = \delta^{(D-p)}(\lambda^i) \, d\lambda^1 \wedge .... \wedge d\lambda^{D-p} \qquad \text{(A.6)}$$

where $\delta^{(D-p)}$ is the usual $D-p$ dimensional Dirac delta function. The well known transformation properties of the Dirac delta function make this object automatically a differential form. (Thus the only meaningful zeros of the λ^i are transversal zeros, i.e. those where λ^i changes sign in any neighborhood of the zero.) If a submanifold is D-dimensional, then the corresponding Dirac delta 0-form is simply the characteristic function: $\delta_0(\mathcal{M}^{D\prime}) = \mathcal{X}_{\mathcal{M}^{D\prime}}$ with

$$
\begin{aligned}
\mathcal{X}_{\mathcal{M}^{D\prime}}(q) &= 1 \qquad q \in \mathcal{M}^{D\prime} \\
&= 0 \qquad q \notin \mathcal{M}^{D\prime}.
\end{aligned}
$$

One may describe submanifolds with boundary by multiplication with an appropriate Dirac delta 0-form c.f. Eqn.(A.4). As an example, if $\mathcal{M}^1$ is the positive x-axis in $\mathbb{R}^3$, then

$$
\delta_2(\mathcal{M}^1) = \delta(y)\delta(z)\Theta(x)dy \wedge dz \tag{A.7}
$$

where the characteristic function $\mathcal{X}(x^\mu)$ is the Heaviside function $\Theta(x)$. Notice that the orientation of this submanifold has been chosen to be along the $+x$ direction, consistent with Eqn.(A.2) and the fact that its boundary is *minus* the point at the origin.

The λ^i do not need to be well-defined on the entire manifold, and in fact they only need to be defined at all in a neighborhood of $\mathcal{M}^p$. Thus despite its appearance in Eqn.(A.6), $\delta_{D-p}(\mathcal{M}^p)$ is not necessarily a total derivative.

If all of the λ^i are well defined everywhere, then $\mathcal{M}^p$ is an algebraic variety. By Eqn.(A.2) and Eqn.(A.6) it can be seen that all algebraic varieties can be written globally as boundaries. It may be that the λ^i are well defined only in a neighborhood of $\mathcal{M}^p$, in which case $\mathcal{M}^p$ is a submanifold. Near points not on $\partial\mathcal{M}^p$ we may think of $\mathcal{M}^p$ locally as a boundary, just as we may think of a closed

differential form as locally exact. Non-orientable submanifolds will correspond to constraints that may be double valued, that is λ^i may return to minus itself upon translation around the submanifold. We consider such cases in section A.5. Another important case occurs when $\mathcal{M}^p$ is only an immersion, i.e. it intersects itself. The λ^i are path dependent here, as well. Consider the immersion $S^1 \subset \mathbb{R}^2$ defined by the constraint $\lambda = 2\arcsin(y) - \arcsin(x) = 0$. This looks like a figure-eight centered on the origin of the plane. Clearly λ is multi-valued, and to get a complete figure eight requires summing over two branches of λ. We suppress the sum in Eqn.(A.6). Notice that the figure eight immersion satisfies

$$\delta_1(S^1) \wedge \delta_1(S^1) = \delta_2(0) - \delta_2(0) = 0.$$

The self intersection of this immersion is twice the point at the origin, but since the orientation (sign) of the intersection is negative for exactly one of the two points of intersection, the total self intersection vanishes. For even co-dimemsion immersions, the sum over branches allows for non-zero self intersection from cross terms. By the antisymmetry of the wedge product, one may show that the self-intersection of an immersion of odd co-dimension will always vanish, assuming $\mathcal{M}^D$ is orientable. One may also compute the nth self intersection of an immersion via

$$\delta_{n(D-p)}(\cap^n \mathcal{M}^p) = \bigwedge_n \delta_{D-p}(\mathcal{M}^p).$$

A.3 Geometry

If we introduce a metric on our manifold, we can measure the volume of our submanifolds with the volume element $\sqrt{|g|}\big|_p$ from the pull-back metric. Looking at the coordinate definition of $\delta_{D-p}(\mathcal{M}^p)$ given in Eqn.(A.5), we see that each of the λ^i is constant along the submanifold, and so $d\lambda^i$ is orthogonal to the submanifold.

Thus, a good candidate for a volume element on $\mathcal{M}^p$ is $*(d\lambda^1 \wedge ... \wedge d\lambda^{D-p})$. To remove the rescaling redundancy in the λ^is we may divide by $\sqrt{*(\bigwedge_i d\lambda^i \wedge *\bigwedge_j d\lambda^j))}$. Equivalently, we may formally write

$$\sqrt{|g|}_p = \frac{*\delta_{D-p}(\mathcal{M}^p)}{||\delta_{D-p}(\mathcal{M}^p)||} \tag{A.8}$$

where the pull-back is implicit on the RHS and

$$||\delta_{D-p}(\mathcal{M}^p)|| = \sqrt{*(\delta_{D-p}(\mathcal{M}^p) \wedge *\delta_{D-p}(\mathcal{M}^p))}.$$

Despite its appearance, $\frac{*\delta_{D-p}(\mathcal{M}^p)}{||\delta_{D-p}(\mathcal{M}^p)||}$ is a p-form living in all D-dimensions, although its only well defined on $\mathcal{M}^p$. This is because in Eqn.(A.8) the Dirac delta function coefficients cancel, leaving dependence only on the smooth λ^is. Because of this, we may define $d * \frac{\delta_{D-p}(\mathcal{M}^p)}{||\delta_{D-p}(\mathcal{M}^p)||}$ using the full D-dimensional exterior derivative. Surprisingly, this is well defined on $\mathcal{M}^p$, and it is not hard to show that (when restricting to points on the submanifold)

$$d * \frac{\delta_{D-p}(\mathcal{M}^p)}{||\delta_{D-p}(\mathcal{M}^p)||} = 0 \quad \Longleftrightarrow \quad \mathcal{M}^p \text{ is extremal.} \tag{A.9}$$

From Eqn.(A.8) it is evident that $||\delta_{D-p}(\mathcal{M}^p)|| = *_p * \delta_{D-p}(\mathcal{M}^p)$, where the Hodge star on $\mathcal{M}^p$ from the pullback metric is denoted by $*_p$. More generally, the action by this Hodge star can be rewritten as

$$*_p F_q = * \frac{F_q \wedge \delta_{D-p}(\mathcal{M}^p)}{||\delta_{D-p}(\mathcal{M}^p)||} \tag{A.10}$$

where F_q is a q-form living on $\mathcal{M}^p$ and the pullback is implicit on the left hand side.

A.4 Topology

One feature of the delta form is that Poincaré duality becomes manifest. Here we assume $\mathcal{M}^D$ is orientable and compact with no boundary. Then Eqn.(A.2) tells

us that $\delta_{D-p}(\mathcal{M}^p)$ is closed if and only if $\mathcal{M}^p$ is a cycle, and $\delta_{D-p}(\mathcal{M}^p)$ is exact if $\mathcal{M}^p$ is a boundary. To complete this correspondence between the p-th Homology and the $D - p$th de Rham Cohomology of $\mathcal{M}^D$ we need to show that

$$\delta_{D-p}(\mathcal{M}^p) = df_{D-p-1} \quad \Longrightarrow \quad \mathcal{M}^p = \partial \mathcal{M}^{p+1}. \tag{A.11}$$

But this is not true when torsion is present. Consider the manifold $\mathbb{RP}^3 = SO(3)$ which has a single nontrivial one-cycle ζ^1, i.e. $H_1(\mathbb{RP}^3; \mathbb{Z}) = \mathbb{Z}_2$. Since the group sum of two of these cycles is trivial, they must form a boundary: $\zeta^1 + \zeta^1 = \partial \mathcal{M}^2$ and so $2\delta_2(\zeta^1) = d\delta_1(\mathcal{M}^2)$ which means

$$\delta_2(\zeta^1) = \frac{1}{2} d\delta_1(\mathcal{M}^2). \tag{A.12}$$

Only by using real coefficients can we make the statement that

$$\mathcal{M}^p \simeq \mathcal{M}^{p'} \quad \Longleftrightarrow \quad [\delta_{D-p}(\mathcal{M}^p)] \simeq [\delta_{D-p}(\mathcal{M}^{p'})] \tag{A.13}$$

De Rham's theorem gives us the isomorphism between homology and cohomology

$$H_p(\mathcal{M}^D; \mathbb{R}) \cong H^p(\mathcal{M}^D; \mathbb{R}),$$

and Poincaré duality asserts that

$$H_p(\mathcal{M}^D; \mathbb{R}) \cong H_{D-p}(\mathcal{M}^D; \mathbb{R}).$$

The delta form provides the isomorphism

$$H_p(\mathcal{M}^D; \mathbb{R}) \cong H^{D-p}(\mathcal{M}^D; \mathbb{R}) \tag{A.14}$$

In fact, if the cohomology basis is chosen such that

$$\int_{\mathcal{M}^{D-p}_{(j)}} \omega^{(i)}_{D-p} = \delta^{ij}$$

then

$$[\delta_{D-p}(\mathcal{M}^p_{(i)})] = [\omega^{(i)}_{D-p}] \qquad \text{(A.15)}$$

where $\mathcal{M}^p_{(i)}$ is the Poincaré dual of $\mathcal{M}^{D-p}_{(i)}$, and together they satisfy

$$\mathcal{M}^p_{(i)} \cap \mathcal{M}^{D-p}_{(j)} = \delta_{ij},$$

i.e. their (net) intersection is a single (positive) point if $i = j$, and is empty otherwise.

A.5 Non-Orientable Submanifolds

If $\mathcal{M}^p$ is non-orientable then an odd number of the functions f^i will be double valued and so $\delta_{D-p}(\mathcal{M}^p)$ will not be well defined. More precisely, $\delta_{D-p}(\mathcal{M}^p)$ is double valued for one-sided submanifolds. We could try to work with the unique orientable double cover $\tilde{\mathcal{M}}^p$ and the well defined $\delta_{D-p}(\tilde{\mathcal{M}}^p)$. But since $\delta_{D-p}(\tilde{\mathcal{M}}^p)$ returns to *minus* itself upon one non-trivial circut, the form seems to vanish:

$$\delta_{D-p}(\tilde{\mathcal{M}}^p) = \delta_{D-p}(\mathcal{M}^p) - \delta_{D-p}(\mathcal{M}^p) = 0. \qquad \text{(A.16)}$$

We can nevertheless construct non-vanishing integrals over $\mathcal{M}^p$ by using twisted p-forms such as the volume form on $\mathcal{M}^p$. $\sqrt{|g|}\big|_p$ is easily seen to be double valued on $\mathcal{M}^p$, and so its wedge product with $\delta_{D-p}(\mathcal{M}^p)$ is well defined:

$$\mathcal{V}ol[\mathcal{M}^p] = \int_{\mathcal{M}^D} \frac{*\delta_{D-p}(\mathcal{M}^p)}{||\delta_{D-p}(\mathcal{M}^p)||} \wedge \delta_{D-p}(\mathcal{M}^p). \qquad \text{(A.17)}$$

The anti-periodicity of $\delta_{D-p}(\mathcal{M}^p)$ is irrelevant in the above equation since it appears twice. Thus the standard formula Eqn.(A.17) applies to *any* immersion, not just oriented submanifolds.

By considering the homology with $\mathbb{Z}_2$ coefficients, we may extend Poincaré duality to non-orientable cycles using a sort of $\mathbb{Z}_2$ cohomology. Consider the manifold $SO(3) \simeq \mathbb{R}P^3$. The zeroth homology is $\mathbb{Z}_2$, which is dual to the $3rd$ cohomology, the volume form normalized to give unit volume modulo $\mathbb{Z}_2$. The first homology is also $\mathbb{Z}_2$, generated by the nontrivial cycle well known to represent "one rotation" of a three dimensional solid. The second cohomology is generated by the twisted 2–form which represents the volume form of an $\mathbb{R}P^2 \subset \mathbb{R}P^3$ with unit surface area. Thus Poincaré duality is again manifest, and intersection number provides a natural non-degenerate mapping between a class and its Poincaré dual.

On $\mathbb{R}P^2$, the single one-cycle satisfies $\zeta^1 \cap \zeta^1 = 1$, that is the cycle intersects *itself* at a single point modulo $\mathbb{Z}_2$. This implies that

$$\int_{\mathbb{R}P^2} \delta_1(\zeta^1) \wedge \delta_1(\zeta^1) = 1 \tag{A.18}$$

which seems odd since the anti-symmetry should make the wedge product vanish. The resolution is that the Poincaré dual of a one-cocycle is a *twisted* one-cocycle. The antisymmetry of the wedge product is cancelled by the antisymmetry of changing which of the two 1-forms is twisted in Eqn.(A.18).

A.6 Complex Notation

If a (complex) codimension m submanifold of $\mathbb{C}^n$ is defined by the zeros of m holomorphic functions $\lambda^j(z)$ then

$$\delta_{m,m}(\mathcal{M}^{n-m}) = \bigwedge_{j=1}^{m} \frac{1}{2\pi i} d^2 \log(\lambda^i(z)). \tag{A.19}$$

For purposes of computing pullback metrics, we may simply write this as proportional to

$$i^m \bigwedge_{j=1}^{m} d\lambda^j \wedge \overline{d\lambda^j}. \tag{A.20}$$

The transformation properties of the Dirac delta function make its extension to differential forms very natural. The computational usefulness of these Dirac delta forms is that they allow a purely target space phrasing of integration, and thus allow one to write *bulk* equations of motion for branes and other localized degrees of freedom. One may compute integrals over submanifolds without invoking a pullback. From a homological point of view, $\delta_{D-p}(\mathcal{M}^p)$ is the Poincaré dual of $\mathcal{M}^p$.

APPENDIX B

LIST OF ABBREVIATIONS AND ACRONYMS

BPS   - Bogolmo'nyi, Prasad, Sommerfeld; usually referring to BPS solitons in supersymmetric theories, which exhibit no force between them

CFT   - Conformal Field Theory

CMB   - Comsic Microwave Background

DBI   - Dirac, Born, Infeld, specifically the DBI action of nonlinear electrodynamics

$D\bar{D}$ - Brane anti-brane

F- & D-   - Fundamental and Dirichlet strings (D1-branes)

FRW   - Friedmann-Robertson-Walker

GP   - Gimon, Polchinski [46]

GR   - General Relativity

GSO   - Gliozzi, Scherk, Olive [121], as in the GSO projection which projects worldsheet supersymmetric theories into modular invariant theories with $\mathcal{N} = (2,0)$, $\mathcal{N} = (1,1)$, or $\mathcal{N} = (1,0)$ spacetime supersymmetry

$G\mu$ - The dimensionless ratio of cosmic string tension to Planck mass squared relevant in 4D cosmic string physics

GUT   - Grand Unified Theory

KKLMMT - Kachru, Kallosh, Linde, Maldacena, McAllister, Trivedi [23]

KKLT   - Kachru, Kallosh, Linde, Trivedi [22]

KS   - Klebanov, Strassler [25]

133

LIGO   - Laser Interferometer Gravitational Wave Observatory

LISA   - Laser Interferometer Space Antenna (launch date: 2015)

LHC   - Large Hadron Collider

NS-NS - Closed string modes arising from holomorphic and antiholomorphic Neveu-Schwarz worldsheet fermions

Planck - A high resolution CMB anisotropy experiment (launch date: 2007)

QFT   - Quantum Field Theory

QUIET - Q/U Image ExperimenT for measureing B-mode polarization of the CMB

R-R   - Closed string modes arising from holomorphic and antiholomorphic Ramond worldsheet fermions

RS   - Randall, Sundrum [122,123]

SM   - The Standard Model of particle physics

SUSY - Supersymmetry

VSF   - Vector superfield

WMAP - Wilkinson Microwave Anisotropy Probe

BIBLIOGRAPHY

[1] G. R. Dvali and S.-H. H. Tye, *Brane inflation*, *Phys. Lett.* **B450** (1999) 72–82, [hep-ph/9812483].

[2] N. T. Jones, H. Stoica, and S. H. H. Tye, *Brane interaction as the origin of inflation*, *JHEP* **07** (2002) 051, [hep-th/0203163].

[3] S. Sarangi and S. H. H. Tye, *Cosmic string production towards the end of brane inflation*, *Phys. Lett.* **B536** (2002) 185–192, [hep-th/0204074].

[4] N. T. Jones, H. Stoica, and S. H. H. Tye, *The production, spectrum and evolution of cosmic strings in brane inflation*, *Phys. Lett.* **B563** (2003) 6–14, [hep-th/0303269].

[5] J. B. Hartle and S. W. Hawking, *Wave function of the universe*, *Phys. Rev.* **D28** (1983) 2960–2975.

[6] H. Firouzjahi, S. Sarangi, and S. H. H. Tye, *Spontaneous creation of inflationary universes and the cosmic landscape*, *JHEP* **09** (2004) 060, [hep-th/0406107].

[7] H. Firouzjahi and S. H. H. Tye, *Brane inflation and cosmic string tension in superstring theory*, *JCAP* **0503** (2005) 009, [hep-th/0501099].

[8] M. Wyman, L. Pogosian, and I. Wasserman, *Bounds on cosmic strings from wmap and sdss*, *Phys. Rev.* **D72** (2005) 023513, [astro-ph/0503364].

[9] D. P. Bennett and F. R. Bouchet, *Evidence for a scaling solution in cosmic string evolution*, *Phys. Rev. Lett.* **60** (1988) 257.

[10] B. Allen and E. P. S. Shellard, *Cosmic string evolution: A numerical simulation*, *Phys. Rev. Lett.* **64** (1990) 119–122.

[11] S. H. H. Tye, I. Wasserman, and M. Wyman, *Scaling of multi-tension cosmic superstring networks*, *Phys. Rev.* **D71** (2005) 103508, [astro-ph/0503506].

[12] M. G. Jackson, N. T. Jones, and J. Polchinski, *Collisions of cosmic f- and d-strings*, *JHEP* **10** (2005) 013, [hep-th/0405229].

[13] S. Dodelson, *Modern cosmology*. Amsterdam, Netherlands: Academic Pr. (2003) 440 p.

[14] W. Hu, *Cmb temperature and polarization anisotropy fundamentals*, *Ann. Phys.* **303** (2003) 203–225, [astro-ph/0210696].

[15] E. W. Kolb and M. S. Turner, *The early universe*, *Front. Phys.* **69** (1990) 1–547.

[16] N. Kaiser and A. Stebbins, *Microwave anisotropy due to cosmic strings*, *Nature* **310** (1984) 391–393.

[17] A. Hanany and K. Hashimoto, *Reconnection of colliding cosmic strings*, *JHEP* **06** (2005) 021, [hep-th/0501031].

[18] L. Pogosian, I. Wasserman, and M. Wyman, *On vector mode contribution to cmb temperature and polarization from local strings*, astro-ph/0604141.

[19] A. H. Guth, *The inflationary universe: A possible solution to the horizon and flatness problems*, *Phys. Rev.* **D23** (1981) 347–356.

[20] A. D. Linde, *A new inflationary universe scenario: A possible solution of the horizon, flatness, homogeneity, isotropy and primordial monopole problems*, *Phys. Lett.* **B108** (1982) 389–393.

[21] A. Albrecht and P. J. Steinhardt, *Cosmology for grand unified theories with radiatively induced symmetry breaking*, *Phys. Rev. Lett.* **48** (1982) 1220–1223.

[22] S. Kachru, R. Kallosh, A. Linde, and S. P. Trivedi, *De-Sitter vacua in string theory*, *Phys. Rev.* **D68** (2003) 046005, [hep-th/0301240].

[23] S. Kachru, R. Kallosh, A. Linde, J. Maldacena, L. McAllister, and S. P. Trivedi, *Towards inflation in string theory*, *JCAP* **0310** (2003) 013, [hep-th/0308055].

[24] S. B. Giddings, S. Kachru, and J. Polchinski, *Hierarchies from fluxes in string compactifications*, *Phys. Rev.* **D66** (2002) 106006, [hep-th/0105097].

[25] I. R. Klebanov and M. J. Strassler, *Supergravity and a confining gauge theory: Duality cascades and chi SB-resolution of naked singularities*, *JHEP* **08** (2000) 052, [hep-th/0007191].

[26] O. DeWolfe, S. Kachru, and H. L. Verlinde, *The giant inflaton*, *JHEP* **05** (2004) 017, [hep-th/0403123].

[27] E. Silverstein and D. Tong, *Scalar speed limits and cosmology: Acceleration from d- cceleration*, *Phys. Rev.* **D70** (2004) 103505, [hep-th/0310221].

[28] M. Alishahiha, E. Silverstein, and D. Tong, *Dbi in the sky*, *Phys. Rev.* **D70** (2004) 123505, [hep-th/0404084].

[29] S. E. Shandera, *Slow roll in brane inflation*, *JCAP* **0504** (2005) 011, [hep-th/0412077].

[30] S. E. Shandera and S. H. H. Tye, *Observing brane inflation*, *JCAP* **0605** (2006) 007, [hep-th/0601099].

[31] C. P. Burgess, M. Majumdar, D. Nolte, F. Quevedo, G. Rajesh, and R. Zhang, *The inflationary brane-antibrane universe*, *JHEP* **07** (2001) 047, [http://arXiv.org/abs/hep-th/0105204].

[32] C. P. Burgess, P. Martineau, F. Quevedo, G. Rajesh, and R. J. Zhang, *Brane antibrane inflation in orbifold and orientifold models*, *JHEP* **03** (2002) 052, [hep-th/0111025].

[33] R. Rabadan and F. Zamora, *Dilaton tadpoles and d-brane interactions in compact spaces*, *JHEP* **12** (2002) 052, [hep-th/0207178].

[34] J. Garcia-Bellido, R. Rabadán, and F. Zamora, *Inflationary scenarios from branes at angles*, *JHEP* **01** (2002) 036, [http://arXiv.org/abs/hep-th/0112147].

[35] E. T. Whittaker and G. N. Watson, *A course in modern analysis*. Cambridge Univesity Press (1902).

[36] P. P. Ewald, *Die berechnung optischer und elektrostatischer gitterpotentiale*, *Ann. Phys.* **64** (1921) 253.

[37] C. Kittel, *Introduction to solid state physics*. John Wiley and Sons (1996).

[38] C. Herdeiro, S. Hirano, and R. Kallosh, *String theory and hybrid inflation / acceleration*, *JHEP* **12** (2001) 027, [http://arXiv.org/abs/hep-th/0110271].

[39] K. Dasgupta, C. Herdeiro, S. Hirano, and R. Kallosh, *D3/D7 inflationary model and M-theory*, *Phys. Rev.* **D65** (2002) 126002, [http://arXiv.org/abs/hep-th/0203019].

[40] M. Gomez-Reino and I. Zavala, *Recombination of intersecting D-branes and cosmological inflation*, *JHEP* **09** (2002) 020, [http://arXiv.org/abs/hep-th/0207278].

[41] T. W. B. Kibble, *Topology of cosmic domains and strings*, *J. Phys.* **A9** (1976) 1387–1398.

[42] J. Polchinski, *String Theory. Vol. 2: Superstring Theory and Beyond*. Cambridge Univ. Pr., 1998.

[43] P. Horava, *Strings on world sheet orbifolds*, *Nucl. Phys.* **B327** (1989) 461.

[44] J. Dai, R. G. Leigh, and J. Polchinski, *New connections between string theories*, *Mod. Phys. Lett.* **A4** (1989) 2073–2083.

[45] R. G. Leigh, *Dirac-born-infeld action from dirichlet sigma model*, *Mod. Phys. Lett.* **A4** (1989) 2767.

[46] E. G. Gimon and J. Polchinski, *Consistency conditions for orientifolds and d-manifolds*, Phys. Rev. **D54** (1996) 1667–1676, [hep-th/9601038].

[47] E. G. Gimon and C. V. Johnson, *K3 orientifolds*, Nucl. Phys. **B477** (1996) 715–745, [hep-th/9604129].

[48] J. Polchinski, *String Theory. Vol. 1: An Introduction to the Bosonic String*. Cambridge Univ. Pr., 1998.

[49] S. Sugimoto, *Anomaly cancellations in type i d9-d9-bar system and the usp(32) string theory*, Prog. Theor. Phys. **102** (1999) 685–699, [hep-th/9905159].

[50] G. Aldazabal, A. Font, L. E. Ibanez, and G. Violero, $D = 4$, $N = 1$, *type IIB orientifolds*, Nucl. Phys. **B536** (1998) 29–68, [hep-th/9804026].

[51] A. Sen, *F-theory and orientifolds*, Nucl. Phys. **B475** (1996) 562–578, [hep-th/9605150].

[52] C. V. Johnson, *D-Branes*. Cambridge, USA: Univ. Pr. (2003) 548 p.

[53] A. Sen, *F-theory and the gimon-polchinski orientifold*, Nucl. Phys. **B498** (1997) 135–155, [hep-th/9702061].

[54] N. Turok and P. Bhattacharjee, *Stretching cosmic strings*, Phys. Rev. **D29** (1984) 1557.

[55] J. Polchinski and J. V. Rocha, *Analytic study of small scale structure on cosmic strings*, hep-ph/0606205.

[56] L. Leblond and S. H. H. Tye, *Stability of d1-strings inside a d3-brane*, JHEP **03** (2004) 055, [hep-th/0402072].

[57] J. Polchinski, *Open heterotic strings*, hep-th/0510033.

[58] E. Witten, *Cosmic superstrings*, Phys. Lett. **B153** (1985) 243.

[59] E. J. Copeland, R. C. Myers, and J. Polchinski, *Cosmic f- and d-strings*, JHEP **06** (2004) 013, [hep-th/0312067].

[60] J. J. Blanco-Pillado, G. Dvali, and M. Redi, *Cosmic d-strings as axionic d-term strings*, Phys. Rev. **D72** (2005) 105002, [hep-th/0505172].

[61] L. Perivolaropoulos, *The rise and fall of the cosmic string theory for cosmological perturbations*, Nucl. Phys. Proc. Suppl. **148** (2005) 128–140, [astro-ph/0501590].

[62] H. Firouzjahi, L. Leblond, and S. H. Henry Tye, *The (p,q) string tension in a warped deformed conifold*, JHEP **05** (2006) 047, [hep-th/0603161].

[63] B. Shlaer and M. Wyman, *Cosmic superstring gravitational lensing phenomena: Predictions for networks of (p,q) strings*, Phys. Rev. **D72** (2005) 123504, [hep-th/0509177].

[64] B. Shlaer and S. H. H. Tye, *Cosmic string lensing and closed time-like curves*, Phys. Rev. **D72** (2005) 043532, [hep-th/0502242].

[65] R. E. Schild, I. S. Masnyak, B. I. Hnatyk, and V. I. Zhdanov, *Anomalous fluctuations in observations of q0957+561 a,b: Smoking gun of a cosmic string?*, Astron. Astrophys. **422** (2004) 477–482, [astro-ph/0406434].

[66] L. Pogosian, S. H. H. Tye, I. Wasserman, and M. Wyman, *Observational constraints on cosmic string production during brane inflation*, Phys. Rev. **D68** (2003) 023506, [hep-th/0304188].

[67] T. Damour and A. Vilenkin, *Gravitational wave bursts from cusps and kinks on cosmic strings*, Phys. Rev. **D64** (2001) 064008, [gr-qc/0104026].

[68] N. Turok, *Grand unified strings and galaxy formation*, Nucl. Phys. **B242** (1984) 520.

[69] X. Siemens and K. D. Olum, *Cosmic string cusps with small-scale structure: Their forms and gravitational waveforms*, Phys. Rev. **D68** (2003) 085017, [gr-qc/0307113].

[70] T. Damour and A. Vilenkin, *Gravitational radiation from cosmic (super)strings: Bursts, stochastic background, and observational windows*, Phys. Rev. **D71** (2005) 063510, [hep-th/0410222].

[71] X. Siemens et al., *Gravitational wave bursts from cosmic (super)strings: Quantitative analysis and constraints*, Phys. Rev. **D73** (2006) 105001, [gr-qc/0603115].

[72] R. A. Battye, R. R. Caldwell, and E. P. S. Shellard, *Gravitational waves from cosmic strings*, astro-ph/9706013.

[73] L. Bildsten, *Gravitational radiation and rotation of accreting neutron stars*, Astrophys. J. **501** (1998) L89, [astro-ph/9804325].

[74] H. Firouzjahi and S. H. H. Tye, *The tension spectrum of cosmic superstrings in a warped deformed conifold*, hep-th/0506264.

[75] A. N. Lommen, *New limits on gravitational radiation using pulsars*, astro-ph/0208572.

[76] V. M. Kaspi, J. H. Taylor, and M. F. Ryba, *High - precision timing of millisecond pulsars. 3: Long - term monitoring of psrs b1855+09 and b1937+21*, Astrophys. J. **428** (1994) 713.

[77] E. Jeong and G. F. Smoot, *Search for cosmic strings in cmb anisotropies*, *Astrophys. J.* **624** (2005) 21–27, [astro-ph/0406432].

[78] A. Vilenkin, *Gravitational field of vacuum domain walls and strings*, *Phys. Rev.* **D23** (1981) 852–857.

[79] A. Vilenkin, *Looking for cosmic strings*, *Nature* **322** (1986) 613–614.

[80] C. Hogan and R. Narayan, *Gravitational lensing by cosmic strings*, *Mon Not. R. astr. Soc.* **211** (1984) 575–591.

[81] J.-P. Uzan and F. Bernardeau, *Cosmic strings lens phenomenology: General properties of distortion fields*, *Phys. Rev.* **D63** (2001) 023004, [astro-ph/0004105].

[82] F. Bernardeau and J.-P. Uzan, *Cosmic string lens phenomenology: Model of poisson energy distribution*, *Phys. Rev.* **D63** (2001) 023005, [astro-ph/0004102].

[83] A. A. de Laix and T. Vachaspati, *Gravitational lensing by cosmic string loops*, *Phys. Rev.* **D54** (1996) 4780–4791, [astro-ph/9605171].

[84] A. de Laix, L. M. Krauss, and T. Vachaspati, *Gravitational lensing signature of long cosmic strings*, *Phys. Rev. Lett.* **79** (1997) 1968–1971, [astro-ph/9702033].

[85] M. Oguri and K. Takahashi, *Characterizing a cosmic string with the statistics of string lensing*, *Phys. Rev.* **D72** (2005) 085013, [astro-ph/0509187].

[86] G. Dvali and A. Vilenkin, *Formation and evolution of cosmic d-strings*, *JCAP* **0403** (2004) 010, [hep-th/0312007].

[87] D. Spergel and U.-L. Pen, *Cosmology in a string-dominated universe*, *Astrophys. J.* **491** (1997) L67–L71, [astro-ph/9611198].

[88] P. McGraw, *Dynamical simulation of non-abelian cosmic strings*, hep-th/9603153.

[89] B. Paczynski, *Will cosmoc strings be discovered using the space telescope?*, *Nature* **319** (1986) 567–568.

[90] M. Landriau and E. P. S. Shellard, *Large angle cmb fluctuations from cosmic strings with a comological constant*, *Phys. Rev.* **D69** (2004) 023003, [astro-ph/0302166].

[91] L. Pogosian, M. C. Wyman, and I. Wasserman, *Observational constraints on cosmic strings: Bayesian analysis in a three dimensional parameter space*, astro-ph/0403268.

[92] J.-H. P. Wu, *Coherence constraint on the existence of cosmic defects*, astro-ph/0501239.

[93] C. Csaki and Y. Shirman, *Brane junctions in the randall-sundrum scenario*, *Phys. Rev.* **D61** (2000) 024008, [hep-th/9908186].

[94] I. Gott, J. Richard, *Gravitational lensing effects of vacuum strings: Exact solutions*, *Astrophys. J.* **288** (1985) 422–427.

[95] A. S. Lo and E. L. Wright, *Signatures of cosmic strings in the cosmic microwave background*, astro-ph/0503120.

[96] A. Vilenkin and E. Shellard, *Cosmic Strings and Other Topological Defects*. Cambridge Univ. Pr., 1994.

[97] T. W. B. Kibble, *Cosmic strings reborn?*, astro-ph/0410073.

[98] A. Vilenkin, *Cosmic strings as gravitational lenses*, *Astrophys. J.* **282** (1984) L51–L53.

[99] A. Vilenkin, *Cosmic strings and domain walls*, *Phys. Rept.* **121** (1985) 263.

[100] I. Gott, J. Richard, *Closed timelike curves produced by pairs of moving cosmic strings: Exact solutions*, *Phys. Rev. Lett.* **66** (1991) 1126–1129.

[101] K. S. Thorne, *Black Holes and Time Warps*. Norton, New York, 1994.

[102] B. Greene, *The Fabric of the Cosmos:Space, Time, and the Texture of Reality*. Knopf, New York, 2004.

[103] S. W. Hawking, *The chronology protection conjecture*, *Phys. Rev.* **D46** (1992) 603–611.

[104] C. V. Johnson and H. G. Svendsen, *An exact string theory model of closed time-like curves and cosmological singularities*, *Phys. Rev.* **D70** (2004) 126011, [hep-th/0405141].

[105] F. J. Tipler, *Singularities and causality violation*, *Annals Phys.* **108** (1977) 1–36.

[106] S. M. Carroll, E. Farhi, A. H. Guth, and K. D. Olum, *Energy momentum restrictions on the creation of gott time machines*, *Phys. Rev.* **D50** (1994) 6190–6206, [gr-qc/9404065].

[107] C. Cutler, *Global structure of gott's two - string space-time*, *Phys. Rev.* **D45** (1992) 487–494.

[108] S. Deser, R. Jackiw, and G. 't Hooft, *Three-dimensional einstein gravity: Dynamics of flat space*, *Ann. Phys.* **152** (1984) 220.

[109] G. 't Hooft, *The evolution of gravitating point particles in (2+1)-dimensions*, Class. Quant. Grav. **10** (1993) 1023–1038.

[110] S. M. Carroll, E. Farhi, and A. H. Guth, *Gott time machines cannot exist in an open (2+1)- dimensional universe with timelike total momentum*, hep-th/9207037.

[111] L.-X. Li and I. Gott, J. Richard, *A self-consistent vacuum for misner space and the chronology protection conjecture*, Phys. Rev. Lett. **80** (1998) 2980, [gr-qc/9711074].

[112] E. Poisson, *Black-hole interiors and strong cosmic censorship*, gr-qc/9709022.

[113] G. 't Hooft, private communication.

[114] A. Albrecht and N. Turok, *Evolution of cosmic strings*, Phys. Rev. Lett. **54** (1985) 1868.

[115] S. W. Kim and K. P. Thorne, *Do vacuum fluctuations prevent the creation of closed timelike curves?*, Phys. Rev. **D43** (1991) 3929–3947.

[116] L. Jarv and C. V. Johnson, *Rotating black holes, closed time-like curves, thermodynamics, and the enhancon mechanism*, Phys. Rev. **D67** (2003) 066003, [hep-th/0211097].

[117] W. J. v. Stockum, *The gravitational field of a distribution of particles rotating around an axis of symmetry*, Proc. Roy. Soc. Edinburgh **57** (1937) 135.

[118] P. O. Mazur, *Spinning cosmic strings and quantization of energy*, Phys. Rev. Lett. **57** (1986) 929–932.

[119] M. P. Headrick and J. R. Gott, *(2+1)-dimensional space-times containing closed timelike curves*, Phys. Rev. **D50** (1994) 7244–7259.

[120] J. D. E. Grant, *Cosmic strings and chronology protection*, Phys. Rev. **D47** (1993) 2388–2394, [hep-th/9209102].

[121] F. Gliozzi, J. Scherk, and D. I. Olive, *Supersymmetry, supergravity theories and the dual spinor model*, Nucl. Phys. **B122** (1977) 253–290.

[122] L. Randall and R. Sundrum, *A large mass hierarchy from a small extra dimension*, Phys. Rev. Lett. **83** (1999) 3370–3373, [hep-ph/9905221].

[123] L. Randall and R. Sundrum, *An alternative to compactification*, Phys. Rev. Lett. **83** (1999) 4690–4693, [hep-th/9906064].